UNIVERSITY OF SÃO PAULO

FACULTY OF MEDICINE OF RIBEIRÃO PRETO

DEPARTAMENT OF INTERNAL MEDICINE

DIEGO ANTONIO PEREIRA MARTINS

Evaluation of the TP53/TP73 pathway in the engraftment of primary acute promyelocytic leukemia cells using a xenotransplantation model

RIBEIRÃO PRETO

2022

DIEGO ANTONIO PEREIRA MARTINS

Evaluation of the TP53/TP73 pathway in the engraftment of primary acute promyelocytic leukemia cells using a xenotransplantation model

Tese apresentada à Faculdade de Medicina de Ribeirão Preto da Universidade de São Paulo para obtenção do título de Doutor em Ciências pelo Programa de Pós-Graduação em Clínica Médica.

Área de concentração: Investigação Biomédica

Orientador: Prof Dr Eduardo Magalhães Rego

RIBEIRÃO PRETO

2022

FICHA CATALOGRAFICA

Serviço de Biblioteca e Documentação Médica

Faculdade de Medicina de Ribeirão Preto da Universidade de São Paulo

Pereira Martins, Diego Antonio

Evaluation of the TP53/TP73 pathway in the engraftment of primary acute promyelocytic leukemia cells using a xenotransplantation model – Ribeirão Preto, 2021.

Avaliação da via TP53/TP73 na enxertia de células de leucemia promielocítica aguda em modelo de xenotransplante.

117p.: 18il.; 30cm

Tese de doutorado, apresentada à Faculdade de Medicina de Ribeirão Preto – USP.

Programa de Pós-Graduação em Clínica Médica. Área de concentração: Investigação Biomédica.

Orientador: Magalhães Rego, Eduardo

1. Prognostic markers. 2. TP53/TP73 pathway. 3. Xenotransplant in acute promyelocytic leukemia.

Nome: Diego Antonio Pereira Martins

Titulo: Evaluation of the TP53/TP73 pathway in the engraftment of primary acute promyelocytic leukemia cells using a xenotransplantation model

Tese apresentada à Faculdade de Medicina de Ribeirão Preto da Universidade de São Paulo para obtenção do título de Doutor em Ciências.

Aprovado em:

Banca Examinadora

Prof. Dr.:_____Instituição:_____

Julgamento:_____Assinatura: _____

Prof. Dr.:_____Instituição:_____

Julgamento:_____Assinatura: _____

Prof. Dr.:_____Instituição:_____

Julgamento:_____Assinatura: _____

Prof. Dr.:_____Instituição:_____

Julgamento:_____Assinatura: _____

Prof. Dr.:_____Instituição:_____

Julgamento:_____Assinatura: _____

APOIO E SUPORTE FINANCEIRO

O presente trabalho foi realizado com o apoio financeiro das seguintes entidades e instituições:

- Fundação de Amparo à Pesquisa do Estado de São Paulo (FAPESP) – Projeto 2017/23117-1;
- Fundação Hemocentro de Ribeirao Preto (FUNDHERP);
- Fundação de Apoio ao Ensino, Pesquisa e Assistência do Hospital das Clínicas da Faculdade de Medicina de Ribeirão Preto da Universidade de São Paulo (FAEPA-HC FMRP/USP);
- Instituto Nacional de Ciência, Tenologia e Inovação (INCT) em Células-Tronco e Terapia Celular – Projeto 14/50947-7;
- Centro de Terapia Celular – Centro de pesquisa, inovação e difusão (CEPID/FAPESP) – Projeto 2013/08135-2.
- Coordenação de Aperfeiçoamento de Pessoal de Nível Superior - Brasil (CAPES) – Código de Financiamento 001

I dedicate this Thesis to my family and friends. Even in my darkest days they never gave up on me. Science will always be the way to move humanity forward and only in a team we can strive and reach our full potential.

ACKNOWLEDGMENTS

Although my believe in a God per se is not well stablished, I would like to acknowledge the fact that without an inexplicable force, superior to our understanding, it would not have been possible to finish this book.

I believe that in life, references are one of the most important things that one can have. I personally use these references, to drive myself to be a better version of me every day, and to one day, be equal to what I used as a fuel to go further. The power of the example is one of the best legacies that we can leave on this earth. In my career, I was extremally lucky to have 4 main examples, that allowed me to be here, and inspired me to reach more than I expected so far. I would like to acknowledge then in a chronological order, but their importance is/was equal to my development:

First, I would like to express my special thanks of gratitude to my first co-supervisor Prof. Antonio Roberto Lucena Araujo. Your example my friend, about not be satisfied with the minimum, not stop to believe and to fight even when the environment is always against us, was what brought me here today. With you I learned that with the right idea, you don't need much more to go far.

Second, I would like to express my eternal gratitude to my supervisor Prof. Eduardo Magalhaes Rego, for accepting me as PhD student and supporting me in my development as a researcher in every possible way. You example about being the best version of a human that we can be, is one of the most impressive things that I experienced. Even after insanely long work journeys, you always kept your humor and was always supportive, patient and kind with all your students.

Third, I would like to express my gratitude to my supervisor Prof. Jan Jacob Schuringa, which received me in the Netherlands. JJ, you always inspired and pushed me in to go far then I believed that I could go. I believed that one of the best qualities as a mentor, is when you don't have to say with words what your students should do, but just with your example, which I always learned with you. Our weekly scientific discussions will be one of the greatest memories of my PhD as they allowed me to see the question from a completely different angle.

Ao meu pai, Jose Martins da Silva. Ao longo dos anos, eu vi o senhor colocar as nossas vidas sempre em primeiro lugar, sacrificando a do senhor por nos. Um exemplo que eu nao tenho palavras para descrever, e que certamente poucas palavras nao conseguirao expressar minha gratidao. Te amo meu pai, e muito obrigado por sempre continuar sendo o senhor.

Next, I would like to thank my family for their lifelong support. Thanks to my mother, Jeciene Amorim, I learned valuable qualities that I carry with me always. Many thanks to my sister, Melissa Martins, which always supported me in every aspect that she could, to my brother-in-law Ilvio Vidal, and my nices Ludmilla and Lyanna. I love you all, and even distant, I always carry you with me.

Following my family, I am extremely grateful that I met Isabel Weinhäuser, who I had the luck to meet in Brazil, against all the odds that this could happen. I can only be here writing this thesis in English (with all the possible mistakes), because she had the patience to teach me, even when I gave up of learning. I cannot express in words my gratitude to her, but I wish that she knows that.

Furthermore, I wish to thank all my colleagues from the laboratory in Brazil and the Netherlands. My special thanks to my brother, which we shared many years together – Juan Luiz Coelho Silva, and to my dear friends Thiago Bianco, Cesar Ortiz, Luciana Yamamoto, Virginia, Mariane, Davinha, Luise, Pedro Luiz, Igor Domingos, and Matheus Bezerra. Moreover, I am grateful for Emmanuel, Alan, Aysegül, Minh, Dianne, whom I met in the Netherlands and always supported me with their friendship.

Likewise, I would like to thank all the people that during this journey, where there to support me. My sincere gratitude to Priscila, Ana Silvia, Patricia, Josi, Amelia, Cleide Lucia, Robin, Annet, and BJ.

Finally, I would like to thank all the financial support I received including the Fundação de Amparo à Pesquisa de São Paulo (FAPESP) and the Abel Tasman Talent Program from the Netherlands.

The current work was sponsored by the Coordenação de Aperfeiçoamento de Pessoal de Nível Superior - Brazil (CAPES) – Code number 001

O presente trabalho foi realizado com apoio da Coordenação de Aperfeiçoamento de Pessoal de Nível Superior - Brasil (CAPES) – Código de Financiamento 001

Ao programa de pós-graduação em Clinica Medica pelo suporte oferecido durante o doutorado e pela excepcional capacitação oferecida.

O presente trabalho foi realizado com apoio da Fundação de Amparo à Pesquisa do Estado de São Paulo (FAPESP) – Processo 2017/23117-1.

“Two things are infinite: the universe and human stupidity; and I'm not sure about the universe.”

Albert Einstein

RESUMO

PEREIRA-MARTINS, DA. **Avaliação da via TP53/TP73 na enxertia de células de leucemia promielocítica aguda em modelo de xenotransplante.** 2022, Ph.D. Tese – Faculdade de Medicina de Ribeirão Preto, Universidade de São Paulo, Ribeirão Preto, 2022.

Os atuais modelos murinos de xenotransplante utilizados como modelos de estudo in vivo dos processos leucêmicos humanos, particularmente na leucemia mieloide aguda (LMA) tem falhado na reconstrução dos processos fisiopatológicos relacionados a doença devido a não similaridade com o nicho medular humano. Deste modo, a avaliação dos processos de alto-renovação, diferenciação e transformação das células tronco hematopoiéticas humanas (HSCs) e leucêmicas (LSCs), bem como sua avaliação quanto a eficácia de novas modalidades de tratamento, devem ser realizadas em microambientes espécie-específicos. Isto é suportado pelo fato de alguns subtipos leucêmicos (presentes no grupo de prognóstico favorável da doença), como a leucemia promielocítica aguda (LPA), apresentam recorrente falha de enxertia em modelos de xenotransplante. Apesar do seu prognóstico favorável frente a outros subtipos de LMA, este subtipo ainda apresenta elevado risco de recaída frequentemente associado a resistência a terapia utilizada. Neste sentido, acredita-se que variações genéticas que confiram maior resistência ao clone leucêmico podem influenciar na capacidade de enxertia destas células, favorecendo sua avaliação in vivo. Estudos prévios do nosso grupo demonstraram que uma maior relação de expressão *ΔNp73*/*TAp73* está associada com pior prognóstico na LPA (menor sobrevida global [SG] e sobrevida livre de doença [SLD]) e resistência à apoptose induzida por citarabina. O ΔNp73, forma truncada do gene *TP73*, atua como um potente inibidor da atividade transcricional das proteínas TP53 e TAp73, desempenhando, desta forma, um importante papel na proliferação e morte celular. Assim, a atividade oncogênica do gene *TP73* é determinada pelo balanço entre suas isoformas transcricionalmente ativa (*TAp73*) e inativa (*ΔNp73*), e essa relação correlaciona-se com o prognóstico clínico e falha no tratamento em diversas neoplasias humanas. Desta forma, o presente trabalho tem como objetivo determinar se alterações na via do TP53/TP73 estão associadas com uma maior capacidade de enxertia em células de pacientes com LPA em modelos de xenotransplante humanizados. Subjacente a isto, investigamos os mecanismos pelos quais a via TP53/TP73 podem conferir às células PML-RARA^{+} vantagens de enxertia, tais como modificações na proliferação, viabilidade e diferenciação celular. Ademais, avaliamos o transcriptoma de pacientes com LPA e LMA com diferentes níveis de expressão do *ΔNp73*/*TAp73*, a fim de identificar possíveis alvos de regulação do TP53/TP73. Em células CD34^{+} isoladas de doadores saudáveis, a hiperexpressão das isoformas *ΔNp73α*/*β* resultou em aumento da capacidade de proliferação e formação de colônias em culturas de longa duração (35 dias) em comparação com o vetor vazio (pMEG). Nas linhagens de LPA (NB4 e NB4-R2), a hiperexpressão do *ΔNp73α*/*β* promoveu um aumento da proliferação, viabilidade

celular em resposta a agentes citotóxicos, e menor diferenciação granulocitíca induzida pelo ácido *all-trans* retinóico. De maneira inversa, a superexpressão de *TAp73α* promoveu a reversão de todos os fenótipos observados com o ΔNp73, resultando em sensibilização ao trióxido de arsênico (ATO) em um modelo de LPA resistente ao ATO. Estes achados foram validados utilizando a linhagem Ba/F3-PML-RARA transduzida com as diferentes isoformas do *TP73*. Ademais, o xenotransplante de animais NSGS com células primárias de pacientes com LPA, transduzidas com o pMEG e o ΔNp73α demonstrou que as células ΔNp73α apresentaram um maior potencial de enxertia na medula óssea, sangue periférico e baço dos animais. No contexto da LMA, pacientes com alta expressão das isoformas *ΔNp73* apresentaram maiores contagens de leucócitos, sendo a razão *ΔNp73*/*TAp73* associada com menor SG e SLD. Ademais, ao nível transcricional, pacientes com alto *ΔNp73* apresentaram enriquecimento para os processos associados com "*HSC UP*" e "*LSC UP*", e negativamente correlacionados com os termos "*GMP UP*" e "*TP53 regulates cell cycle arrest*". Em modelos celulares, a superexpressão das isoformas *ΔNp73α*/*β* resultou em vantagens proliferativas e de sobrevivência celular nos modelos celulares que não continham mutações no gene *TP53* (MOLM13, MV4-11, OCI-AML3 e HL60), embora nenhum efeito tenha sido observado nas linhagens celulares contendo mutações em *TP53* (TF-1 e KG1). O silenciamento da expressão do gene *TP53* em linhagens *TP53 wild-type* reduziu os efeitos da superexpressão das isoformas *ΔNp73α*/β. Mecanisticamente, elevada expressão de *ΔNp73* resultou em redução da expressão de *TP53* e aumento da expressão de *DHODH*, cujo efeitos puderam ser revertidos com o uso do inibidor farmacológico de DHODH - Brequinar, em combinação com o agente demetilante Decitabina. Em conclusão, a hiperexpressão das isoformas *ΔNp73* conferiu vantagens de sobrevivência celular as células de LMA, resultando na enxertia das células primarias de pacientes diagnosticados com LPA em modelo de xenotransplante.

Palavras-chave: Marcadores prognósticos, Via TP53/TP73, Xenotransplante.

ABSTRACT

PEREIRA MARTINS, DA. **Evaluation of the TP53/TP73 pathway in the engraftment of primary acute promyelocytic leukemia cells using a xenotransplantation model.** 2022, Ph.D. Thesis – Faculdade de Medicina de Ribeirão Preto, Universidade de São Paulo, Ribeirão Preto, 2022.

Current murine xenotransplantation models used as in vivo study models of human leukemic processes, particularly in acute myeloid leukemia (AML) have failed to reconstruct the pathophysiological processes related to the disease due to their non-similarity to the human bone marrow (BM) niche. Thus, the evaluation of the processes of self-renewal, differentiation, and transformation of human hematopoietic (HSCs) and leukemic (LSCs) stem cells, as well as their evaluation of the effectiveness of new treatment modalities, must be carried out in species-specific microenvironments. This is supported by the fact that some leukemic subtypes (categorized with favorable prognosis regarding the disease course), such as the acute promyelocytic leukemia (APL), present recurrent graft failure in xenotransplantation models. Despite their favorable prognosis against other subtypes of AML, this subtype still has a high risk of relapse often associated with drug-resistance. In this sense, it is believed that genetic variations that confer greater resistance to the leukemic clone may influence the grafting capacity of these cells, favoring in vivo evaluation. Previous studies from our group have shown that a higher *ΔNp73*/*TAp73* expression ratio is associated with a worse prognosis in APL (lower overall survival [OS] and disease-free survival [DFS]) and resistance to cytarabine-induced apoptosis. ΔNp73, a truncated form of the *TP73* gene, acts as a potent inhibitor of the transcriptional activity of TP53 and TAp73 proteins, thus playing an important role in cell proliferation and death. Thus, the oncogenic activity of the *TP73* gene is determined by the balance between its transcriptionally active (*TAp73*) and inactive (*ΔNp73*) isoforms, and this relationship is correlated with the clinical prognosis and treatment failure in several human neoplasms. Thus, the present work aims to determine whether alterations in the TP53/TP73 pathway are associated with an engraftment capacity of cells isolated from APL patients in humanized xenotransplantation models. Moreover, we investigated the mechanisms by which the TP53/TP73 pathway can confer grafting advantages to PML-RARA^{+} cells, such as changes in cell proliferation, viability, and differentiation. Furthermore, we evaluated the transcriptome of patients with APL and AML with different expression levels of *ΔNp73*/*TAp73*, to identify possible targets of TP53/TP73 regulation. In CD34^{+} cells isolated from healthy donors, overexpression of *ΔNp73α*/*β* isoforms resulted in increased cell proliferation and colony formation in long-term cultures (35 days) compared to the empty vector control (pMEG). In APL cell lines (NB4 and NB4-R2), overexpression of *ΔNp73α*/*β* promoted an increase in cell proliferation, viability in response to cytotoxic agents, and decreased granulocytic differentiation induced by *all-trans* retinoic acid. Conversely,

overexpression of *TAp73α* promoted the reversal of all phenotypes observed with *ΔNp73*, resulting in sensitization to arsenic trioxide (ATO) in an ATO-resistant APL model. Furthermore, in vivo patient derived xenotransplant models using NSGS mice demonstrated that primary APL blasts transduced with ΔNp73 had a superior engraftment in the BM, peripheral blood, and spleen of the mice. In the context of AML, patients with high expression of *ΔNp73* isoforms had higher leukocyte counts, with the *ΔNp73*/*TAp73* ratio being associated with lower OS and DFS. Furthermore, at the transcriptional level, patients with high *ΔNp73* were associated with the terms "HSC UP" and "LSC UP", and negatively correlated with the terms "GMP UP" and "TP53 regulates cell cycle arrest". In cell lines, the overexpression of the *ΔNp73α/β* isoforms resulted in proliferative and cell survival advantages in cell models that did not contain mutations in the *TP53* gene (MOLM13, MV4-11, OCI-AML3 and HL60), although no effect was observed in the cell lines containing mutations in *TP53* (TF-1 and KG1). The silencing of *TP53* gene expression in wild-type *TP53* cells reduced the effects of overexpression of *ΔNp73α/β* isoforms. Mechanistically, high *ΔNp73* expression resulted in reduced *TP53* expression and increased *DHODH* expression. In conclusion, overexpression of ΔNp73 isoforms conferred cell survival advantages on AML cells, resulting in engraftment of primary cells from patients diagnosed with APL in a xenotransplantation model.

Keywords: Prognostic markers, TP53/TP73 pathway, Xenotransplant models.

LIST OF ABBREVIATIONS AND ACRONYMS

AC220	Quizartinib
AML	Acute Myeloid Leukemia
ACTB	Actin Beta
ANOVA	Analysis of Variance
AGM	Aorta Gonad Mesonephros
ANGPT1	Angiopoietin
APL	Acute Promyelocytic Leukemia
AraC	Cytarabine
ATO	Arsenic Trioxide
ATRA	*All-trans* Retinoic acid
AUC	Area Under the Curve
BM	Bone Marrow
BiNGO	The Biological Networks Gene Ontology tool
BSA	Bovine Serum Albumin
CB	Cord Blood
CD	Cluster of Differentiation
cDNA	Copy Deoxyribonucleic acid
CPHM	Cox Proportional Hazard Model
CR	Complete Remission
CEBPA	CCAAT Enhancer Binding Protein Alpha
CMP	Common Myeloid Progenitor
CLP	Common Lymphoid Progenitor
CPT1A	Carnitine palmitoyl transferase I
CSFE	Carboxyfluorescein Succinimidyl Ester
CXCL	C-X-C motif chemokine

DAPI	4´,6-Diamidine-2´-phenylindole dihydrochloride
DFS	Disease Free Survival
DHODH	Dihydroorotate dehydrogenase
DNA	Deoxyribonucleic acid
DNMT3A	DNA Methyltransferase 3 Alpha
EDTA	Ethylenediaminetetraacetic Acid
ELN	European Leukemia Net
ES	Enrichment Score
FAB	French-American-British
FACS	Fluorescence-activated cell sorting
FAO	Fatty Acid Oxidation
FBS	Fetal Bovine Serum
FcR	Fc Receptor
FCS	Fetal Calf Serum
FDR	False Discovery Rate
FHS	Fetal Horse Serum
FLT3	Fms-Like Tyrosine Kinase 3
G-CSF	Granulocyte colony-stimulating factor
GEO	Gene Expression Omnibus
GM-CSF	Granulocyte-macrophage colony-stimulating factor
GMP	Granulocyte/Macrophage Progenitor
GO	Gene Ontology
GSEA	Gene Set Enrichment Analysis
HCL	Hydrochloric acid
HD	Healthy Donor
HMR	HyperPrep Kit with RiboErase
HPCA	Human Primary Cell Atlas

HPRT1	Hypoxanthine Phosphoribosyl transferase 1
HR	Hazard Ratio
HSC	Hematopoietic Stem Cell
IHC	Immunohistochemistry
IL	Interleukin
Kit	Stem Cell Factor
KM	Kaplan Meier
LMPP	Lymphoid-Primed-Progenitor
LRP6	LDL receptor related protein 6
LSC	Leukemic Stem Cells
LT-HSC	Long-Term Hematopoietic Stem Cells
MCSF	Macrophage Colony Stimulating Factor
MCP	Microenvironment Cell Populations-counter
MEMα	Modification of Minimum Essential Medium
MEP	Megakaryocyte/Erythrocyte Progenitors
MFI	Mean Fluorescent Intensity
MGG	May Grunwald-Giemsa
$MgSO_4$	Magnesium sulfate
MNC	Mononuclear cell
MPP	Multipotent Progenitor
MSC	Mesenchymal Stem cells
NANOG	Nanog homeobox
NES	Normalized Enrichment Score
NK	Natural Killer
NPM1	Nucleophosmin
NSG	NOS scid gamma (mice strain)
OS	Overall Survival

OXPHOS	Oxidative Phosphorylation
PB	Peripheral Blood
PBS	Phosphate-buffered saline
PBMSC	Peripheral Blood Mononuclear-Stem Cell
PCA	Principal Component Analysis
PCR	Polymerase Chain Reaction
PDX	Patient Derived Xenograft
PH	Proportional Hazards
PHF8	PHD finger protein 8
PIM2	Pim-2 proto-oncogene, serine/threonine kinase
PKC	Midostaurin
PML	Promyelocytic leukemia protein
PS	Penicillin Streptomycin
ROC	Receiver Operating Characteristic Curve
RNA	Ribonucleic acid
RPL30	Ribosomal Protein L30
RPMI	Roswell Park Memorial Institute medium (culture medium)
RT-PCR	Real Time Polymerase Chain Reaction
SCF	Stem Cell Factor
SLAM	Signaling Lymphocyte Molecule
SPSS	Statistical Package for the Social Sciences
ST-HSC	Short-Term Hematopoietic Stem Cells
TCGA	The Cancer Genome Atlas
TNFα	Tumor Necrosis Factor
Tris	Trisaminomethane
TP53	Tumor protein 53
TP73	Tumor protein 73

TPO	Thrombopoietin
USP	University of São Paulo
UMCG	University Medical Center Groningen
VEN	Venetoclax
WT	Wild Type

LIST OF FIGURES AND ILLUSTRATIONS

LIST OF TABLES

SUMMARY

Introduction

1 INTRODUCTION

1.1 The generation of blood cells: the normal hematopoiesis process

Hematopoiesis is the process by which hematopoietic stem cells (HSC) differentiate into different progenitor cells to continuously sustain the supply of blood cells (GRENIER-PLEAU et al., 2020). Since the first report bringing the notion about a common precursor cell giving rise to all blood lineages (GASPARETTO et al., 2017; LORENZ; CONGDON; UPHOFF, 1952; TILL; MCCULLOCH, 1961), countless studies, have shaped our knowledge about the structure of the hematopoietic system, which led to the classical portraiture of a hierarchically organized hematopoietic differentiation tree (Figure 1A).

Studies in mice demonstrated that hematopoiesis first develops in the yolk sac (primitive or embryonic hematopoiesis), followed by the para-aortic splanchnopleure region and the aorta-gonad-mesonephros region (ANA CUMANO; FRANCOISE DIETERIAN-LIEVRE; ISABELLE GODIN, 1996; LINNEKIN, 1999; MATSUOKA et al., 2001; MEDVINSKY; DZIERZAK, 1996). Subsequently, the process of hematopoiesis ensues in the fetal liver and finally settles in the bone marrow (BM) (EMA; NAKAUCHI, 2000). Experimental data provides evidence to support three distinct theories describing the origin of the hematopoietic lineage. The first theory proposes the Haemangioblast, a common mesodermal progenitor cell with bidirectional potential, to generate hematopoietic cells to initiate embryonic hematopoiesis and endothelial cells for the formation of Blood Islands (CHOI et al., 1998; CHUNG et al., 2002; FALOON et al., 2000; HIRAI et al., 2003). Other studies suggest that hematopoietic cells derive from the hemogenic endothelium, a mesoderm-derived primitive endothelium structure, while others presume that hematopoietic and endothelial cells develop independently from a gastrulation-specified progenitor (GARCIA-PORRERO; GODIN; DIETERLEN-LIÈVRE, 1995; TAM; BEHRINGER, 1997).

In a field with remaining questions about the hematopoietic process, one of the well-established theories is that the different blood lineages emanate from HSCs during adult/definitive hematopoiesis. The HSC gives rise to different types of blood cells responsible for the associated roles of the blood system (AKASHI K et al., 2000; CABEZAS-WALLSCHEID et al., 2014). The HSC are multipotent cells defined by its ability to self-renew and initiate the lineage differentiation process, which is characterized by the loss of self-renewal ability to generate oligo- and subsequently unipotent progenitor cells. As a result, the hematopoietic system must maintain a rigorous balance between HSC self-renewal and

differentiation to avoid HSC depletion or the excessive proliferation of undifferentiated cells causing the emergence of hematological malignancies (YAMASHITA et al., 2020).

Figure 1. The normal hematopoiesis processes

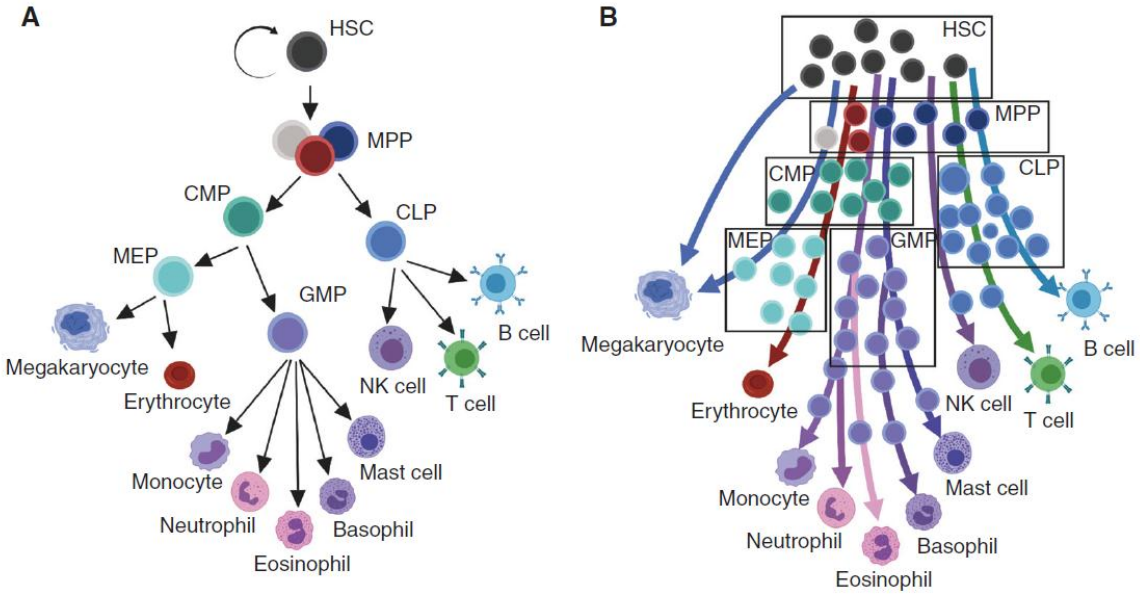

Olson et al., 2020 Normal Hematopoiesis Is a Balancing Act of Self-Renewal and Regeneration, Cold Spring Harb Perspect Med

Representative picture depicting the process of hematopoietic stem cell commitment. **(A)** Classical tree-like model of hematopoietic differentiation. **(B)** The continuous differentiation model.

HSC can be divided into long-term (LT), short term (ST) HSC (HIRAI et al., 2003; IKUTA; WEISSMAN, 1992; MORRISON; WEISSMAN, 1994; SPANGRUDE, 1991). LT and ST distinguish themselves by their self-renewal ability, whereby LT-HSC possess long-lasting abilities to repopulate the BM in the event of lethal irradiation (CHRISTENSEN; WEISSMAN, 2001; SMITH; WEISSMAN; HEIMFELD, 1991), while ST-HSC promotes only short-term reconstitution of the blood lineage (MORRISON; SCADDEN, 2014; MORRISON; WEISSMAN, 1994; YANG et al., 2005). While LT-HSC display a more quiescent nature, the ST-HSC can differentiate into multipotent progenitors (MPPs) (MORRISON et al., 1997). MPP can be classified into four distinct groups, being the MPP1 the most similar with the ST-HSC, while MPP2 and MPP3 differentiate into common myeloid progenitor (CMP) cells (PIETRAS et al., 2015) and MPP4 are associated with lymphoid-primed multipotent progenitors (LMPPs) to initiate lymphoid lineage development (ADOLFSSON et al., 2001, 2005; BOYER et al., 2011; FORSBERG et al., 2006). Finally, CMP can give rise to megakaryocyte/erythrocyte progenitors

(MEP) and granulocyte/macrophage progenitors (GMP) (Figure 1B) (AKASHI K et al., 2000; NAKORN et al., 2002).

1.2 Murine models to study the human hematopoiesis

Over the last few decades, murine models for xenotransplantation have undergone significant improvements, with the capacity to support grafting of different types of hematological neoplasms (REINISCH et al., 2016; THEOCHARIDES et al., 2016). In summary, the main contributions of xenotransplantation systems are i) the identification of normal hematopoietic stem cell (HSC) and leukemic counterpart (LSC), ii) the characterization of the hierarchy of human hematopoiesis and iii) the usage as preclinical models for the development of targeted therapies for malignant hematologic disorders (GOULD; JUNTTILA; DE SAUVAGE, 2015; VALENT et al., 2012). Underlying the contribution to the characterization of the physiological process of normal human hematopoiesis, one of the greatest contributions of humanized transplant systems was in the discovery and understanding of the processes of malignant hematopoiesis and leukemic hierarchy (SHULTZ; ISHIKAWA; GREINER, 2007; WARNER et al., 2005). In this context, the application of these models in understanding the pathophysiology of this disease was capable of reproducing the clinical heterogeneity observed in patients (SONTAKKE et al., 2016), which can be studied at the clonal evolution level, with identification and characterization of the sub clonal leukemic architecture (KOKKALIARIS et al., 2016; SHLUSH et al., 2017). However, among the remaining limitations of this system, the different components of the bone marrow niche, emerge as a problem associated with failure in faithfully recapitulating the process of human hematopoiesis and impaired maintenance of long-term engraftment in many cases (VAN GOSLIGA et al., 2007).

Overall, the success of xenotransplantation models relies on three main factors i) the immunological tolerance of the recipient animal; ii) the presence of a correct spatial niche distribution that will support the homing and expansion of the transplanted cells and; iii) the appropriate support by the host with the correct contribution of cytokines and molecules of the major histocompatibility complex II (MHC-II) (PACZULLA et al., 2017). In order to promote a bone marrow microenvironment with greater similarity to that found in human BM and thus provide the factors that positively influence the success of xenotransplantation, co-transplantation strategies with human stromal mesenchymal cells (MSCs) have been used in xenotransplant models (ANTONELLI et al., 2016; REINISCH et al., 2016).

1.3 The emergence of acute myeloid leukemia

In hematological malignancies such as Acute Myeloid Leukemia (AML) the hematopoietic system is disrupted impeding the development of terminally differentiated myeloid cells. Acute Myeloid Leukemia (AML) is an aggressive hematological cancer characterized by clonal expansion of myeloid lineage progenitors and bone marrow failure (DÖHNER et al., 2010). The two main clinical-pathological hallmarks of AML are the clonal expansion and bone marrow failure. The 5-year overall survival rate is approximately 25% and the typical symptoms upon disease progression are anemia, leukocytosis, and thrombocytopenia. An initial classification for AML patients was proposed by the French-American-British (FAB) classification system categorized patients based on morphological and cytochemistry aspects into eight subtypes (M0-M7) (BENNETT et al., 1976). Although useful for the laboratory classification of AML samples, the FAB system showed unsatisfactory results regarding its efficiency into the AML clinics. Therefore, a new system was established by the European LeukemiaNet (ELN) to stratify patients into favorable, intermediate, and adverse risk groups based on their cytogenetic and molecular landscape (Figure 2) (DÖHNER et al., 2017).

Figure 2. Classification systems for Acute Myeloid Leukemia

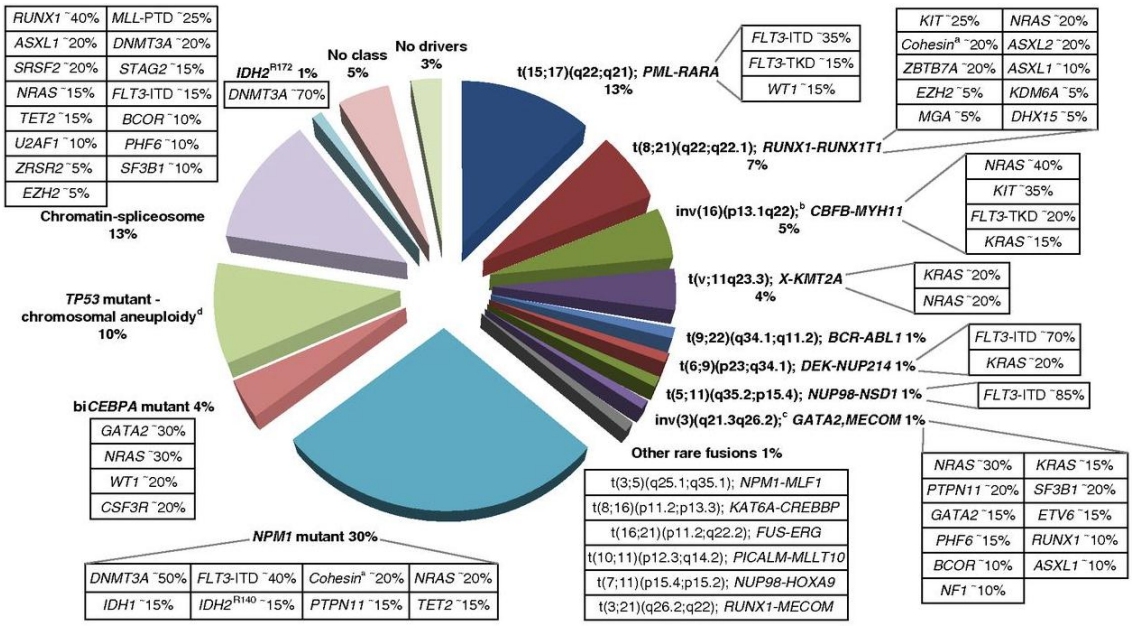

Döhner et al., 2017 Diagnosis and management of AML in adults: 2017 ELN recommendations from an international expert panel, Blood

Pie chart depicting the molecular classes of AML and concurrent mutations in adult patients.

Risk scoring systems, such as the ELN, reflects therapy-refractoriness and risk of relapse. Whereas therapy escalation or de-escalation is indicated for high and low-risk patients, respectively, patients with intermediate-risk (IR) scores constitute the largest group of AML patients and are most heterogeneous (DÖHNER et al., 2017; PAPAEMMANUIL et al., 2016). Further refinement of scoring systems is required here, particularly when it comes to the post-remission therapy choice, which includes allogeneic stem cell transplantation in first complete remission (CR) (CALLENS et al., 2005).

One of the characteristics that contributes to the higher difficulty in treating AML patients is the AML clonal evolution (Figure 3A). Emerged in the last decade, this term roots in the idea that a common ancestral cell can give rise to different leukemic cells carrying different mutations known as subclones (MORITA et al., 2021). These data suggest that the AML bulk population is a highly heterogenous population and each cell displayed different biological characteristics. Moreover, these differences become also apparent in patient derived xenograft (PDX) models, whereby commonly only one or few clones is able to engraft probably due to intrinsic advantages compared to the other subclones injected (KLCO et al., 2014).

Figure 3. AML clonal dynamics and evolution

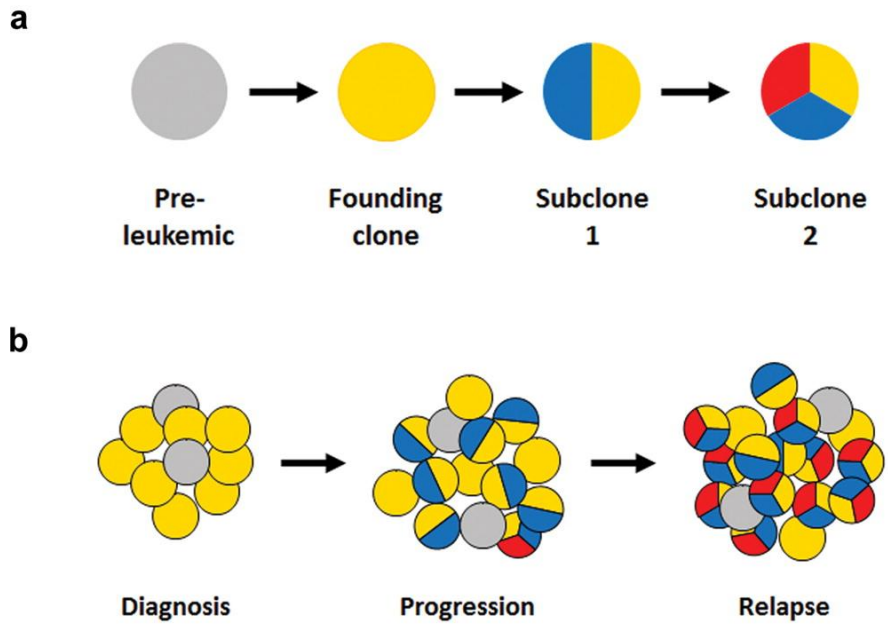

Graubert et al., 2014 New Molecular Abnormalities and Clonal Architecture in AML: From Reciprocal Translocations to Whole-Genome Sequencing, ASCO Educational Book.

Representative picture depicting the process of AML clonal evolution frequently resulting in relapse. **(A)** Accumulation of random somatic mutations in an age-dependent fashion in normal HSCs. **(B)** Representation of the BM of an AML patient typically composed by an admixture of cells from the founding clone and residual, non-clonal cells. Later on, new clones emerge during the natural progression of the disease.

In the clinical setting, the presence of distinct subclones is associated with an increased chance of resistant to AML therapies by one of the subclones, which consequently survive and reemerge causing the disease relapse (Figure 3B) (SHLUSH et al., 2017). As a result, it a better understanding of AML clonal evolution and patient-tailored therapies become ever so more necessary to prevent AML relapse and improve the clinical outcome of AML patients.

1.4 Xenograft models for acute myeloid leukemias

Acute myeloid leukemias (AML) constitute a heterogeneous group of clonal bone marrow diseases that affect hematopoietic progenitors, making them incapable of terminally differentiating and responding to natural regulators of cell proliferation and death. As a result, these malignant cells (leukemic blasts) accumulate in the bone marrow and impair the normal production of blood cells; additionally, these cells can also accumulate in other tissues and organs, compromising their functions (ESTEY, 2016; VERHAAK et al., 2009). From xenotransplantation studies in murine models, such as diabetic/severe combined immunodeficient (NOD/SCID), it is known that the maintenance of this group of diseases is given by the presence of LSC, which have a hierarchical organization similar to that seen in the process of normal hematopoiesis. Thus, xenotransplantation models for AML not only define LSC and serve as preclinical models for therapy but are also a valuable representative tool in the dissection process of the clonal architecture of the AML and the functional properties of the present subclones, which are also targets of therapy (THEOCHARIDES et al., 2016).

However, in AML xenograft models a limited engraftment rate (between 40-50% of patient samples) is observed in a reproducible and robust way (in successive transplants). In this sense, the work by Kennedy et al. (BARABÉ et al., 2007), evaluating 307 AML samples, observed that only 44% of these were grafted and reproduced the disease phenotype seen in humans. Associated with these findings, the same authors observed a high proportion of grafting in samples from relapsed patients when compared to the sample at diagnosis (66% versus 44%), correlating the grafting capacity of the samples with the observed aggressiveness of the disease.

Other studies (NG et al., 2016; VARGAFTIG et al., 2012) have shown that the failure to graft a large proportion of AML samples is particularly observed in samples from patients belonging to the favorable risk group. AMLs present in the favorable risk group constitute

approximately 40% of new cases of de novo AML, being common in young patients under 60 years of age (DÖHNER et al., 2017). Due to the lesser biological aggressiveness observed and because they benefit better from therapy, patients included in this group have greater survival when compared to patients allocated to intermediate or high-risk groups. However, only 66% of young patients and 33% of adult patients, present in the favorable risk group, survive for more than 3 years after diagnosis (ELLEGAST et al., 2016). Thus, the study of different clones found in patients in xenotransplantation models is of relevant importance in the development of therapies aimed at preventing future relapse (WUNDERLICH; MULLOY, 2016).

In order to improve the engraftment rate of AML samples in the favorable- and intermediate-risk group, several murine models were engineered in order to provide a BM niche more similar to the human one. The NSGS (or NSG-SGM3) model (*NOD.Cg-Prkdc^{scid}Il2rg^{tm1Wjl}Tg(CMV-IL3,CSF2,KITLG)1Eav/MloySzJ*) (ZHANG et al., 2017), express the human *IL3*, *GM-CSF* and *KITLG* genes into the murine BM. Although initial reports displayed promising results to this model, one of the main limitations is the induction of exhaustion in the HSC/LSC, due to the high levels of cytokines (KORNBLAU et al., 2018; PEREIRA-MARTINS et al., 2021). Subsequently, the MISTRG mice (*C;129S4-Rag2$^{tm1.1Flv}$Csf1$^{tm1(CSF1)Flv}$Csf2/Il3$^{tm1.1(CSF2,IL3)Flv}$Thpo$^{tm1.1(TPO)Flv}$Il2rg$^{tm1.1Flv}$Tg(SIRPA)1Flv/J*) (ELLEGAST et al., 2016), was developed to express four genes encoding cytokines important for innate immune cell development. The human cytokines were able to support the development and function of monocytes/macrophages and NK cells derived from human fetal liver or adult $CD34^+$ progenitor cells, when injected into the mice. Human macrophages were able to infiltrate the tumor xenograft in a manner resembling the observed in the patients. Unfortunately, the lack of mice available in the market, together with the scarce literature regarding the model, constitutes the main limitation in its use.

Also in this sense, another subtype that has a high percentage of graft failure in xenotransplantation models is acute promyelocytic leukemia (APL) (MATSUSHITA et al., 2014; PATEL et al., 2012). Considered as a leukemic subtype with a good prognosis, only two studies were successful in reproducing the disease in patient-derived models using only immunodeficient mice. The first, published in 2012 by Patel et al (PATEL et al., 2012), using a NOD/shi-SCID IL2R$\gamma^{-/-}$ (hereafter called NSG) murine model, the authors obtained an engraftment rate of 50% (4/8 samples) of human $CD45^+CD33^+CD19^-$ cells. Out of these 04 samples, only in two, the molecular characteristics of APL (presence of the PML-RARA transcripts) could be confirmed and the engraftment capacity upon serial transplantation was

retained. Subsequent to this report, Matsushita et al. (MATSUSHITA et al., 2014) proposed an in vivo model of APL using cord blood (CB) $CD34^+$ cells transduced with the PML-RARA (short isoform/bcr3) using the retroviral vector MIGR1. While the overexpression of the PML-RARA does not provide cell transformation per se, the authors transplanted them into pre-conditioned NSG mice and followed the levels of human CD45 cells in the peripheral blood (PB) of the mice until engraftment was detected. Within 1-year post-transplant, the authors managed to observe histopathological signs of APL in the transplanted mice. Immunophenotypic analysis of the engrafted cells associated with serial transplantation, suggested that the cell-of-origin of APL is probably residing in the common myeloid progenitor (CMP, $CD34^+CD38^+CD123^+CD45RA^-$) pool (REINISCH et al., 2016). Later, the report from Paczulla et al., (PACZULLA et al., 2017), described the engraftment of AML samples with a favorable prognosis, including APL samples into immunodeficient mice (2 independent patients). The authors suggested that since engraftment capacity is correlated with clinical presentation of the disease in patients, samples with lower engraftability are most likely less efficient in homing into the murine BM. This, together with the lack of a proper tumor microenvironment, results in longer latency periods to engraft. The authors provided two examples, where one APL sample displayed engraftment in 10 weeks, while the other sample only showed signs of engraftment at week 26 into irradiated NSG mice. A major drawback in this study was the methodology to access engraftment (by only measuring the human CD45 levels and not confirming the PML-RARA transcript). Furthermore, both samples displayed poor levels of engraftment, with BM engraftment inferior to 4%, no invasion on the PB, and the lack of a secondary recipient to show if the LSC properties remained preserved.

These observations suggest that the presence of a cellular microenvironment with greater similarity to the human bone marrow is necessary in the recapitulation of acute myeloid leukemias in patient-derived xenotransplantation (PDX) models (ANTONELLI et al., 2016). This can be explained by the species-specific need for myeloid growth factors, which when produced by the murine bone marrow are not sufficient to provide an adequate environment for staging, survival, and expansion of LSC (REINISCH et al., 2016).

Thus, the development of new approaches for xenotransplant samples from patients allocated in the favorable risk group has included the use of scaffolds filled with human mesenchymal cells (MSCs), in the search for a microenvironment more similar to that found by human LSC (SONTAKKE et al., 2016).

1.5 Humanized models of xenotransplantation

In order to solve the graft problems found in some leukemic subtypes (such as APL, for example) and other hematological disorders (myelodysplastic syndromes and chronic myeloproliferative neoplasms), current studies have used strategies for co-transplantation of leukemic cells with mesenchymal cells isolated from the human BM stroma (KORNBLAU et al., 2018; RAU, 2017). The hematopoiesis process takes place in specialized microenvironments in the bone marrow, known as medullary niches (MENDELSON; FRENETTE, 2014), where, in these sites, the HSCs establish intimate contact with a complex cellular network that includes: mesenchymal stromal cells, osteoblasts, adipocytes, endothelial cells, and Schwann cells. These niches are essential to support the survival of LSC (SHULTZ; ISHIKAWA; GREINER, 2007; YAMASHITA et al., 2020).

In this sense, three main approaches have been used to recreate this medullary microenvironment in a xenotransplantation model. The first, proposed in 2015 for Reinisch et al (REINISCH et al., 2016; REINISCH; MAJETI, 2016), proposed mixing stromal mesenchymal cells from human BM with an extracellular matrix, for subcutaneous implantation in the flanks of NOD/SCID mice, recreating a medullary microenvironment capable of recruiting and support the engraftment of cells in xenotransplantation experiments. Reinisch et al demonstrated the ability to engraft particularly difficult to engraft samples, such as APL and myelofibrosis samples, using the ectopic scaffold. The authors demonstrated that when injected intravenously, human cells migrated into the humanized microenvironments but not into the murine ones. These humanized ectopic niches proved to be able to recruit cell lines, maintaining the normal hematopoiesis process within them. The second methodology, proposed by the Schuringa`s lab (University Medical Centre Groningen/Netherlands), similarly to the first one, proposes the use of ceramic scaffolds, filled with BM-isolated human MSCs, which are implanted in NOD/SCID mice to develop mimetic structures to the human BM microenvironment (ANTONELLI et al., 2016; DE BOER et al., 2018; SONTAKKE et al., 2016). The authors reported increased engraftment levels, particularly for the AML samples allocated in the favorable risk group. Transcriptionally, AML blasts engrafted into the human niche presented increased similarities with the diagnosis samples when compared to blasts that invaded the murine BM, suggesting the ability of the humanized microenvironment to preserve the clonal architecture observed in the patients. Regardless of the methodology used, the results suggest that these structures provide a more permissive microenvironment for LSC, directing them to the process of commitment to the myeloid

lineage, thus facilitating the recreation of these leukemia subtypes (ANTONELLI et al., 2016).

Recently, the group of Dominique Bonnet (MÉNDEZ-FERRER et al., 2020)(ABARRATEGI et al., 2017) proposed the use of gelatin-based porous scaffolds pre-seeded with autologous MSCs isolated from the BM samples of the patients (or allogeneic MSCs, when an autologous MSC could not be retrieved). The authors demonstrated that regardless of the murine model used as a recipient (NSG versus NSGS), human engraftment was detected around week 8-10, with murine vasculature around the scaffold. Additionally, the authors demonstrated the preference of human cells to the human microenvironment, by transplanting intravenously animals containing empty scaffolds filled with human and murine MSCs. Human $CD45^+$ cells could be detected inside the scaffolds seeded with human, but not in the ones with murine MSCs.

In addition to providing adequate engraftment for most of the leukemic subtypes, the use of humanized xenotransplantation systems is of paramount importance in maintaining the clonal genetic signature of leukemic cells (KLCO et al., 2014; WANG et al., 2017). Particularly in the context of sub-clonal mutations (such as *FLT3*-ITD and *NPM1* mutations), where the concordance in variant allele frequency (VAF) that is observed in the patient sample and in the PDX is relatively poor (KOKKALIARIS et al., 2016). When comparing the differences between transcriptomes from cells derived from murine microenvironments versus cells obtained from humanized microenvironments (ectopic scaffolds), prominent differences were observed in the signature of genes associated with hypoxia signaling, mitochondria, and metabolism. Within the differentially expressed genes, the enrichment for genes such as *CDKN1C*/*p57*, *SALL4*, and *BMI1*, associated with cell cycle inhibitors and contribution to stemness of HSCs/LSCs (SONTAKKE et al., 2016). This could explain the better engraftment observed for different leukemic subtypes in these humanized models.

However, in addition to providing the proper BM microenvironment, genetic modulators inherent to the pathophysiology of the disease can act as enhancers of the engraftment capacity in PDX models (CARRETTA et al., 2017; CELLS et al., 2016). These factors can favor the engraftment of cells from patients allocated in the favorable risk groups, such as APL.

In this sense, our group found an association between increased expression of the truncated isoform of the *TP73* gene, *ΔNp73*, and a worse clinical outcome in APL patients treated with *all-trans* retinoic acid (ATRA) plus anthracycline-based chemotherapy (LUCENA-ARAUJO et al., 2015). Moreover, we demonstrated that the overexpression of the

ΔNp73 gene in PML-RARA^{+} cells increased the cell proliferation rate and promoted a greater resistance to drug-induced apoptosis (LUCENA-ARAUJO et al., 2017a).

1.6 The TP53 pathway in APL

In this regard, acute promyelocytic leukemia (APL) accounts for about 20 to 25% of AMLs in Latin American countries and has peculiar clinical, morphological, and biological characteristics that distinguish it from other subtypes of this disease. From a morphological point of view, it corresponds to the M3 subtype of the French-American-British (FAB) classification and is characterized by the interruption of myeloid maturation and accumulation of leukemic blasts similar to promyelocytes in the bone marrow (BENNETT et al., 1976; SANZ et al., 2019). Clinically, APL differs from other subtypes of AMLs due to their association with hemorrhagic manifestations in approximately 60% to 90% of patients (CORRÊA DE ARAUJO KOURY et al., 2017; SANZ et al., 1999; SILVA et al., 2019), this being the main cause responsible for the high mortality rates during the initial phases of treatment.

This leukemia is found, in approximately 98% of cases, associated with a reciprocal and balanced translocation between chromosomes 15 and 17 which, from a molecular point of view, is located at the breakpoints of the *PML* (Promyelocytic Leukemia) and *RARA* (Retinoic Acid Receptor Alpha) genes, respectively (KAMLER; PIZANIS, 2013; REGO et al., 2013). This translocation leads to the production of a hybrid gene that encodes for the PML-RARA fusion protein, which conserves most of the functional domains of the parental proteins and acts as a dominant-negative oncogenic product, interfering with both the functions of the wild PML protein and the normal retinoid pathway (ABLAIN et al., 2014; INSINGA et al., 2004; LI; MASON; MELNICK, 2016).

In vitro (KAWASAKI et al., 2003) and *in vivo* (REGO et al., 2001) experiments demonstrated that the *PML* gene acts as a tumor suppressor controlling cell apoptosis, differentiation, and senescence. Interestingly, the PML protein co-localizes with the TP53 tumor suppressor protein in the nuclear bodies, acting as a co-activator of the latter and playing a role as a TP53-dependent cell senescence controller (ABLAIN et al., 2014). Similarly, the PML protein also it is able to physically interact with TAp73, inhibiting the ubiquitination of this protein via CBP/p300 and, consequently, its degradation (CAMPBELL et al., 2020).

In the case of APL, the PML protein levels are significantly compromised since at least one allele of the *PML* gene is involved in t(15;17)/PML-RARA. Furthermore, the PML-RARA oncoprotein maintains its binding capacity to the parental PML protein and interferes in a dominant-negative way in its function (ABLAIN et al., 2014). Heterodimerization between PML and PML-RARA results in an abnormal localization pattern of the PML protein, which leaves the nuclear bodies and begins to have a speckled distribution throughout the nucleus. This shift suggests that the PML-RARA protein may interfere in the physiological function of PML (CAMPBELL et al., 2020). In addition, it is attributed to the PML-RARA fusion protein the ability to destabilize the TP53 protein, promoting its deacetylation and subsequent degradation via MDM2 (BERNARDI et al., 2004).

1.7 The *TP73* gene: sixteen in one

The first homolog of the tumor suppressor TP53 gene was described by Kaghad et al. in 1997 (KAGHAD et al., 1997), located on chromosome 1, locus 1p36. This gene, called *TP73*, consists of 14 exons that encode a 2.2 kb mRNA and its respective 73,000 dalton protein, called TAp73. Functionally, TAp73 exerts a similar action to the tumor suppressor TP53, due to its high degree of homology in the main domains of its structure. The DNA-binding domain shows 63% homology with TP53, while the oligodimerization domains in COOH-terminal and NH2-terminal transactivation ends, show 38% and 29% homology, respectively (JOST; MARIN; KAELIN, 1997) (Figure 4A). Another common feature of the *TP73* gene is its ability to produce multiple isoforms through multiple mechanisms, including alternative splicing of the mRNA at the COOH-terminal end, which can result in up to nine different permutations (BOYAPATI; KANBE; ZHANG, 2004), although it is still debatable how many of these variants are actually translated into proteins (RUFINI et al., 2011). Additionally, one of the most important distinctions between its variants involves the use of two distinct promoters: the first located in the 5' UTR region of exon 1 (P1), and the second (P2) located in the intron 3. The transcription of the *TP73* gene through these different promoters, associated or not with the use of alternative splicing involving exon 2 and exon 3 (Figure 4B), gives rise to variants without the NH2-terminal (ΔN) transactivation domain and, therefore, unable to activate transcriptionally the target genes (DI et al., 2013).

Figure 4. The TP73 gene structure

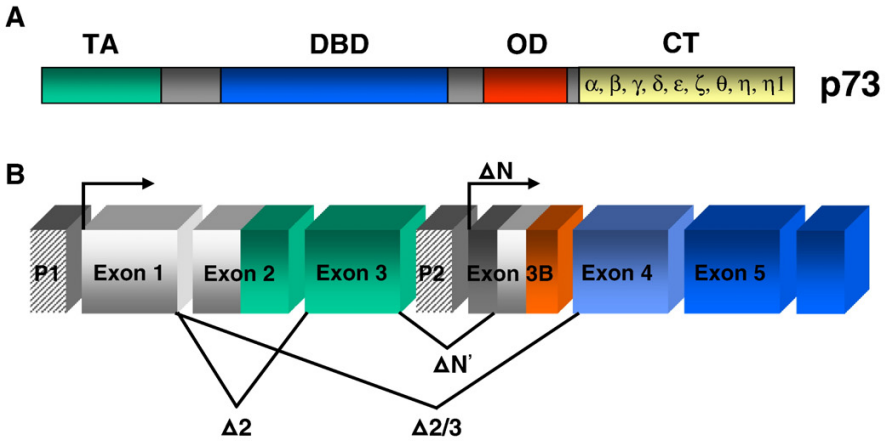

Lucena-Araujo et al., 2012. *In vivo* and *in vitro* analysis of the truncated isoform ΔNp73 in acute promyelocytic leukemia.

(A) Structure of the functional domains of the *TP73* gene. TA, NH2-terminal transactivation domain (green); DBD, DNA binding domain (blue); OD, oligomerization domain (red); CT, carboxy-terminal (COOH-terminal) end (yellow). **(B)** Alternative splicing associated with truncated isoforms of the *TP73* gene. Exons are represented as colored boxes according to the domains they give rise to and which have been represented in the respective colors in (A). Transcription sites are indicated by arrows. The two promoter regions (P1 and P2) are displayed as striped boxes. Alternative splicing of transcripts originating from the P1 promoter are labeled as Δ2 (ΔEx2p73), Δ2/3 (ΔEx2/3p73) and ΔN' (ΔN'p73). The P2 promoter, responsible for the transcription of the truncated isoform ΔNp73, is represented in dark gray.

The transcriptionally active protein encoded by the *TP73* gene (TAp73) has the same inherent capacity to the TP53 protein, which is the ability to control the expression of genes associated with cell cycle control and apoptosis (JOST; MARIN; KAELIN, 1997). Given its chromosomal location in a region frequently altered in human tumors (KAGHAD et al., 1997), it is conceivable that this protein has also a tumor suppressor activity. In fact, the expression of the *TP21* gene, whose TP21 protein acts as a regulator of the G1/S checkpoint of the cell cycle, can be regulated by both TP53 and TAp73 (LEVRERO et al., 1999). Several TP53 target genes, such as *GADD45*, *14-3-3σ*, *MDM2*, *Bax*, *NOXA*, *PUMA*, and *IGFBP3*, also have their transcription regulated by *TAp73* (LEVRERO et al., 2000; STIEWE; PÜTZER, 2001).

However, some evidence obtained from the analysis of human tumors and knock-out mice for the *TP73* gene (*TP73*$^{-/-}$) does not support the hypothesis that the *TP73* gene is a tumor suppressor gene. The first reports in the literature showed that the frequency of mutations and/or deletions in *TP73* is extremely low (LEVRERO et al., 1999), different from what was observed for the *TP53*, which is mutated in more than 50% of the solid tumors in

humans (TYNER et al., 2018). Stiewe and Pützer analyzed more than 1,000 different specimens of human tumors and determined that the mutation rate in the *TP73* gene is approximately 0.5% (STIEWE; PÜTZER, 2002). The recent studies conducted by two independent groups from the Memorial Sloan Kettering Cancer Center (BOLTON et al., 2020; ZEHIR et al., 2017), evaluating sequencing data from 10,945 and 24,146 patients diagnosed for several different types of solid tumors, found no patient carrying mutations in the *TP73* gene. Furthermore, unlike *TP53*$^{-/-}$ mice, *TP73*$^{-/-}$ mice do not spontaneously develop neoplasms, being only alterations in the development of the central and peripheral nervous system observed (DROPULIĆ, 2011; YANG et al., 1993).

One of the problems in the study of tumor development using the *TP73*$^{-/-}$ mice, is the complete deletion of all variants of this gene (transcriptionally active and truncated ones). To study the functions of its variants, researchers generated knock-out mice for specific isoforms of the *TP73* gene. Tomasini et al (TOMASINI et al., 2008) were the first to generate and characterize mice deficient for the complete isoform TAp73. The authors observed that the animals deficient for this isoform (*TAp73*$^{-/-}$) showed an intermediate phenotype between *TP53*$^{-/-}$ and *TP73*$^{-/-}$ mice, with a higher incidence of tumors, especially lung tumors, and alterations in the development of the central nervous system. Furthermore, murine *TAp73*$^{-/-}$ cells displayed aneuploidy associated with genomic instability, which may explain the increased incidence of spontaneous tumors (TOMASINI et al., 2008). Therefore, despite the low frequency of mutations in this gene, the results from *TAp73*$^{-/-}$ mice point to the involvement of the *TP73* gene in the tumorigenesis process.

Through additional promoters or by using alternative splicing at the NH2-terminal end, the *TP73* gene can generate truncated mRNAs, which can be translated into proteins lacking the NH2-terminal transactivation domain (YANG et al., 1993). The transcripts generated from the P1 promoter and which undergo alternative splicing (*ΔN'p73*, *ΔEx2p73*, *ΔEx2/3p73*), are collectively known as *ΔTAp73*, while mRNA transcribed exclusively from the P2 promoter is called *ΔNp73* (Figure 4B). Ishimoto et al. (ISHIMOTO et al., 2002) described for the first time the occurrence of the truncated isoform ΔNp73 in humans and demonstrated that this protein exerts a dominant-negative action on the TP53 and TAp73 proteins, suppressing their transcriptional activity by competing for the DNA binding site in the case of TP53, or by direct association with the protein, in the case of *TAp73* (KARTASHEVA et al., 2002; STIEWE; THESELING; PÜTZER, 2002).

In summary, the *TP73* gene, described as the first homolog of the tumor suppressor gene *TP53*, performs antagonistic functions, in which transcriptionally active isoforms have

pro-apoptotic characteristics, while truncated isoforms have anti-apoptotic properties (MCKEON; MELINO, 2007; STIEWE, 2007). TAp73 isoforms are able to bind to TP53 responsive elements and activate the transcription of genes related to apoptosis induction and cell cycle arrest. On the other hand, the truncated isoforms ΔTAp73 (ΔN'p73, ΔEx2p73, ΔEx2/3p73) and ΔNp73, due to the remaining DNA-binding domain, are able to bind to the DNA binding sites but fail in transcribing the target genes of TP53 and TAp73, since they lack the transactivation domain.

1.8 The oncogenic isoforms of TP73 and their functions: the ΔNp73 isoforms

The works of Ishimoto et al (ISHIMOTO et al., 2002), Stiewe et al (STIEWE; THESELING; PÜTZER, 2002), and Ghandi et al (GHANDI et al., 2019), using the Cancer Cell Line Encyclopedia (CCLE), demonstrated that the truncated isoform *ΔNp73* was significantly expressed in a number of human cancer cell lines. Petrenko et al. demonstrated that the *ΔNp73* overexpression resulted in immortalization of primary fibroblasts from mouse embryos through inhibition of TP53/TAp73-dependent apoptosis, resistance to gene-induced senescence from the Ras family, and by cooperating with *cMYC*/*E1A*-induced cell proliferation and colony formation (PETRENKO; ZAIKA; MOLL, 2003). Interestingly, as far as we know, no human cell line or primary tumor cells expresses a single specific isoform (truncated or complete) of the *TP73* gene (CAMPBELL et al., 2020; GHANDI et al., 2019; ISHIMOTO et al., 2002). Thus, the expression of truncated isoforms of the *TP73* gene occurs concomitantly with the expression of complete isoforms, which suggests the existence of a balance between the actions of these two types of variants.

In this sense, several studies suggest that the balance between the ΔNp73 and TAp73 isoforms is more important to determine the fate of cancer cells than the isolated expression of each one of them (GROB et al., 2001; PÜTZER et al., 2003; ZAIKA et al., 2002). Overall, in some cancer types what is observed is a preferential transcription of the *ΔNp73* isoform, resulting in an imbalance in the TAp73/ΔNp73 ratio, while in the majority of the cases, both the transcriptionally competent (TAp73) and the truncated ΔTAp73 isoforms are expressed (CONCIN et al., 2004; STIEWE et al., 2004). Our group reported higher expression levels of both variants of the *TP73* gene in AML patients compared to healthy hematopoietic progenitors ($CD34^+$ cells) (LUCENA-ARAUJO et al., 2008). Furthermore, comparative analysis between the AML subtypes revealed that leukemic blasts carrying the t(15;17), t(8;21) and inv16/t(16;16) translocations (all favorable-prognosis – (GRIMWADE et al.,

2010)), the *ΔNp73*/*TAp73* ratio was significantly lower when compared to other AML subtypes (LUCENA-ARAUJO et al., 2008).

Moreover, even in tumors in which the mRNA levels of the *TAp73* and *ΔNp73* isoforms were found at similar and/or high levels, a higher intracellular concentration of the ΔNp73 variant was detected due to superior stability of this truncated protein (GROB et al., 2001; STIEWE; THESELING; PÜTZER, 2002). A better understanding of the transcriptional control of the *TP73* gene isoforms, as well as the mechanisms associated with the stabilization and degradation of TAp73 and ΔNp73 proteins, may be of interest for the development of new therapies against cancer.

Likely in solid tumors, mutations in the *TP73* gene in AML are also rare (LEY et al., 2013; TYNER et al., 2018), with a reported frequency of 0.001%-0.1%. In addition to structural alterations, epigenetic mechanisms may be involved in the regulation of *TP73* gene expression in neoplastic cells (SHIN et al., 2000). Sahu et al (SAHU et al., 2005), evaluated the methylation status of *TP73* in patients with *de novo* AML, of which none of them presented methylation. Corroborating these findings, Chim et al. investigated the *TP73* methylation profile in APL patients and demonstrated that there was no methylation detected as well (CHIM; WONG; KWONG, 2003). On the other hand, Ekmekci et al. reported hypermethylation in the promoter region of *TP73* in 10% of patients with *de novo* AML (GU et al., 2018). Schmelz and colleagues demonstrated that 5-Aza-2'-deoxycytidine (5-Aza), a known hypomethylating agent used in the treatment of patients with Myelodysplastic Syndrome (MDS) and AML that are ineligible to receive intensive chemotherapy, was able to reverse *TP73* methylation, increasing TP21 protein expression and inducing apoptosis (SAWYERS et al., 1992). Therefore, the literature regarding the TP73 methylation status in hematologic malignancies is still controversial.

1.9 The TP73 isoforms and their role in APL

Besides the role of TP53 in the pathogenesis of APL, previous reports already pointed to a possible role for a gene with very similar functions to *TP53*, the *TP73*, in the pathogenesis of APL (MAINARDI et al., 2007; MEIER et al., 2016). The report of Rizzo et al. (MAINARDI et al., 2007) demonstrated that the expression of the truncated isoform *ΔNp73* was inferior in APL samples when compared to other AML subtypes. Worth it to mentioning that the conclusions obtained from this study are limited due to the small cohort of APL patients evaluated and the methodology for gene expression analysis (Nested reverse

transcription polymerase chain reaction – RT-PCR). Subsequently, Mainardi and collaborators demonstrated *in vitro* that the promoter region of the *ΔNp73* isoform has elements responsible for retinoic acid and that its expression is compromised in the presence of the PML-RARA fusion protein (MAINARDI et al., 2007). However, even though it is a transcriptional target of the fusion protein PML-RARA, our group observed that a group of APL patients had significantly higher levels of the *ΔNp73* transcript, which was correlated with resistance to cytarabine-induced apoptosis *in vitro* (BIOLOGY, 2016; LUCENA-ARAUJO et al., 2017b). Using a larger cohort of APL patients, we demonstrated a wide range in expression for the *TP73* isoforms, with some patients displaying a higher *ΔNp73*/*TAp73* ratio (LUCENA-ARAUJO et al., 2015). Clinically, patients with a high *ΔNp73*/*TAp73* ratio correlate with the poorest clinical outcomes in APL, although its functional implications with the disease progression remain unknown (Figure 5).

Figure 5. The role ΔNp73 in the drug-induced apoptosis in APL

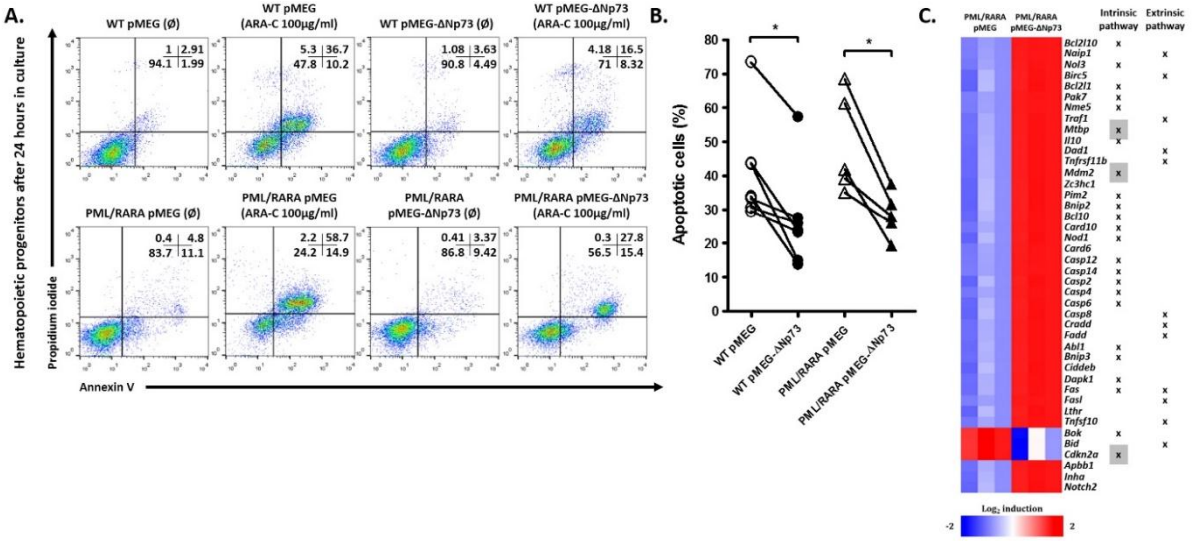

Lucena-Araujo et al., 2017. ΔNp73 overexpression promotes resistance to apoptosis but does not cooperate with PML/RARA in the induction of an APL-leukemic phenotype.

(A) Representative dotplot from one of five independent apoptosis experiments using cytarabine (Ara-C 100 µg/ml, 24 hours) as standard apoptosis stimulus for BM mononuclear cells isolated from PML-RARA mice (CD45.2) transduced with the empty vector and the *ΔNp73α* gene. (B) Percentage of apoptotic cells (Annexin-V$^+$ cells) after 24 hours of treatment. (C) Heatmap displaying the fold-change of differentially expressed genes between Kit$^+$ cells overexpressing *ΔNp73α* compared to the empty vector, in murine hCG-PML-RARα cells.

Since the functions of the PML protein are compromised in the blasts of APL patients, it is theoretically possible that there is a greater degradation of proteins responsible for cell

cycle control and apoptosis, such as TP53 and TAp73, which, consequently, would influence the balance of the ΔNp73/TAp73 ratio. Thus, due to the fact that cells with a high ΔNp73/TAp73 ratio have greater resistance to drug-induced apoptosis, resulting in greater selective advantage, it is theoretically likely that this signaling pathway can act as a genetic modulator in the engraftment capacity of APL cells in PDX models.

The publication of Gould et al (GOULD; JUNTTILA; DE SAUVAGE, 2015) suggests that the failure in the results of clinical trials with drugs that apparently showed success in treatment *in vitro* and *in vivo* is in part associated with the cellular and murine model used, in which a humanized microenvironment is not considered. In agreement with these findings, results published by different groups (ANTONELLI et al., 2016; KOKKALIARIS et al., 2016; REINISCH et al., 2016) showed the assessment of heterogeneity and clonal displacement as important parameters to be evaluated *in vitro* and *in vivo*. The presence of a humanized niche is necessary for the maintenance of clonal heterogeneity that is observed in samples at diagnosis, which is commonly lost in a murine microenvironment, significantly compromising the evaluation of the pharmacological response.

The ability to satisfactorily engraft APL samples remains limited to the use of some specific xenotransplantation strategies in humanized models and with limited reports (PEREIRA-MARTINS et al., 2021; REINISCH et al., 2016). Previous results published by our group suggest that the presence of higher levels of ΔNp73, confer proliferative advantages to APL cells. With this in mind, it is theoretically conceivable that a molecular imbalance in the *TP53*/*TP73* pathway may favor the expansion of APL blasts, aiding in the engraftment of this leukemic subtype in PDX models.

Thus, the development of xenotransplantation models for APL is of paramount importance in understanding the cell biology and in the development of new therapeutic approaches more focused on eradicating the leukemic clone, thus contributing to the understanding and prevention of disease relapses.

1.10 The scope of this thesis

Within this thesis, we uncover clear heterogeneity within the levels of the TP73 isoforms across different AML/APL patients. We show that this has clinical importance since the presence of high ΔNp73/TAp73 ratio in the blasts of AML patients correlates with the poorest clinical outcomes, being associated with a cell-of-origin more similar to the HSC. We demonstrated that the overexpression of *ΔNp73* in AML/APL cells is associated with

increased resistance to drug-induced apoptosis and differentiation, resulting in increased engraftment of APL blasts in a PDX model. Additionally, we demonstrated that mutations or downregulation in TP53 abrogated the pro-tumorigenic phenotypes created by *ΔNp73* overexpression. Our studies also provide mechanistic insight into the ΔNp73/TAp73 ratio mediated phenotypes in leukemic blasts, reprogramming them into more aggressive leukemia initiating cells in vivo.

Objectives

2 OBJECTIVES

2.1 General objective

The overarching aim of the current thesis is to determine if the modulation of genes in the TP53/TP73 pathway are associated with a higher success rate of xenografts in acute promyelocytic leukemia using patient-derived xenotransplantation models.

2.2 Specific objectives

1. Establish a cellular model of acute promyelocytic leukemia (APL) in healthy primary human hematopoietic stem progenitor cells ($CD34^+$) using a lentiviral transduction of the PML-RARA (bcr-1) fusion gene;
2. Evaluate the potential of the interaction between the induced expression of the truncated variant *ΔNp73* and the *PML-RARA* fusion gene in the cellular model of human APL (leukemic blasts and transduced $CD34^+$ cells) *in vitro* and *in vivo*;
3. Perform the screening of genetic modifiers that support the engraftment capacity of human primary APL cells, in xenotransplantation models based on transcriptomic evaluation;
4. Evaluate the phenotypic changes upon overexpression of the *TP73* isoforms in cellular models of acute myeloid leukemia (AML) *in vitro;*
5. Determine whether the expression of different *TP73* isoforms can interfere with AML treatment;
6. Evaluate the clinical outcomes of AML patients regarding the expression of the *TP73* isoforms.

Material and Methods

3 MATERIAL AND METHODS

3.1 Reagents

REAGENT or RESOURCE	SOURCE	IDENTIFIER
Antibodies		
Anti-Human CD45 PE-Cy7	BioLegend	304016
Anti-Human HLA-DR PE	BioLegend	980416
Anti-Human CD14 PercP Cy5	BioLegend	301848
Anti-Human CD33 PE	BD Biosciences	561816
Anti-Human CD117 APC	BD Biosciences	550412
Anti-Human CD34 eFluor 450	eBiosciences	48-0341-82
Anti-Human CD11b FITC	Immunotools	21279113X2
Anti-human CD11b Alexa Fluor 594	BioLegend	101254
Anti-human CD11c APC	BD Biosciences	560895
Anti-human CD15 PE	BD Biosciences	562371
Annexin APC	Immunotools	31490016X2
Anti-Mouse Gr1 APC	BioLegend	108412
Anti-Mouse CD117 APC-Cy7	BioLegend	105826
Anti-Mouse CD34 PE-Cy7	BioLegend	128618
Anti-Mouse CD45.1 PE	BioLegend	110708
Ki-67 PE	BioLegend	350502
Bacterial and virus strains		
Biological samples		
Human AML blast cells	UMCG/USP	Ethical committee NL43844.042.13
Human APL blast cells	UMCG/USP	Ethical committee #13496/2005
Murine hCG-PML-RARa blast cells	USP	Ethical committee #176/2015
Chemicals, peptides, and recombinant proteins		
Propidium Iodide	ThermoFisher	P1304MP
4′,6-diamidino-2-phenylindole	Sigma-Aldrich	28718-90-3
Paraformaldehyde	Sigma-Aldrich	30525-89-4
RNAseA	ThermoFisher	12091021
Dnase I	Roche	11284932001
MgSO4	Sigma-Aldrich	M7506
Heparin		
Arsenic Trioxide	Sigma-Aldrich	1327-53-3
All Trans Retinoic Acid	Sigma-Aldrich	302-79-4
Midostaurin	Sigma-Aldrich	M1323
Quizartinib	Selleckchem	S1526
Venetoclax	Selleckchem	S8048
Decitabine	MedChemExpress	HY-A0004
Brequinar	MedChemExpress	HY-108325

Human Granulocyte-macrophage colony-stimulating factor	Peprotech	300-03
Human Interleukin 6	Peprotech	200-06
Human Interferon Gamma	Peprotech	300-02
Human Interleukin 3	Peprotech	200-03
Human Granulocyte colony-stimulating factor	Peprotech	300-23
Human Thrombopoietin	Amgen	
Carboxyfluorescein succinimidyl ester	BioLegend	423801
β-mercaptoethanol	Merck Sharp & Dohme BV	60-24-2
SsoAdvanced Universal SYBR® Green Supermix	BioRad	1725274
iScript cDNA synthesis Kit	BioRad	1708891BUN
Tetramethylrhodamine, Ethyl Ester, Perchlorate	Thermofisher	T669
MitoTracker DeepRedTM	Thermofisher	M22426
MitoTracker GreenTM	Thermofisher	M7514
Thiazolyl blue tetrazolium bromide	Sigma-Aldrich	M5655-5X1G
RetroNectin GMP grade	Takara	T202
Amicon® Ultra-15 Centrifugal Filter Unit	Merck	UFC910024
Critical commercial assays		
Seahorse XFe96 Flux Analyzer	Agilent	
Experimental models: Cell lines		
MOLM-13	DSMZ	ACC 554
MV4-11	ATCC	CRL-9591™
HL60	ATCC	CCL-240™
OCI-AML2	DSMZ	ACC 99
OCI-AML3	DSMZ	ACC 582
TF-1	DSMZ	ACC 334
NB4	Harvard Medical School	Prof. Pier Paolo Pandolfi
NB4-R2	Harvard Medical School	Prof. Pier Paolo Pandolfi
MS-5	DSMZ	ACC 441
HS27A	ATCC	CRL-9591™
U-937	DSMZ	ACC 5
HEL	DSMZ	ACC 11
KG-1	DSMZ	ACC 14
KASUMI-1	DSMZ	ACC 220
K-562	DSMZ	ACC 10
THP-1	DSMZ	ACC 16
HEK293T	ATCC	CRL-3216
Experimental models: Organisms/strains		
NSGS (NOD.Cg-Prkdcscid Il2rgtm1Wjl Tg (CMV-IL3,CSF2,KITLG)1Eav/MloySzJ)	Jackson Laboratory	013062
NSG (NOD.Cg-Prkdcscid Il2rgtm1Wjl/SzJ)	Jackson Laboratory	005557
C57BL/6J	Jackson Laboratory	000664
Oligonucleotides		

ΔEx2p73 Forward primer	Eurofins	GACGGCTGCAGGGAACCAGA
ΔEx2p73 Reverse primer	Eurofins	TGCCCTCCAGGTGGAAGACG
ΔN`p73 Forward primer	Eurofins	CAGTCAAGCCGGGGGAATAATG
ΔN`p73 Reverse primer	Eurofins	TCCGCAGCTAGTGAGGCAG
ΔNp73 Forward primer	Eurofins	CAAACGGCCCGCATGTTCCC
ΔNp73 Reverse primer	Eurofins	TGGGACGAGGCATGGATCTG
TAp73 Forward primer	Eurofins	GCACCACGTTTGAGCACCTCT
TAp73 Reverse primer	Eurofins	GCAGATTGAACTGGGCCATGA
p73α Forward primer	Eurofins	GTTCGGCAGCTACACCCAAC
p73α Reverse primer	Eurofins	CACCCCAATCCTGTTAAAAAACTGAC
p73β Forward primer	Eurofins	GTTCGGCAGCTACACCCAAC
p73β Reverse primer	Eurofins	CCCAGGTCCTGACGAGG
PIM2 Forward primer	Eurofins	ATCCTGATAGACCTACGCCG
PIM2 Reverse primer	Eurofins	ACACCCTTGTCCCATCAAAG
LPR6 Forward primer	Eurofins	CCCATGCACCTGGTTCTACT
LPR6 Reverse primer	Eurofins	CCAAGCCACAGGGATACAGT
NANOG Forward primer	Eurofins	ACCTTGGCTGCCGTCTCTGG
NANOG Reverse primer	Eurofins	AGCAAAGCCTCCCAATCCCAAACA
PHF8 Forward primer	Eurofins	GGGAAGAACCAACAACGCAG
PHF8 Reverse primer	Eurofins	TCTGGACGATAGCGCGG
TP53 Forward primer	Eurofins	CTTCCCTGGATTGGCAGC
TP53 Reverse primer	Eurofins	TTTTCAGGAAGTAGTTTCCATAGGT
DHODH Forward primer	Eurofins	TGGAGACACCTGAAAAAGCG
DHODH Reverse primer	Eurofins	GGCATCAGGTGTTCAGCATA
HPRT1 Forward primer	Eurofins	GAACGTCTTGCTCGAGATGTGA

HPRT1 Reverse primer	Eurofins	TCCAGCAGGTCAGCAAAGAAT
ACTB Forward primer	Eurofins	AGGCCAACCGCAAGAAG
ACTB Reverse primer	Eurofins	ACAGCCTGGATAGCAACGTACA
RPL30 Forward primer	Eurofins	ACTGCCCAGCTTTGAGGAAAT
RPL30 Reverse primer	Eurofins	TGCCACTGTAGTGATGGACAC
Recombinant DNA		
pLenti6/V5-p53_wtp53	Addgene	#22945
HA-p73α-pcDNA3	Addgene	#22102
pLKO.1-mCherry	Addgene	#8453
HA-ΔNp73α-pcDNA3	Regina Elena Cancer Institute	Dr Maria Giulia Rizzo
HA-ΔNp73β-pcDNA3	GenScript	OHu22244
pCDH1-MCS1-EF1-RFP/GFP-PURO	GenScript	CD73B-1
pMEG-PMLRARA Bcr1	This study	
pMEG-TAp73/pMER-TAp73	This study	
pMEG-ΔNp73α	This study	
pMEG-ΔNp73β	This study	
pLKO.1-mCherry-shTP53	This study	
Software and algorithms		
FlowJo v10.0.6	Treestar	http://www.flowjo.com/
Prism 9	GraphPad	http://www.graphpad.com/
SPSS Statistical package 19.1	IBM	https://www.ibm.com/
Wave	Agilent	https://www.agilent.com/
RStudio	CRAN	www.r-project.org
GSEA 4.0.1	Broad Institute	https://software.broadinstitute.org/gsea/
Cytoscape 3.4		http://apps.cytoscape.org/apps/bingo
Other		
FcR Blocking reagent, human	Miltenyi Biotec	130-059-901
CD34 MicroBeads Kit UltraPure, Human	Miltenyi Biotec	130-100-453
CD117 MicroBeads Kit, Human	Miltenyi Biotec	130-091-332
CD3 MicroBeads, Human	Miltenyi Biotec	130-050-101
Streptavidin MicroBeads	Miltenyi Biotec	130-048-102
TrypLE™ Express Enzyme	Thermo Fischer Scientific	12604021
MethoCult™	Stemcell	H4435/H4230

3.2 Cloning, expansion and purification of *TP53, TAp73, ΔNp73* (alpha and beta) and *PML-RARA* genes

The cDNA encoding the *TP53* (pLenti6/V5-p53_wtp53 - #22945) and *TAp73* (HA-p73α-pcDNA3 - #22102) genes were acquired from the Addgene Public Repository (Cambridge, MA), and extracted according to the supplier's recommendations. The *ΔNp73β* gene was purchased from GeneSci Biosciences (California, USA). For cloning the *ΔNp73α* gene, its cDNA was kindly provided by Dr. Maria Giulia Rizzo of the Regina Elena Cancer Institute (Rome, Italy) and similarly, the cDNA of the *PML-RARA* fusion gene (bcr1 isoform) was kindly provided by Dr. Pier Paolo Pandolffi of the Cancer Research Institute, Harvard Medical School. Short-hairpin vectors to knockdown the expression of *TP53* were cloned and extensively validated, as previously described (AMODEO et al., 2017; GOMEZ-PUERTO et al., 2016). An shRNA sequence that does not target human genes (referred to as scrambled) was used as a control. All the shRNA sequences were expressed using the lentiviral expression plasmid pLKO.1-mCherry (https://www.addgene.org/8453/). After expansion on LB agar medium, the material was subjected to plasmid DNA purification, using the S.N.A.P. MidiPrep (Invitrogen, USA), following the manufacturer's instructions.

After expansion, cDNA from *TP53, TAp73α* and *ΔNp73α/β* genes were subcloned into the lentiviral expression plasmid pCDH1-MCS1-EF1-RFP-PURO or into pCDH1-MCS1-EF1-GFP-PURO (hereafter called pMER and pMEG, respectively). The cDNA of the *PML-RARA* fusion gene in turn was subcloned into the lentiviral expression plasmid pMEG. Once the expansion and purification of the lentiviral expression vectors pMER-*TP53*, pMER/pMEG-*TAp73α,* pMER/pMEG-*ΔNp73α/β,* and pMEG-*PML-RARA* were completed, confirmation of the presence of the insert was performed through digestion with restriction enzymes, followed by sequencing in both directions.

3.3 Cell lines

All cell cultures were maintained in a humidified atmosphere at 37°C with 5% CO2. NB4 (all-trans retinoic acid, ATRA-sensitive) and NB4-R2 (ATRA-resistant) cell lines were kindly provided by Dr. Pier Paolo Pandolfi (Harvard Medical School, USA), and maintained in RPMI 1640 (Gibco, USA) supplemented with 10% fetal calf serum (FCS) (Gibco, USA), L-glutamine (2 mM), Sodium Pyruvate (1 mM), 1% penicillin/streptomycin (PS, Invitrogen, USA). NB4-ATOr resistant cells were kindly

provided by Dr. Tiziana Ottone (University of Tor Vergata, Rome, Italy), and were generated by long-term exposure of NB4 cells to increasing concentrations of ATO. Resistance to ATO was confirmed by apoptosis assessment. Mycoplasma contamination was routinely tested. All leukaemia cell lines were authenticated by short tandem repeat analysis. The cell lines used for the *in vitro* experiments are described in section 3.1. – Reagents and were cultured using the described medium in their respective datasheets. All-trans retinoic acid (ATRA), Midostaurin (PKC), and arsenic trioxide (ATO) were obtained from Sigma-Aldrich (St. Louis, USA) and cytarabine (citarax) was obtained from Blau pharmaceuticals (Sao Paulo, Brazil). Venetoclax (VEN) and quizartinib (AC220) were obtained from Selleckchem (Houston, USA). Brequinar and Decitabine was obtained from MedChemExpress (Groningen, NL).

3.4 Lentivirus production

Recombinant lentivirus encoding the *PML-RARA* fusion transcript (bcr1 isoform) and the isoforms of the *TP73* gene (hereinafter called *TAp73α*, *ΔNp73α* and *ΔNp73β* genes) were generated using the pMEG lentivector (#CD713B-1; System Biosciences, USA) in HEK293T cells according to the three-plasmid packaging procedure as described elsewhere (LUCENA-ARAUJO et al., 2017a). After production, lentiviral particles were concentrated using the Amicon® Ultra-15 Centrifugal Filter Units (Merck, USA), following the manufacturer's instructions. Lentiviral particles to overexpress/knockdown the target genes were used to infect healthy CB $CD34^+$ cells, primary human leukemic blasts (AML and APL), and the AML cell lines. For primary cells, we performed two rounds of transduction using a multiplicity of Infection (MOI) superior to 40, by spinoculation (800 xg for 1 hour) in retronectin coated plates (Takara Bio, USA), with the addition of polybrene (8 µg/mL). For cell lines, a MOI equal to 8 was used to assure a transduction efficiency superior to 50%. Cells were sorted based on their GFP, RFP or mCherry protein expression (alone or in combination, when a double transduction was performed), and posteriorly used for *in vitro* assays. The efficiency of infection was further confirmed by gene expression quantification and western blotting analysis. For the PML-RARA construct, the effectiveness of infection was tested by qPCR and by fluorescence microscopy (to detect the “speckled” pattern of the nuclear bodies of the PML protein when fused to RARA).

3.5 Patient analysis

3.5.1 Human sample collection and patient information

Bone marrow samples of APL patients used for *in vitro* and *in vivo* experiments were studied after informed consent and protocol approval by the Ethical Committee in accordance with the Declaration of Helsinki (registry #12920; process number #13496/2005; CAAE: 155.0.004.000-05 and CAAE: 819878.5.1001.5440; Supplemental document A and B, respectively). Mononuclear cells (MNCs) were isolated via Ficoll (Sigma-Aldrich) separation and cryopreserved. Peripheral blood (PB) and bone marrow (BM) samples of AML patients were studied after informed consent and protocol approval by the Medical Ethical committee of the UMCG in accordance with the Declaration of Helsinki. An overview of patient characteristics can be found in Table 1. Neonatal cord blood (CB) was obtained from healthy full-term pregnancies from the Obstetrics departments of the University Medical Center (UMCG) and Martini Hospital in Groningen, The Netherlands, after informed consent. The protocol was approved by the Medical Ethical Committee of the UMCG. Donors are informed about procedures and studies performed with CB by an information sheet that is read and signed by the donor, in line with regulations of the Medical Ethical Committee of the UMCG (protocol #NL43844.042.13). Peripheral blood mononuclear cell derived $CD34^+$ stem cells (PBMSCs) and CB derived $CD34^+$ cells were isolated by density gradient separation, followed by a hematopoietic progenitor magnetic associated cell sorting kit from Miltenyi Biotech (#130-046-702) according to the manufacturer's instructions.

3.5.2 Cord blood CD34 isolation

Peripheral blood mononuclear cells were isolated by a density gradient using Ficoll (Sigma-Aldrich) from cord blood. Mononuclear cells were washed once at 450g with PBS-EDTA (5 mM) and resuspended in 300 µL of PBS. Next, 100 µL of FcR blocking reagent and 100 µL of CD34 MicroBeads (Miltenyi Biotech) were added to the suspension and incubated for 30 min at 4°C. After incubation cells were washed for 10 min at 450g and resuspended in 2 mL of PBS–EDTA (5 mM). Cells were passed through a cell strainer (70 µM) and isolated by magnetic separation on the autoMACS (Program – Possedels, Miltenyi Biotech). The purity of the isolated cells was routinely evaluated by FACS and in the range of 85% to 95%. All $CD34^+$ healthy cells were pre-stimulated

for 24-48hrs prior to experimental use. CB derived cells were pre-stimulated with Stemline II hematopoietic medium (SigmaAldrich; #S0192), 1% penicillin/streptomycin (PS) supplemented with SCF (255-SC, Novus Biologicals), Flt3 ligand (Amgen) and N-plate (TPO) (Amgen) (all 100 ng/ml). PBMSC $CD34^+$ cells were pre-stimulated with Stemline II, 1% PS, along with SCF, Flt3 ligand, N-plate (all 100 ng/ml) and IL-3 (Sandoz) and IL-6 (both 20 ng/ml).

3.5.3 Gene expression profile of *TP73* isoforms in AML patients

All APL/AML samples used for gene expression analyses were obtained at diagnosis from bone marrow aspirates and were processed according to standard techniques. The gene expression profile was performed as described previously elsewhere (LUCENA-ARAUJO et al., 2017c). Briefly, the expression of the isoforms of the *TP73* gene (*TAp73*, *ΔNp73*, *p73α* and *p73β*) was determined by real-time reverse transcriptase polymerase chain reaction using SsoAdvanced Universal SYBR® Green Supermix (BioRad), following the manufacturer's instructions. Primers used for the reactions are described in section 3.1 – Reagents. The gene expression values of *TP73* isoforms were calculated as relative quantification using the ΔCt method and expressing the results as $2^{-\Delta\Delta Ct}$, in which $\Delta\Delta Ct = \Delta Ct_{patients} - \Delta Ct_{THP1\ cell\ line}$ (THP1 cell line, a human acute myeloid leukemia cell line, expressing high levels of all *TP73* isoforms) (WEINHÄUSER et al., 2020).

3.5.4 Flow cytometry

Cryopreserved MNC fractions of AML/APL patients were thawed, resuspended in newborn calf serum (NCS) supplemented with DNase I (20 Units/mL), 4 µM MgSO4 and heparin (5 Units/mL) and incubated at 37°C for 15 minutes (min). To analyze the myeloid differentiation of the transduced AML/APL bulk samples with the different isoforms of *TP73*/*TP53* genes, $1x10^5$ mononuclear cells were blocked with human FcR blocking reagent (Miltenyi Biotec) for 5 min and stained with the following antibodies in two tubes: Tube I) CD45-PE-Cy7, HLA-DR-PE, CD14-PerCP, CD16-APC-Cy7, CD11c-APC and Tube II) CD45-PE-Cy7, CD11b-PE, and CD15-APC for 20 min at 4°C. At the end of staining, cells were resuspended in RPMI 1640 + 10% FCS containing 4′,6-diamidino-2-phenylindole (DAPI, 1 µg/mL), the latest used as a viability marker for the analysis. The more mature myeloid population was detected inside the population of cells positive for

the Green Fluorescent Protein (GFP), based on the SSC-A^{high}CD45^{high} population, analyzing the staining for the different myeloid-associated markers of cell differentiation. Fluorescence was measured on the BD FACS LSRII or FACS CantoII and analyzed using FlowJo (Tree Star, Inc). For each sample a minimum of 5000 events were acquired inside the single cell fraction, DAPI^{-}GFP^{+} population.

3.5.5 Clinical endpoint analysis

Survival analyzes were performed in AML patients treated with intensive chemotherapy (3+7 scheme) as an induction protocol (BEZERRA et al., 2020). According to survival receiver operating characteristic (ROC) curve analysis, the cut-off used to dichotomize AML patients into two groups (i.e., low expression and high expression) was set by simulating all possibilities (CHANG et al., 2017), followed by the inspection of Kaplan-Meier (KM) curves. Overall survival was defined as the time from diagnosis to death from any cause related to the disease; those alive or lost to follow-up were censored at the date last known alive. For patients who achieved complete remission (CR), disease-free survival (DFS) was defined as the time from CR achievement to the first adverse event: relapse, development of secondary malignancy, or death from any cause, whichever occurred first. Univariate and multivariate proportional hazards regression analysis was performed for potential prognostic factors for overall survival (OS). Potential prognostic factors examined and included in multivariable regression analysis were ELN2010 (2017 when possible) risk stratification, age at diagnosis (analyzed as continuous variable), and our proposed categorization regarding the *TP73* expression. Proportional hazards (PH) assumption for each continuous variable of interest was tested. Linearity assumption for all continuous variables was examined in logistic and PH models using restricted cubic spline estimates of the relationship between the continuous variable and log relative hazard/risk. Descriptive analyses were performed for patient baseline features. Fisher's exact test or Chi-square test, as appropriate, was used to compare categorical variables. Kruskal-Wallis test was used to compare continuous variables. Details of the statistical analysis and clinical endpoints were described elsewhere. All P values were two sided with a significance level of 0.05. All statistical analyses were performed using the statistical package for the social sciences (SPSS) 21.0 and R 3.3.2 (The CRAN project, www.r-project.org) software.

3.6 *In vitro* assays

3.6.1 Cell proliferation assays

Transduced AML and APL cell lines with the different constructs were treated with thymidine (2 mM; CallBiochen, USA) for 18 h twice to induce cell cycle arrest at the G1/S boundary. Cells were subsequently seeded in 6-well plates and 1 million cells were collected and fixed with 70% ethanol at distinct timepoints: Day 1, 2, 3, 4, 6 and 8 and stored at -20°C. Ki-67 staining was performed following the manufacturer's instructions (Ki-67 PE clone SolA15; BioLegend, USA). Next, the mean of fluorescence intensity (MFI) was obtained by flow cytometry standard techniques using a FACS CantoII instrument (Becton-Dickinson, USA). IgG isotype was used as a negative control for each condition. As a confirmatory assay, cells were seeded at a density of 1.5×10^4 cells/ml in 12-well plates and the cell proliferation was assessed with a hemocytometer each 3 days for 10 consecutive days. For primary leukemic blasts and healthy CB $CD34^+$ cells, transduced cells were seeded at a density of $1x10^5$ cells/ml in co-culture with a monolayer of MS5 cells. Primary AMLs were grown on MS5 stromal cells in gartners medium (alpha-MEM supplemented with 12.5% of Fetal Calf Serum [FCS], 12.5% of Fetal Horse Serum [FHS] and 1% PS) with G-CSF (Amgen), N-Plate and IL-3, all 20 ng/mL, and proliferation was evaluated by weekly counts using a hemocytometer for 35 days. The levels of GFP and myeloid differentiation markers (CD11c, CD11b, CD14, CD15, and CD34) were measured by flow cytometry using a BD FACS LSRII instrument (Becton-Dickinson, USA) and analyzed using FlowJo (Tree Star, Inc).

3.6.2 Colony forming unit assay

For transduced AML cell lines, colony formation capacity was evaluated out in semisolid methylcellulose medium (1.5×10^3 cells/mL; MethoCult 4230; StemCell Technologies Inc., Canada). Colonies were detected after 10 days of culture by adding 1 mg/mL of thiazolyl blue tetrazolium bromide (MTT) reagent and scored with the Image J quantification software (US National Institutes of Health, USA). For primary leukemic blasts and CB $CD34^+$ cells, cryopreserved MNC fractions of AML cells were thaw and the isolation of the $CD34^+$ or $CD117^+$ cells was performed. A total of $1x10^3$ transduced AML/CB $CD34^+$ cells were plated in semisolid methylcellulose medium supplemented with human cytokines

MethoCultTM H4435 (StemCell). Colonies were detected after 10 (to evaluate the burst forming unit erythroid – BFU-E) and 14 days and scored.

3.6.3 Apoptosis assay drug screen in the presence of cytotoxic therapy

Drug screen assays were performed using liquid culture systems for AML cell lines and the co-culture systems employing transduced primary AML blasts and MS-5 cells as a stromal layer. A total of transduced $5x10^4$ APL/AML cell lines were seeded in 24 well plates and incubated in complete medium for 72 hours in the presence of vehicle, ATO (1 µM) alone or in combination with ATRA (1 µM) (For APL cell lines only), cytarabine (Ara-C, dose range: 10 – 500 nM), venetoclax (VEN, dose range: 100 to 500 nM), midostaurin (PKC, dose range: 40-100 nM), quizartinib (AC220, dose range: 40 to 100 nM), decitabine (DEC, dose range: 50 to 500 nM – daily added), and brequinar (BRQ, dose range: 50 to 100 nM). The apoptosis rate was determined using the Annexin V-APC/PE and DAPI binding assay (BD Biosciences, San Jose, CA, USA). All specimens were acquired by flow cytometry (BD FACS CantoII/ FACS LSRII; Becton-Dickison) and analyzed with the FlowJo software (Treestar, Inc., USA). All experiments were performed in triplicate and for each sample a minimum of 10 000 events were acquired.

3.6.4 Granulocytic differentiation induction

A total of 2×10^5/mL transduced APL/AML cells were cultured in their respective medium in the presence of ATRA (1 µM) alone or in combination with ATO (1 µM, only for APL cell lines) for 48 and 72 h at 37 °C (DMSO and NaOH were used as vehicle control for ATRA and ATO, respectively). The differentiation rate was determined by evaluating the number of CD11b-, CD11c-, CD15-, CD14-, HLA-DR-, and CD16-positive cells (percentage and MFI levels). Experiments were conducted using the BD FACS CantoII/FACS LSRII flow cytometer (Becton-Dickinson) and analyzed with the FlowJo software (Treestar, Inc.). In parallel, cytospin preparations stained with May-Grünwald-Giemsa (MGG) were used to evaluate morphological changes in transduced NB4 cells treated with ATRA (1 µM) for 5 days (compared to DMSO control).

3.6.5 Gene expression profile of genes associated with *TP73* biology

Total RNA from transduced AML cell lines with the different constructs at basal conditions or treated with Ara-C (100 nM for 48 h), ATRA (1 µM for 72 h) and decitabine (100 nM for 72 h) at different time-points was obtained using the Trizol reagent (Thermo Fisher Scientific, USA). For primary AML blasts/CB $CD34^+$ cells, $1x10^5$ cells were used for RNA isolation. The cDNA was synthesized from 1 µg of RNA using the iScript cDNA synthesis kit (Bio-Rad) and amplified using SsoAdvanced SYBR Green Supermix (Bio-Rad) on a CFX384 Touch Real-Time PCR Detection System (Bio-Rad). Real-time quantitative polymerase chain reaction (RQ-PCR) assays with sample-derived cDNA were performed in duplicate on Optical 384-well plates with the *RPL30*, *ACTB* and *HPRT1* as endogenous control. The primer sequences used to evaluate the gene expression of *PIM2*, *LRP6*, *NANOG*, *PHF8*, *DHODH*, and *TP53* are listed in the key resources table (section 3.1 – Reagents). The gene expression of the target genes was calculated relative to a reference cDNA (THP1 cell line) and set to 1. In all experiments, the same reference cDNA was used as an internal control to ensure that the results would be fully comparable among experiments. The gene expression values of the genes of interest were calculated as relative quantification using the ΔCt method and expressing the results as $2^{-\Delta\Delta Ct}$, in which $\Delta\Delta Ct = \Delta Ct_{sample} - \Delta Ct_{THP1}$ cell line. All the results regarding the gene expression analysis, were normalized as a fold relative to wild-type THP1 cells.

3.7 *In vivo* APL patient derived xenotransplant (PDX) model

3.7.1 Animal welfare

All animals were housed under specific pathogen free conditions in individually ventilated cages during the whole experiment. The animals were maintained according to the Guide for Care and Use of Laboratory Animals of the National Research Council, USA, and to the National Council of Animal Experiment Control recommendations. All experiments were approved by the Animal Ethics Committee of the University of São Paulo (protocols #176/2015).

3.7.2 *In vivo* APL patient derived xenotransplant (PDX) model using transduced blast cells

Eight to ten weeks old female NSGS (NOD.Cg-Prkdcscid Il2rgtm1Wjl Tg(CMV-IL3,CSF2,KITLG)1Eav/MloySzJ) mice were purchased from the Jackson Laboratory. Five different cryopreserved MNC fractions of APL patient samples (each one isolated from a different APL patient) were thaw as described in the section "Flow cytometry" (clinical characteristics in table 2), depleted for $CD3^+$ cells and transduced twice with empty vector or ΔNp73α vector (multiplicity of infection, MOI > 40) using Retronectin-coated plates (Takara). Forty-eight hours post transduction, GFP levels were checked by FACS (empty vector (mean ± Standard Deviation): 31.2 ± 4.7% and ΔNp73α: 9.2 ± 3.4%) and $2x10^6$ primary human transduced APL cells were injected via the retro-orbital sinus into recipient mice (n = 2 mice per patient sample; total of 10 mice per group – empty vector/ΔNp73α). Human $CD45^+$ levels were measured regularly in blood obtained by sub-mandibular bleeding. Twelve- and eighteen weeks post-transplant mice were sacrificed, and cells from the mouse organs including BM, spleen and liver were isolated and analyzed for the presence of human $CD45^+$ cells, regardless of GFP expression (to analyze the transduced and non-transduced human cells). Using FACS analysis, we evaluated the presence of human APL blasts and the more differentiated myeloid committed cells defined by the expression of human $CD45^+CD117^+CD33^+HLADR^-CD19^-$ and $CD45^+CD117^-CD33^+$ markers respectively (PASSLICK; FLIEGER; ZIEGLER-HEITBROCK, 1989), inside the GFP^- (non-transduced) and GFP^+ (transduced cells) cell populations. All antibodies used for the staining were incubated following manufacturer's instructions (see section 3.1 - Reagents). All specimens were acquired by flow cytometry (BD FACS CantoII) and analyzed with the FlowJo software (Treestar, Inc., USA). For each sample a minimum of 20 000 viable events were acquired. In addition, spleen weight was evaluated to access leukemia dissemination to secondary tissues and cytospin preparations using BM isolated cells stained with May-Grünwald-Giemsa (MGG) were used to evaluate the morphology of human APL blasts. Left over cells from BM were sorted for human APL blasts: $GFP^+CD45^+CD117^+CD33^+$ cells, to perform *ex vivo* experiments and stored in liquid nitrogen.

3.8 *Ex vivo* drug screen using xenotransplant engrafted APL blasts

HS27A cells were plated on gelatin coated culture flasks and expanded to form a confluent layer. Next, sorted human APL blasts were cultured in gartner's medium with 20 ng/mL G-SCF, N-plate and IL-3. Cells were incubated for 72 hours in the presence of vehicle, ATO (1 µM) alone or in combination with ATRA (1 µM). The apoptosis rate was determined using the Annexin V-APC and DAPI binding assay (BD Biosciences, San Jose, CA, USA). All specimens were acquired by flow cytometry (BD FACS CantoII; Becton-Dickison) and analyzed with the FlowJo software (Treestar, Inc., USA). All experiments were performed in triplicate and for each sample a minimum of 10 000 events were acquired.

3.9 Microarray and RNA-seq data analysis

3.9.1 Gene expression profile using public datasets

To validate our gene expression data in APL/AML patients, we analyzed the expression of the *TP73* isoforms (using the platform TSV.db - http://www.tsvdb.com/) and their targets using the following datasets: TCGA study for acute myeloid leukemia (LEY et al., 2013), the BeatAML study (TYNER et al., 2018) and the BloodSpot database (BAGGER; KINALIS; RAPIN, 2019). Patients were analyzed regarding the individual expression of the *TP73* isoforms, as well as the *ΔNp73*/*TAp73* ratio. Additionally, global transcriptional and protein expression profile, as well as drug sensitivity to the chemotherapeutic agents commonly used into AML clinics from 17 AML cell lines included in the Cancer Cell Line Encyclopedia (CCLE), were retrieved using the DepMap portal (https://depmap.org/portal/).

3.9.2 Gene ontology (GO) and Gene set enrichment analysis (GSEA) for *TP73* biological pathways in APL/AML

Gene ontology (GO) was performed using the online platform (Panther - http://geneontology.org/) and the BiNGO plugin using Cytoscape (NHI, USA). Gene set enrichment analysis (GSEA) was performed using the Broad Institute software (http://software.broadinstitute.org/gsea/index.jsp). All genes from the RNA-seq of the TCGA AML cohort were pre-ranked according to their differential expression (fold change) and

intensively treated AML patients (n=121) were categorized into high and low expression of *ΔNp73*/*TAp73* ratio, using their median expression rate as a cut-off. Enrichment scores (ES) were obtained with the Kolmogorov-Smirnov statistic, tested for significance using 1000 permutations, and normalized (NES) to consider the size of each gene set. As suggested by the GSEA, a false discovery rate (FDR) cut-off of 25% (FDR q-value < 0.25) was used (SUBRAMANIAN et al., 2005). The limma-voom tool (http://usegalaxy.org) was used to examine differentially expressed genes and genes with ≥1log difference and adjusted p-value of <0.05 were considered significant (PEREIRA-MARTINS et al., 2021). Data visualization was performed with the ClustVis platform.

Results

4 RESULTS

4.1 The ΔNp73α overexpression promotes increased cell proliferation in APL cell lines, which is reversed by the overexpression of TAp73α.

Previously (LUCENA-ARAUJO et al., 2015), our group demonstrated that APL patients displayed increased expression of ΔNp73 isoforms in comparison with the TAp73. In collaboration with another PhD student (Cesar Alexander Ortiz Rojas), we demonstrated that BM samples isolated from APL patients, presented increased expression of ΔNp73, ΔEx2p73, and ΔN`p73 in comparison with healthy BM-MNCs (Figure 6A). We also detected decreased levels of TAp73 in APL patients, suggesting that in APL, the TP73 gene might work as an oncogene (Figure 6B). Survival analysis using the expression of the *TP73* isoforms revealed that the single expression of ΔNp73 and ΔEx2p73 was associated with poor overall survival (OS) in APL, while only the ratio ΔEx2p73/TAp73 was significantly associated with OS in a multivariate analysis (Figure 6C-E). Furthermore, we demonstrated that the usage of ΔEx2p73/TAp73 ratio had superior prediction capacity than the ΔNp73 expression alone (Figure 65F).

Next, we investigated the functional consequences of APL cell lines (NB4 and NB4-R2) transduced with ΔNp73α and its respective empty vector (pMEG). As depicted in Figure 6, the transduced APL cells with ΔNp73α displayed increased cell proliferation when evaluated by daily counts (from day 6 onwards), Ki-67 staining and clonogeneic capacity (Figure 6G-I). Of note, NB4-R2 cells exhibited mild proliferative advantage upon ΔNp73α overexpression, which can be explained by the increased basal proliferation of NB4-R2 cells in comparison with the parental NB4 cells.

Regarding the overexpression of the transcriptionally active isoform TAp73α, NB4 and NB4-R2 cells showed a reduction in proliferative potential (Figure 6J-K), which was confirmed by evaluating the colony formation capacity where cells containing TAp73α had a lower potential for colony formation (Figure 6L).

Figure 6. The role of TP73 isoforms in APL models

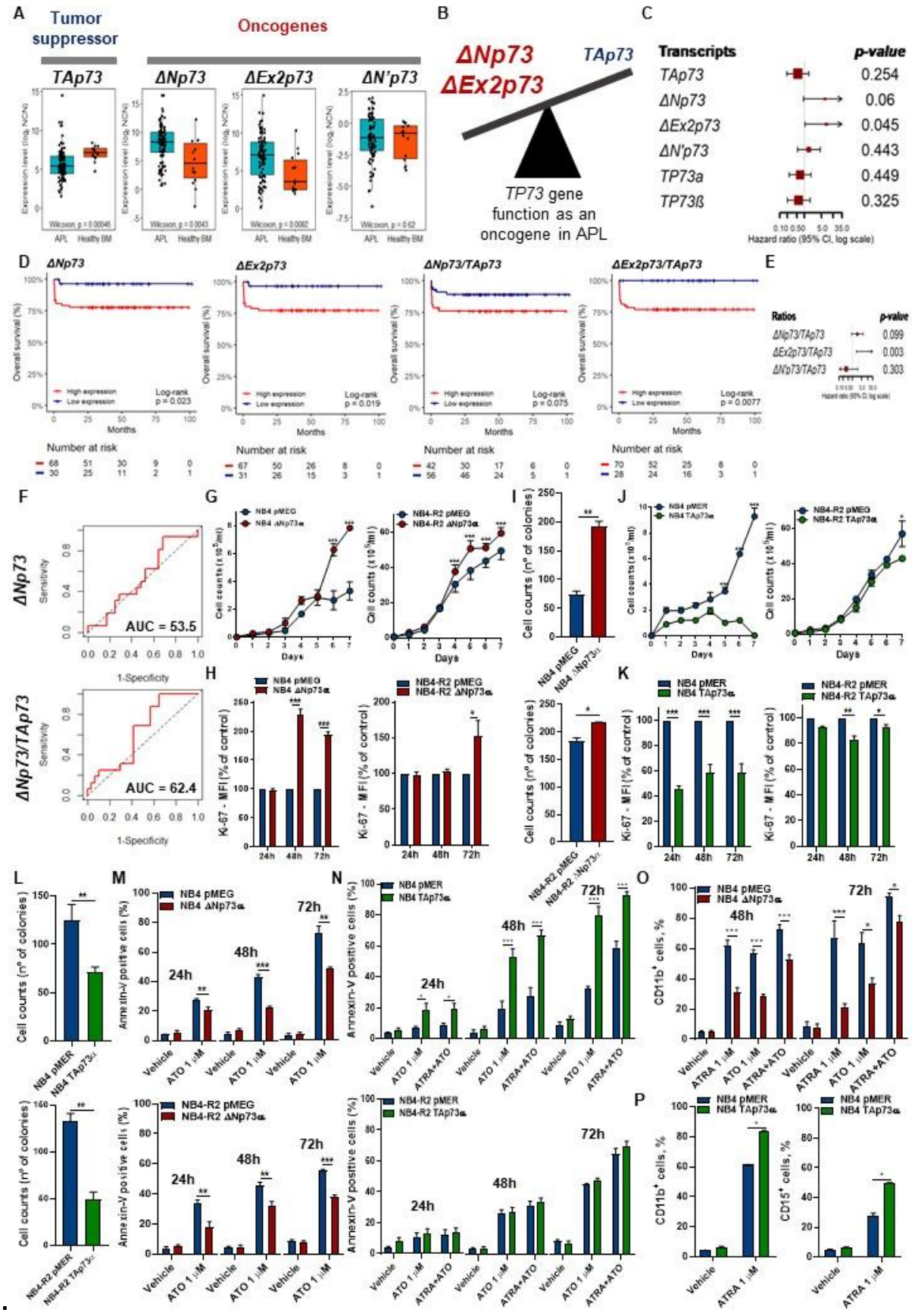

(A) Differential expression of *TP73* isoforms in the IC APL cohort. Gene expression is expressed as log2 values. Horizontal lines represent the median. (B) Scheme for the role of TP73 isoforms in APL. (C) Forest plot depicting the overall survival (OS) analysis for the different TP73 isoforms in APL patients from the IC-APL cohort. (D) Kaplan-Meier (KM) for OS regarding the expression of the TP73 isoforms (alone or in a ratio) in the IC-APL cohort. (E) Forest plot for OS of the different ratios ΔNp73/TAp73 in APL patients. (F) ROC curve analysis for OS considering the ΔNp73 isoform alone or in a ratio with TAp73. (G) Growth curves were analyzed in ΔNp73 overexpressing NB4 and NB4-R2 cells relative to the empty vector (pMEG) control. (H) Ki67 staining of NB4 and NB4-R2 cell lines lentivirally transduced with ΔNp73 or empty vector (pMEG, control). (I) colony formation assay in methylcellulose using lentivirally transduced NB4 and NB4-R2 cell lines. Graphic bars represent the number of colony-forming cells in each well. (J) Growth curves were analyzed in TAp73 overexpressing NB4 and NB4-R2 cells relative to the empty vector (pMEG) control. (K) Ki67 staining of NB4 and NB4-R2 cell lines lentivirally transduced with TAp73 or empty vector (pMEG, control). (L) colony formation assay in methylcellulose using lentivirally transduced NB4 and NB4-R2 cell lines with TAp73. Graphic bars represent the number of colony-forming cells in each well. Drug induced apoptosis after 24, 48, and 72h of treatment with ATO (1 μM) alone or in combination with ATRA (1 μM) were analyzed in ΔNp73 (M) and TAp73 (N) overexpressing cells relative to the empty vector control. Apoptosis was evaluated using Annexin V APC and DAPI to distinguish the apoptotic cells, by FACS. Percentage of $CD11b^+$ and $CD15^+$ in NB4 cells infected with empty vector or pMEG- ΔNp73 (O) and pMER-TAp73 (P) lentiviruses after 48 (left panel) and 72 (right panel) hours of ATRA (1 μM) alone or in combination with ATO (1 μM each) treatment used as the standard stimulus for differentiation.

(C-E) Survival curves were compared using the log-rank test.
(G-P) Wilcoxon signed rank test (2-sided). ***P<0.0001, NS, not significant.
(A) Mann Whitney test for unpaired data (2-sided). *P<0.05.

4.2 The ΔNp73α overexpression of reduces the drug-induced apoptosis in APL models, while TAp73α induces it.

Since we observed increased cell proliferation, we sought to assess whether these effects could modulate the apoptosis induced by the main drugs used in the APL clinics (ATRA and ATO). To do so, NB4 and NB4-R2 cells transduced with the different *TP73* isoforms were treated with ATO (1 µM, NaOH 0.1% was used as vehicle control) alone or in combination with ATRA (1 µM, DMSO 0.01% was used as vehicle control) for 24, 48 and 72 hours, and apoptosis analysis was performed using annexin-V APC and DAPI by flow cytometry. For each condition, analyzes were performed in triplicate and at least four independent experiments were performed for each treatment time.

NB4 and NB4-R2 ΔNp73α cells exhibited decreased drug-induced apoptosis in a time-dependent manner in comparison to pMEG cells (Figure 6M). This data is in agreement with our previously reported one regarding the treatment of primary PML-RARA^{+} murine cells transduced with ΔNp73α, where cytarabine was used as an apoptosis-inducing agent. Regarding TAp73α, the results were inversely proportional to those obtained with ΔNp73α, with NB4 TAp73α cells showing higher levels of apoptosis induction at 24, 48, and 72 hours, in relation to NB4 pMER cells (Figure 6N, upper panel). However, NB4-R2 TAp73α cells did not show an increase in apoptosis at any of the evaluated time-points (Figure 6N, lower panel).

4.3 ΔNp73α overexpression reduces ATRA-induced granulocytic differentiation in APL cells.

Since the previous report about the role of ΔNp73 in the control of the myeloid differentiation (GAILLARD et al., 2018; MAINARDI et al., 2007), we next evaluated the effect of ΔNp73α overexpression regarding their ATRA-induced cell differentiation in NB4 cells. Upon 48 and 72 hours of treatment with ATRA (1 µM), NB4 ΔNp73α cells showed a lower expression of membrane markers CD11b and CD11c, when compared to pMEG cells, although this effect was not observed more in the presence of ATO (1 µM) after 72 hours (Figure 6O). In agreement with these findings, analysis of the morphology of NB4 cells (pMEG/ΔNp73α) after 5 days of treatment with 1 µM ATRA showed a pattern of nuclear lobulation with the acquisition of secondary and tertiary granulation, suggestive of myeloid differentiation in pMEG cells but not in ΔNp73α cells, which remained with a more immature cellular appearance (data not shown).

Although the role of ΔNp73α in modulating myeloid differentiation has been previously suggested, to date, no work has evaluated the impact of TAp73α on drug-mediated myeloid differentiation. As expected, NB4 TAp73α cells showed a higher expression of the granulocytic differentiation membrane markers, CD11b and CD15, compared to NB4 pMER cells, after treatment with ATRA (1 μM) for 72 h (Figure 6P).

4.4 Development of a PDX model of systemic APL using transduced primary APL cells

To evaluate the effects of the *ΔNp73α* gene regarding the engraftment of APL samples in xenotransplantation models, we transduced 10 different samples isolated from the BM of patients diagnosed with APL in the HC/FMRP-USP with ΔNp73α and pMEG. After transduction, $2x10^6$ CD3-depleted cells were transplanted via the retro-orbital plexus into 10–12-week-old female NSGS (or NSG-SGM3) animals. The animals were weekly monitored for physical signs of engraftment and leukemic dissemination (weight loss greater than 10%, changes in motor rhythm and eating disorders), and each 5 weeks, peripheral blood counts and assessment of the percentage of human cells were monitored through blood samples collected by puncture in mandibular vein (Figure 7A).

Figure 7. ΔNp73 overexpression results in superior PDX engraftment in APL models

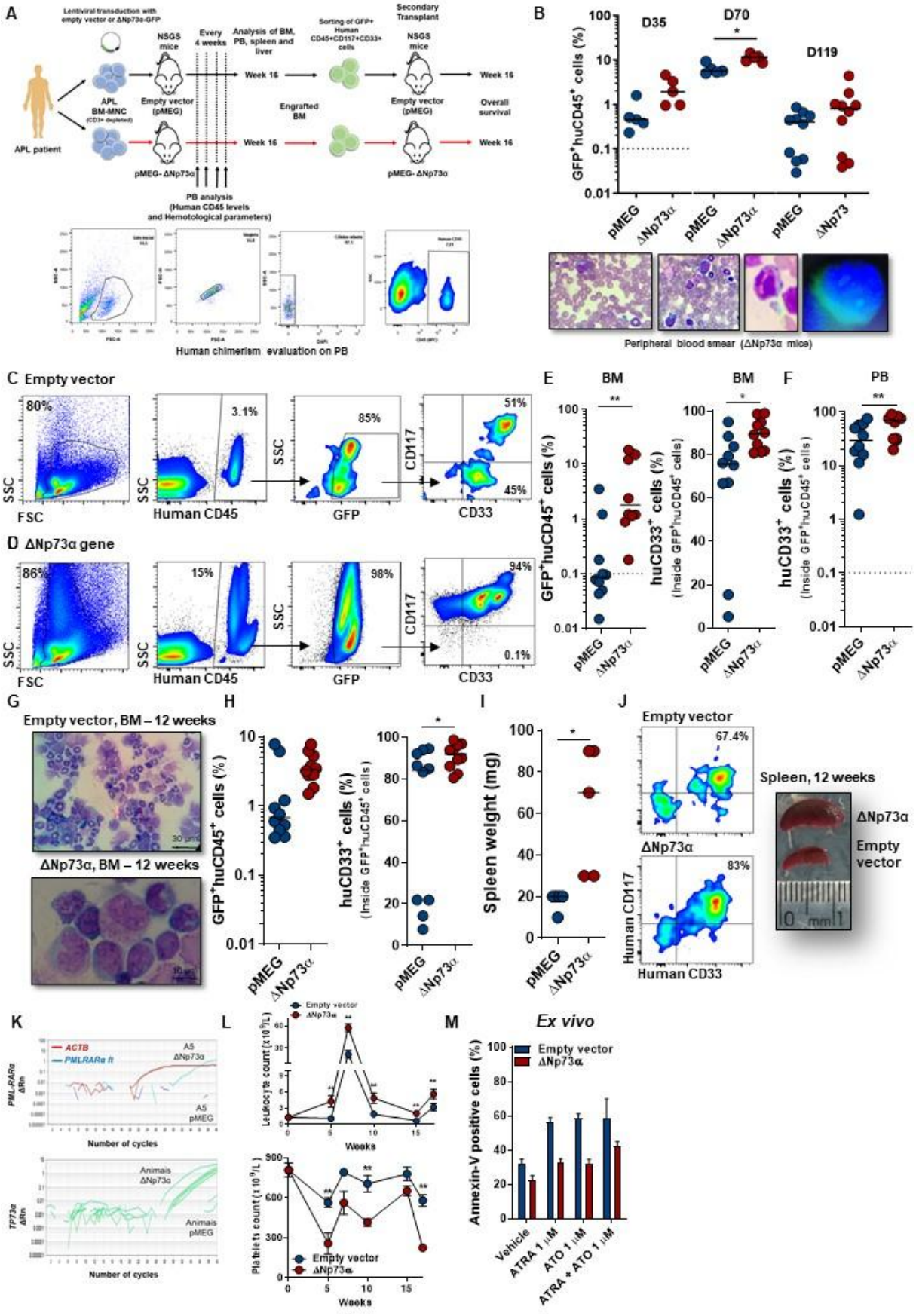

(A) Schematic representation of the generation of the xenograft mouse model for APL engraftment using NSGS mice. (B) Peripheral blood levels of human $CD45^+$ cells through the whole period of the transplant. Representative FACS phenotype from a primary murine bone marrow transplanted with human transduced APL blasts with the empty vector (C) or the ΔNp73 gene (D) at sacrifice. APL blasts and mature myeloid committed cells were analyzed by flow cytometry using markers against CD117, CD33 and CD11b as indicated (inside the population $huCD45^+$ and GFP^+). Scatter plots showing engraftment of donor human $CD45^+$ cells in bone marrow (E) and peripheral blood (F). Representative images of May-Grünwald-Giemsa-stained cytospins of murine bone marrow cells isolated from pMEG and pMEG-ΔNp73 mice. (H) Percentual of engraftment in the spleen and spleen weight (I) of transplanted mice at sacrifice. (J) Representative FACS phenotype from a primary murine spleen of transplanted mice (left panel) and morphological aspect of the organ (right panel). (K) Representative qPCR analysis for detection of the PML-RARA in peripheral blood samples of transplanted mice. The ACTB gene was used as an endogenous control gene. *Ex vivo* analysis of transduced APL blasts reinforces in vitro findings. (L) Incubation of bone marrow sorted APL blasts cells ($GFP^+CD45^+CD117^+CD33^+$) from pMEG/ΔNp73 engrafted mice, with ATRA plus ATO (1 μM each) led to increased induction of apoptosis over the course of 72 hours in empty vector cells. Data were expressed as mean ± standard error of the mean. * indicates $P < 0.05$. ** indicates $P<0.01$. *** indicates $P < 0.001$. NS indicates not significant.

4.4.1 ΔNp73α mice presented increased levels of human CD45$^+$GFP$^+$ cells in the peripheral blood until week 10

We evaluated the engraftment levels of the mice, by quantification of the percentage of human CD45 (huCD45$^+$) and GFP in the peripheral blood samples of the mice. Five weeks post-transplant, we were able to detect the presence of huCD45$^+$GFP$^+$ cells in the animals present in both groups, and although not significant, the animals in the ΔNp73α group showed higher levels (median, [minimum and maximum]: 1.92%; [0.95-4.56%]) compared to mice in the pMEG group (0.46%; [0.23-1.59%]). Significant differences were observed at week 10 post-transplant with mice in the ΔNp73α group having a median of huCD45$^+$GFP$^+$ cells of 11.1% [8.37-13.6%], whereas the mice in the pMEG group displayed a median of 5.41% [4.83-8.88%] (Figure 7B). Furthermore, using fluorescence microscopy to identify the presence of circulating GFP$^+$ cells in PB smears, we confirmed the presence of GFP$^+$ cells, as well as cells with characteristics of human promyelocytes (Figure 7B, lower panel).

4.4.2 ΔNp73α overexpression resulted in increased engraftment in APL PDX model

Surprisingly, although the detectable engraftment in the PB, and the increased leukocyte counts in the ΔNp73α group, after 16 weeks post-transplantation, none of the animals allocated in the two groups (pMEG and ΔNp73α) showed clinical signs of disease, so we decided to terminate the experiment and evaluate the degree of cell infiltration in the bone marrow and spleen of the mice. The BM of the animals was obtained from the maceration and collection of released cells from the tibia, femur, and spine of the animals and the spleen was obtained by gentle tissue maceration and purification using a cell filter with a size of 70 µm. BM and spleen cells were stained with human CD45, CD33, CD117 (as markers of human APL blasts – CD117$^+$CD33$^+$), and CD19 (to exclude the possibility of B-lineage engraftment) (Figure 7C-D). ΔNp73α mice showed higher levels of huCD45$^+$GFP$^+$ cells in the BM when compared to the pMEG group (Median, [minimum-maximum] - ΔNp73α: 6.75%; [0.18-18.1%] versus pMEG: 0.08%; [0.015 -3.5%]), as well as the levels of huCD45$^+$GFP$^+$CD33$^+$ cells (Figure 7C-E). Evaluation for the presence of huCD33$^+$ cells (evaluated inside the huCD45$^+$GFP$^+$ population) in the PB, revealed increased levels of those cells in the ΔNp73α group (Figure 7F). Analyses of the morphology of BM cells in BM smears revealed the presence of cells with characteristics of human blasts, followed by a reactional increase in the number of intermediate murine myeloid cells (a known marker of leukemic infiltration in the

mice) (Figure 7G). The higher engraftment levels observed in the ΔNp73α mice were also reflected in higher levels of $GFP^+huCD45^+CD33^+$ cells in the spleen of ΔNp73α mice (3.9%; [1.5-7.8%]) compared to pMEG animals (0.68%; [0.35-7.8%]) (Figure 7H), with increased spleen weight and size (Figure 7I-J).

Finally, analysis of PB samples revealed a positive signal for the presence of PML-RARα transcripts in all the mice transplanted with ΔNp73α cells, while only 04/10 of the animals in the pMEG group showed detectable signal (Figure 7K). Moreover, we could also observe two important findings: 1) the translocation pattern of PML-RARα (defined as Bcr; Breakpoint chromosome region) remained unchanged in the samples after engraftment (and at termination); and 2) It was possible to detect (using specific primers that are not similar to the murine form of *Trp73*) the expression of ΔNp73α in the PB of ΔNp73α mice, but in only in 02/10 animals, which also showed engraftment of APL cells in the pMEG control group.

4.4.3 ΔNp73α mice exhibited leukocytosis and thrombocytopenia after engraftment

Prior to the transplant, animals allocated in both groups (empty vector control cells – hereafter called pMEG mice, and the ΔNp73α overexpressing cells, hereafter called ΔNp73α mice) were sorted in order to promote similar levels for baseline hematological counts (leukocyte and platelet counts, and hemoglobin levels) (Figure 7L). At the week five post-transplant, ΔNp73α mice had 3-fold higher levels of leukocytes than pMEG animals, and this difference persisted throughout the whole transplant course (Figure 7L, upper panel). Unexpectedly, at week 7, the median leukocyte levels in ΔNp73α mice was $55.4x10^9$/L and in pMEG mice was $23.3x10^3$/L, suggesting increased cell proliferation of the ΔNp73α cells. Evaluation of platelet counts revealed that ΔNp73α mice had lower platelet counts since the fifth-week post-transplant (median [minimum and maximum value]; ΔNp73α: $199x10^9$/L [45-$476x10^9$/L] and pMEG: $555x10^9$/L [476-$684x10^9$/L]), with some fluctuations during the time of the transplant, for both groups (Figure 7L, lower panel). No differences were observed regarding the hemoglobin levels between the two groups (data not shown).

To further study cellular characteristics of engrafted ΔNp73α cells, BM cells from empty vector and ΔNp73α-transplanted mice were sorted (based on GFP^+ and human $CD45^+CD33^+CD117^+$ expression for *ex vivo* experiments. Sorted GFP^+ human APL blasts were cultured for 3 days with ATRA (1 μM) and ATRA+ATO (1 μM each) to evaluate drug-induced apoptosis. Xenograft-derived *ex vivo* cultures, revealed that ΔNp73α-expressing cells

presented decreased sensitivity to ATO, mono or combined therapy, induced apoptosis after 72h of treatment compared to control cells (Figure 7M).

4.5 ΔNp73 isoforms are up-regulated in AML patients, being a high ΔNp73/TAp73 ratio correlated with an HSC/LSC-like proteomic signature

We investigated the role of *TP73* isoforms in AML, a more heterogeneous disease than the previously studied so far, APL. Using the BloodSpot databank, the expression of *TP73* was increased in AML patients (n=198) compared to healthy HSPCs (Figure 8A). Based on the TCGA dataset, we classified the AML patients (n=121, all treated with 3+7 chemotherapy) according to the differential expression of the *TP73* isoforms. Using the area under the curve (AUC) obtained from ROC curve analysis, we dichotomized AML patients into two groups: high and low *ΔNp73*/*TAp73* ratio. Patients with a high ratio were frequently *FLT3*-wild-type displaying increased leukocyte count and a trend of low OS and DFS (Figure 8B-E).

Clustered analysis, using the transcriptome of AML patients with high versus low *ΔNp73*/*TAp73* ratio from the TCGA dataset demonstrated a distinguished gene expression signature between the two groups (high vs low ratio) (Figure 8F). Moreover, gene ontology and gene set enrichment analysis associated a high *ΔNp73*/*TAp73* ratio in AML patients with terms like “RNA pol II transcription”, “HSC_UP”, and “LSC_UP” while a low ratio was associated with “oxidative phosphorylation”, “mitochondrial ribosome binding”, and “GMP_UP” (Figure 8G-H). These results suggest that AML patients with low *ΔNp73*/*TAp73* ratio differ in their metabolic and proliferative state compared to patients with a high *ΔNp73*/*TAp73* ratio.

Next, we correlated the global gene expression of AML patients included in the TCGA cohort with the *ΔNp73*/*TAp73* ratio. We noticed that a high ratio was correlated with the expression of genes associated with cell proliferation (*MKI67*) and anti-apoptotic process (*MDMX*/*MDM2*), whereas a low ratio was correlated with genes associated with the TP53 downstream signaling pathway (*TP53*/*TP53I3*) and with the myeloid differentiation control (*CEBPA*/*CEBPE*) (Figure 8I). Moreover, using the BeatAML cohort dataset, which evaluated in an ex vivo screen the drug sensitivity of AML blasts towards several chemotherapeutic agents used to treat cancer, we correlated the expression of *TP73* with the sensitivity to the main drugs used in leukemia treatment. Low *TP73* expression was associated with increased sensitivity to most of the FLT3-inhibitors (Midostaurin, Quizartinib, Crenolanib, Sorafenib,

and Gilterinib) (Figure 8J), and to some potential drugs used in leukemia, such as JAK1/2 inhibitors (Ruxolitinib) and BCR-ABL inhibitors (Ponatinib).

Finally, using our own cohort of patients diagnosed at the University Medical Center Groningen (UMCG), we confirmed that AML patients displayed increased expression of *ΔNp73* in comparison with *TAp73* (Figure 8K). These results suggest that, as observed in APL, the *TP73* gene seems to act more as an oncogene than as a tumor suppressor in AML.

Figure 8. ΔNp73 isoforms are up-regulated in AML and correlates with a HSC-like signature.

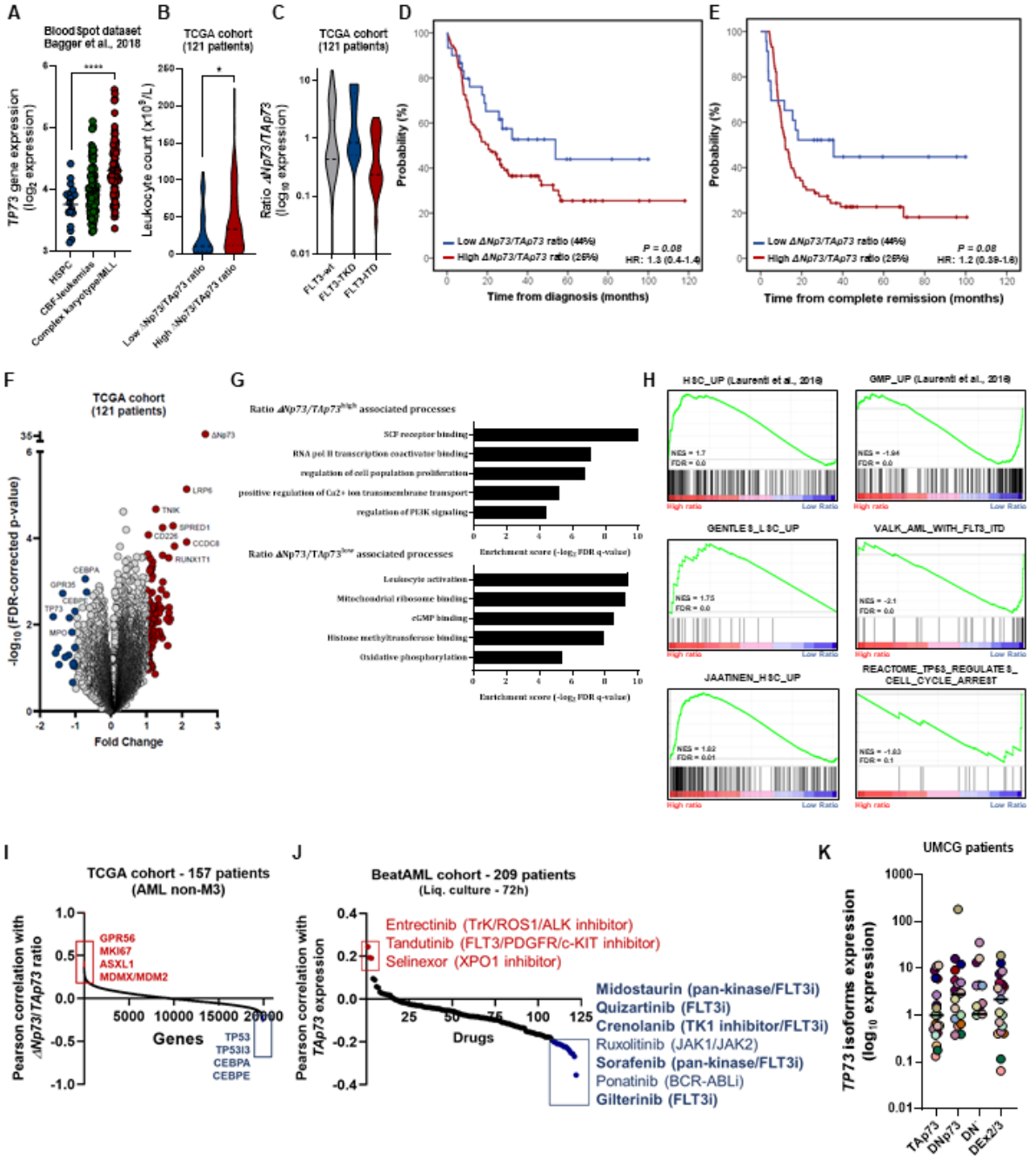

(A) *TP73* transcript levels were evaluated in acute myeloid leukemia patients (AML) compared to healthy hematopoietic stem- and progenitors-cells (HSPCs) using the BloodSpot dataset. Gene expression is expressed as log2 values. Horizontal lines represent the median. ∗p<.05, ∗∗∗p<0.0001. (B) High expression ratio between *ΔNp73*/*TAp73* isoforms it is associated with increased leukocyte count. (C) The ratio *ΔNp73*/*TAp73* isoforms in AML patients grouped by the *FLT3* mutational status. The probability of overall survival (D) and disease-free survival (E) in AML patients from the ICAPL study according to the *ΔNp73*/*TAp73* ratio. Survival curves were estimated using the Kaplan- Meier method and the log- rank test was used for comparison. (F) Volcano plot comparing AML patients with low ratio with AML patients with high ratio of *TP73* isoforms. Fold change was set at 1 for upregulated and downregulated gene expression. Significance was set at corrected FDR <0.05. (G) Gene ontology (GO) and (H) gene set enrichment analysis (GSEA) on a ranked gene list based on the leading-edge genes for the ratio *ΔNp73*/*TAp73* expression in 121 de novo AML patient samples from TCGA study. Genes were ranked based on Pearson correlation with *ΔNp73*/*TAp73* expression. Normalized enrichment score (NES) and false discovery rate (FDR) was used for significance. (I) Pearson correlation between the *TP73* ratio and the global gene expression profile in AML patients followed in the TCGA cohort (J) Pearson correlation between *TP73* gene expression and the drug sensitivity against 124 drugs used in cancer therapy, using the BeatAML cohort. (K) Differential expression of TP73 isoforms in the UMCG cohort of AML patients. Gene expression is expressed as log10 values. Horizontal lines represent the median.

4.6 ΔNp73 overexpression in primary AML cells resulted in heterogeneous phenotypes

To investigate the role of ΔNp73 isoforms in the hematopoietic tissue, we decided to transduce primary $CD34^+$ cells isolated from cord blood (CB) with the *ΔNp73α*, *ΔNp73β* isoforms, and the empty vector control (Figure 9A). Cells were maintained in co-culture with stromal cells (MS-5 cells) to provide the necessary support for long-term cultures. The weekly cell count of $CD34^+$ cells overexpressing ΔNp73 isoforms indicated increased cell proliferation (Figure 9A), which was followed by an increased number of $CD34^+$ cells after 35 days in culture (Figure 9B). Additionally, we observed a trend in fewer myeloid mature cells ($CD11b^+/CD14^+$) (Figure 9C). The increased proliferation was further confirmed by overtime measurements of GFP^+ cells at day 7 and day 35 and increased colony formation after 35 days in culture (Figure 9D-F). Taken together, these results suggest that both isoforms expressed in AML patients resulted in increased cell proliferation and maintenance of CD34 expression in healthy CB $CD34^+$ cells.

To validate our findings from CB $CD34^+$ cells in primary patient samples, we opted to transduce primary AML blasts with the *ΔNp73α*, *ΔNp73β* isoforms, and the empty vector control (Figure 10A). Interestingly, while the *ΔNp73* overexpression resulted in indubitable increased proliferation in healthy $CD34^+$ cells, we observed a heterogeneous response on the cell proliferation of primary AML cells expressing *ΔNp73* measured by daily counts and GFP levels. Overall, 45% of the transduced cells presented increased cell proliferation for at least one of the transduced isoforms (Figure 10A), whereas 55% of the samples presented no differences or even a negative phenotype upon the transduction with *ΔNp73* isoforms (Figure 10B-C). In line with the daily counts for the samples where *ΔNp73* was able to increase cell proliferation, GFP levels were increased after 35 days in culture (Figure 10D). The CD11b expression (a marker of myeloid differentiation) was decreased in the ΔNp73 expressing cells in comparison with the empty vector control (Figure 10E). In general, seems that the overexpression of *ΔNp73β* results in stronger phenotypes in primary AML blasts, in comparison with the *ΔNp73α* isoform.

Figure 9. Expression of ΔNp73 isoforms in healthy CB CD34$^+$ cells resulted in increased cell proliferation and clonogenicity capacity.

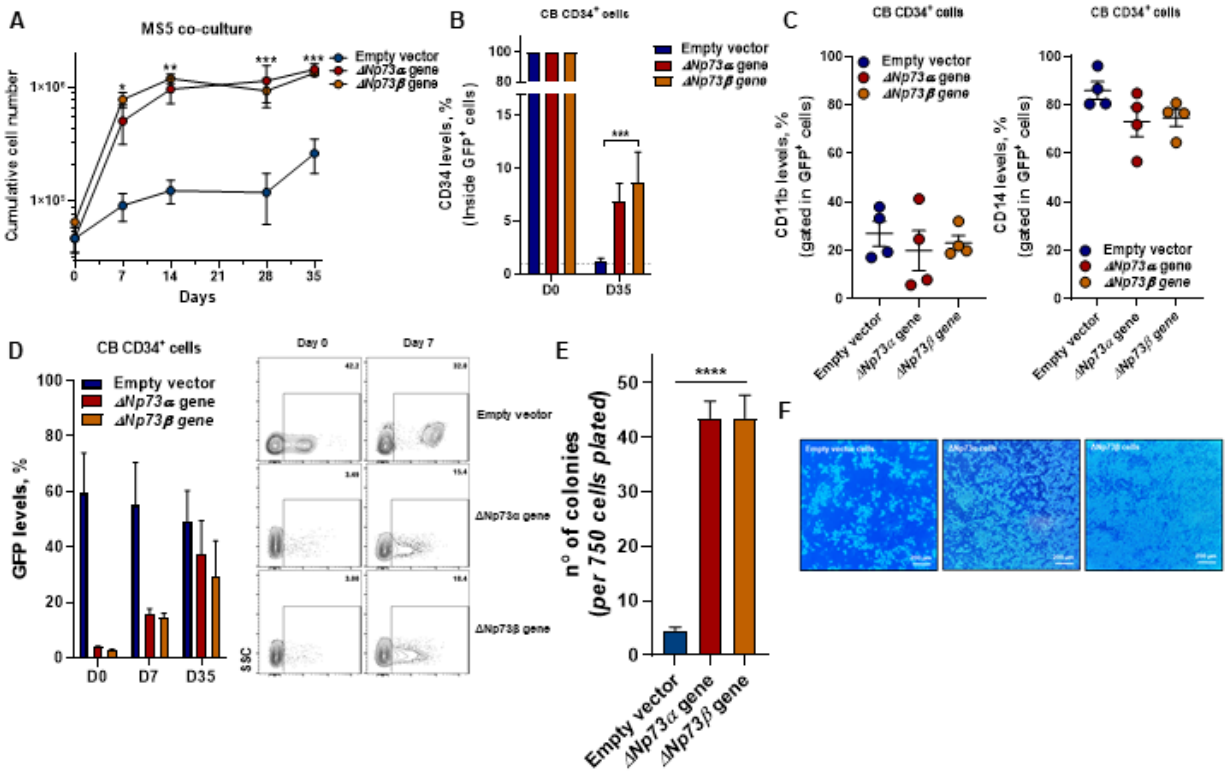

(A) Growth curves using four different CB CD34$^+$ cells, transduced with ΔNp73α/β or empty vector. (B) Surface expression of CD34 marker and (C) CD11b and CD14 markers in CB CD34$^+$ transduced cells after 35 days in culture. Horizontal lines represent the median. (D) Green fluorescent protein (GFP) levels (used as a report for clonal expansion in transduced cells) at different timepoints of culture. Results are shown as mean ± standard error mean (SEM) of, at least, 4 independent experiments. Representative Fluorescence-activated cell sorting (FACS) phenotype from a primary healthy CD34$^+$ cells transduced with the empty vector, or with the *ΔNp73α/β* gene. (E) Graphic bars represent the number of colony-forming cells in each well in CB CD34$^+$ cells transduced with ΔNp73α/β or empty vector (pMEG, control). Results are shown as mean ± standard error mean (SEM) of, at least, 4 independent experiments. (F) Snapshots of MS5 co-cultures with transduced cells at day 12 of the co-cultures.

Figure 10. Expression of *ΔNp73* isoforms in primary AML blasts resulted in different behaviors regarding the genetic/cell-component background.

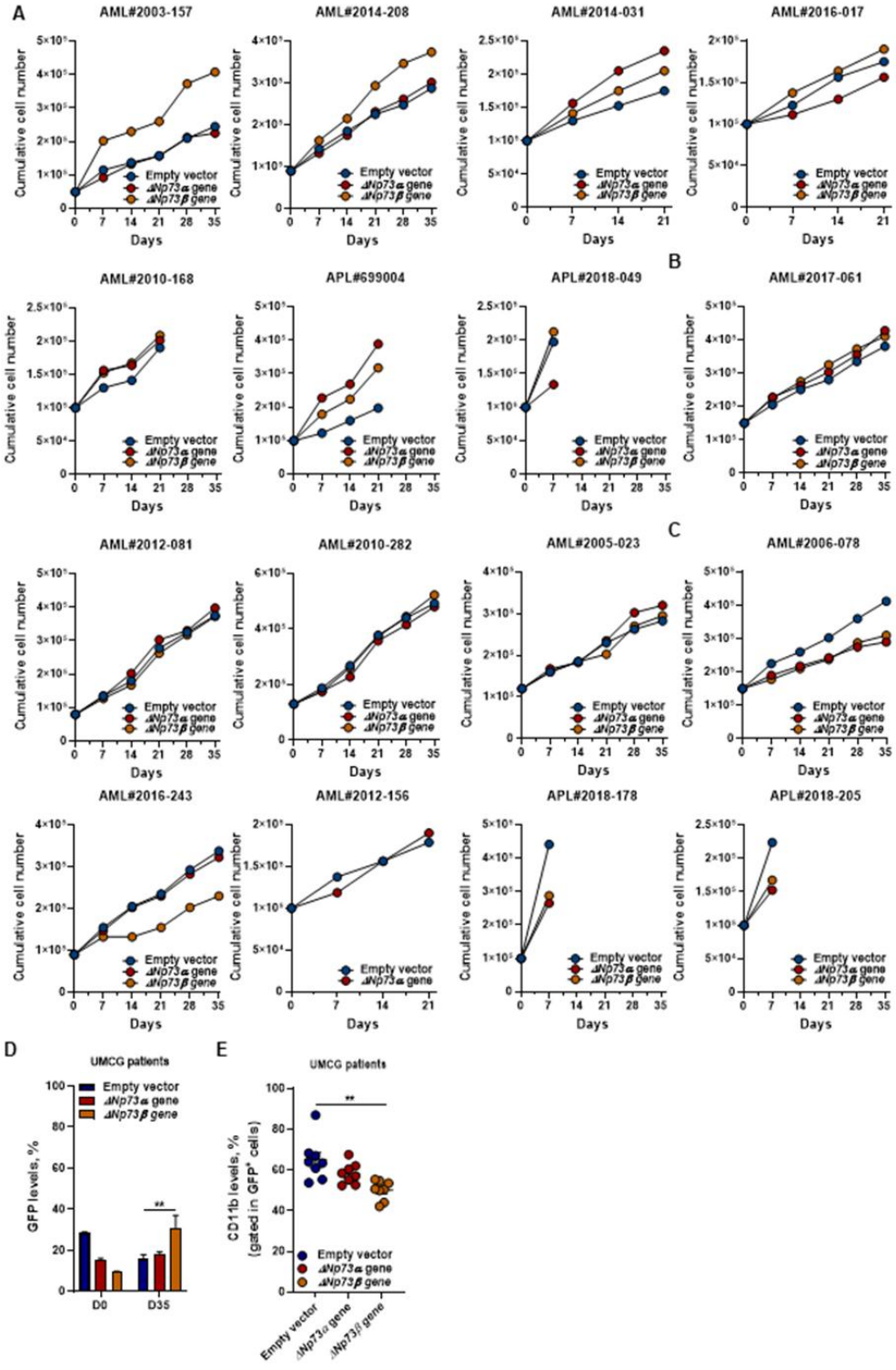

(A-C) Growth curves using sixteen different AML blasts, transduced with *ΔNp73* isoforms or empty vector. Green fluorescent protein was used as a report for clonal expansion in transduced cells. (D) Green fluorescent protein (GFP) levels (used as a report for clonal expansion in transduced cells) at different timepoints of culture (Day 0 and Day 35). Results are shown as mean ± standard error mean (SEM) of, at least, 4 independent experiments. (E) Surface expression of CD11b marker in primary AML blasts transduced after 35 days in culture. Horizontal lines represent the median. ∗∗p<0.01

4.7 AML cell lines presented increased *ΔNp73* isoforms

As a next step, we decided to evaluate the expression of *TP73* isoforms using a broad dataset of AML cell lines. In total, we screened 17 AML cell lines, of which multi-omic datasets were available at the CCLE and DepMap portal. Overall, for all the AML cell lines (n = 17), the expression of the *ΔNp73* isoforms was up regulated in comparison with the *TAp73* isoforms (Figure 11A). We also noticed that the cell line OCI-AML3 exhibited higher levels of *TAp73* isoforms in comparison with OCI-AML2 cells, being the only difference between these two cells the presence of a mutation in the NPM1 gene, detected in the OCI-AML3. For the NB4 resistant cells (to ATRA [NB4-R2] or ATO [NB4-ATOr]), we observed decreased expression of *TAp73* in comparison with the wild type one, suggesting a role for this isoform in the drug sensitivity.

Using the transcriptome from the AML cell lines available in the CCLE dataset, we observed that the high expression of *TAp73* was positively correlated with the *TP73* expression and the high *ΔNp73*/*TAp73* ratio was negatively correlated with *TP53* expression (Figure 11B). Next, we decided to correlate the expression of *ΔNp73*/*TAp73* ratio with the global gene expression data using the CCLE RNA-seq for 13 of the 17 AML cell lines. We observed that high ratio was positively correlated with *SMADs* and *COL1* expression, which are downstream targets of *ΔNp73*, and positively correlated with the expression of some genes involved in the spliceosome machinery, such as *SF3B1* and *U2AF1*, and *DHODH* (Figure 11C, upper panel). As also observed in the TCGA cohort, a low ratio was associated with increased expression of genes associated with cell cycle control and apoptosis induction, such as *TP53*, *PIG3*, *SLIT2*, and *BAX*, and with genes associated with cell differentiation, such as *PHF*/*RARa*. At the protein level, a high ratio was positively correlated with proteins involved in TP53 regulation and cell proliferation while a low ratio was correlated with proteins involved in cell cycle control (Figure 11C, lower panel). Mutational analysis revealed no association between the *ΔNp73*/*TAp73* ratio and the mutational status of *TP53* and *TP73* in the AML cell lines (Figure 11D). Since in the TCGA cohort, the mutation in genes associated with the spliceosome (*SF3B1*, *U2AF1*, and *SRSF2*) was correlated with increased *ΔNp73*/*TAp73* ratio, we decided to also look at that in the AML cell line panel, but only TF1 cells presented a mutation in the *SF3B1* gene. This data suggests that the TP73 isoforms could mimic *TP53* mutant cell biology, in a *TP53* wild-type setting.

Finally, we screened the relation between the *ΔNp73* expression alone or in a ratio with *TAp73* and the sensitivity to several chemotherapeutic agents used in AML clinics. Our analysis revealed that high *ΔNp73* levels were associated with resistance to venetoclax, ruxolitinib, and sorafenib, and increased sensitivity to Decitabine (Figure 11E, upper panel). When we looked at the

correlations with the *ΔNp73/TAp73* ratio, we could see that a high ratio was correlated with resistance to cytarabine, daunorrubicin, and venetoclax, and sensitivity to DHODH inhibitor leflunomide (Figure 11E, lower panel). This data indicates that cells with high *ΔNp73* expression may have a therapeutic vulnerability against decitabine, which could be explained by the restored levels of *TAp73* post-decitabine treatment. Moreover, since cells with a high ratio presented increased *DHODH* expression (probably linked with cell proliferative supportive function of the enzyme), these cells can be also more sensitive to DHODH inhibitors. Overall, at the RNA and protein level, a high *ΔNp73/TAp73* ratio was associated with downregulation of the TP53 signaling pathway suggesting that functionally, AML cells would display decreased drug-induced apoptosis and differentiation upon *ΔNp73* expression.

To functionally evaluate some of these correlations that we observed before, we started looking at the balance of TP73 isoforms in some biological contexts. First, we investigated the case of NB4 ATO-resistant cells. Upon ATO treatment, some APL patients can relapse the disease acquiring mutations in the PML protein, which results in reduced binding capacity for ATO, and decreased degradation of the PML-RARA protein (ALFONSO et al., 2019). In our screening, we observed that NB4 cells carrying the mutation A216T exhibited decreased expression of TAp73 in comparison with the wild-type ones. So, we decided to overexpress the *TAp73* in NB4 ATOr cells, to evaluate the sensitivity upon ATO treatment. As we can see, at 48 and 72h, the treatment with ATO alone or in combination with ATRA was successful to induce apoptosis in NB4 ATOr cells (Figure 11F). Of note, the overexpression of *TAp73* might represent a limitation in these observations (due to the non-physiological levels), so we decided to pharmacologically induce *TAp73* expression. Since 2005, a first report published by a German group described that the treatment with Azacitidine can induce in a dose-dependent way the *TP73* expression in AML cell lines (SCHMELZ et al., 2005). Further, another group demonstrated that upon decitabine therapy for 72h, Kasumi-1 cells exhibited decreased methylation in the *TP73* locus (GU et al., 2018), we hypothesized that NB4 ATOr cells would be sensitive to decitabine therapy. As we can see, NB4 ATOr cells exhibited sensitivity to decitabine, but the combination with ATO was not additive to the Decitabine monotherapy (Figure 11G). Treatment with decitabine (100 nM) for 72h was able to rescue the expression of *TAp73* in NB4 ATOr cells and OCI-AML2 cells, although it was not effective for KG1 cells (*TP53* frameshift mutant) (Figure 11H). In primary AML cells, decitabine treatment resulted in heterogeneous phenotypes regarding the rescue of *TAp73* expression (Figure 11I), which was not directly correlated with the decitabine-induced apoptosis (Figure 11J). These results point to the fact the regulation of the TP73 locus is still at large to be explored.

Figure 11. Differential TP73 isoforms content in AML cell lines reveal molecular targets related to cell cycle and apoptosis control.

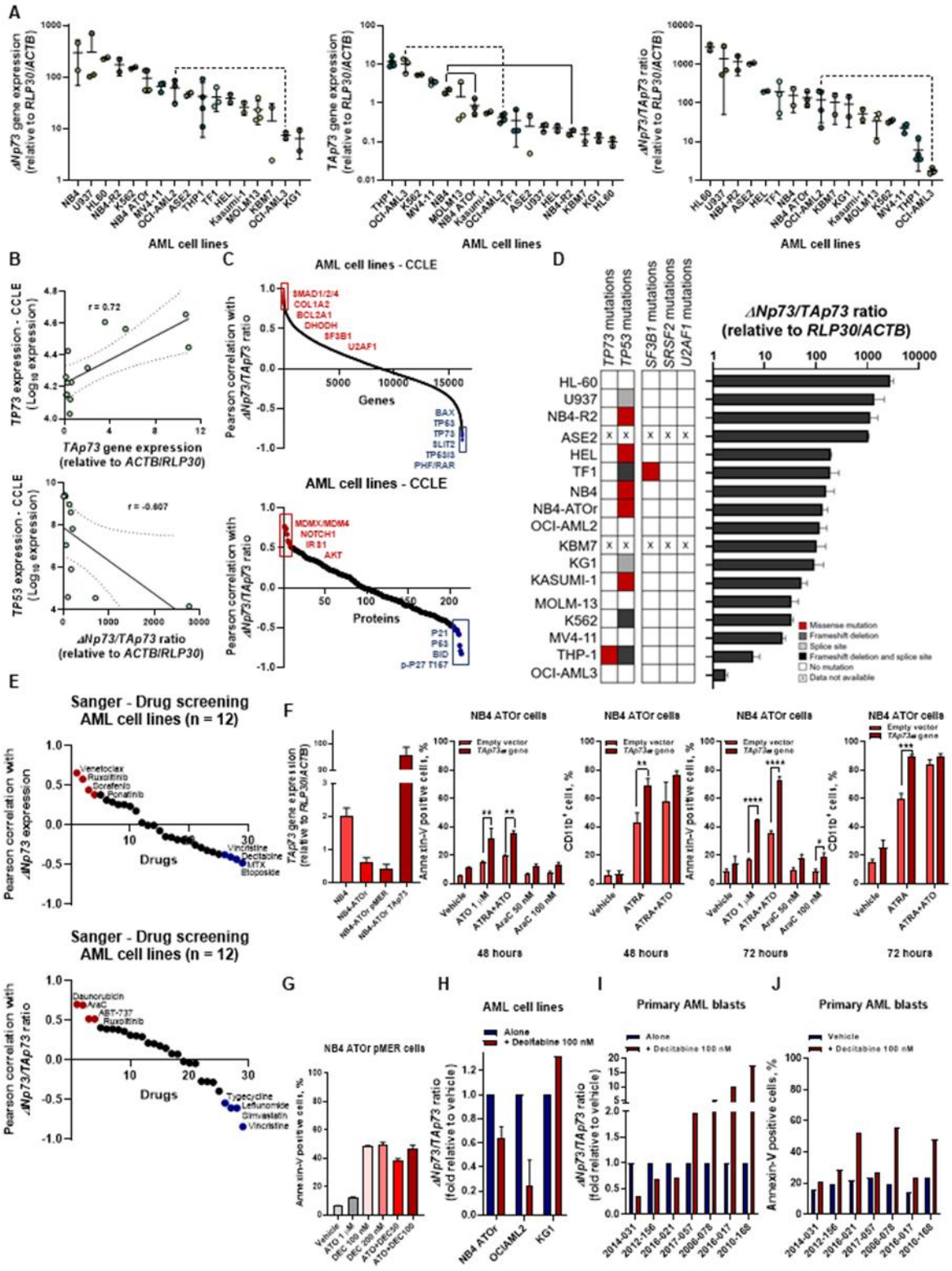

(A) The TP73 isoforms (ΔNp73 and TAp73) content were evaluated in AML cell lines (n = 17). Content is expressed as relative quantification to endogenous controls (ACTB and RLP30) values. Horizontal lines represent the median. ∗p<.05, ∗∗∗p<0.0001. (B) Pearson correlation using the *TAp73* levels evaluated by us and the *TP73* gene expression deposited in the CCLE dataset (upper panel); Pearson correlation between the ΔNp73/TAp73 ratio evaluated by us and the *TP53* gene expression deposited in the CCLE dataset (lower panel). (C) Pearson correlation using CCLE Broad Institute datasets to correlate the ΔNp73/TAp73 ratio and the positively and negatively associated genes (upper panel) and proteins (lower panel) in AML cell lines. Highlighted in red and blue are the top correlated targets (positively and negatively). (D) Mutational profile regarding *TP73* and *TP53* genes, and genes associated with the spliceosome machinery, and the ΔNp73/TAp73 ratio for all the evaluated AML cell lines. (E) Pearson correlation using Sanger Institute datasets to correlate the *ΔNp73* expression alone (upper panel) or the *ΔNp73*/*TAp73* ratio (lower panel) and the sensitivity to 30 drugs used in AML clinics. Highlighted in red and blue are the top correlated targets (positively and negatively). (F) NB4 ATOr cells were transduced with lentivirus containing the empty vector or the *TAp73* cDNA. Quantitative gene expressions of *TAp73* were analyzed in overexpressing cells relative to the EV control, respectively. Values were normalized to the expression level of housekeeping genes (*ACTB* and *RLP30*). Results are shown as mean ± standard error mean (SEM) of, at least, 4 independent experiments. Each independent experiment was performed in triplicate. Student's t-test was used for statistical analysis. Drug induced apoptosis and differentiation in transduced NB4 ATOr cells at 48 and 72h. Apoptosis was evaluated using Annexin V FITC and DAPI to distinguish the apoptotic cells; differentiation was evaluated based on the CD11b expression on the surface of the cells, by FACS. Quantitative gene expressions of *TP73* isoforms upon decitabine (100 nM) treatment in AML cell lines (G) and primary AML blasts (I). Values were normalized to the expression level of housekeeping genes (*ACTB* and *RLP30*). Results are shown as mean ± standard error mean (SEM) of, at least, 4 independent experiments. Each independent experiment was performed in triplicate. Student's t-test was used for statistical analysis. (J) Decitabine induced apoptosis in primary AML cells after 72h of exposure. Decitabine (100 nM) was replenished each day.

4.8 *ΔNp73* overexpression in AML cell lines resulted in increased cell proliferation and drug resistance, in part due to *PIM2* expression

With these results, we were interested to evaluate how does the expression of TP73 isoforms modulate AML cell proliferation and survival. To perform this screening, we used a set of 6 AML cell lines (Four *TP53* wild-type cells and two *TP53* mutant cells), where we overexpressed both *ΔNp73α*/β isoforms. As we can see, the *ΔNp73* overexpression resulted in increased cell proliferation in the *TP53* wild-type cell lines (Figure 12A-D, first panel). To investigate how the *ΔNp73* overexpression could promote resistance to drug-induced apoptosis, we treated the AML cell lines with different cytotoxic drugs for 72h and evaluated the cell death using Annexin-V staining. As we can see, the treatment with cytarabine for OCI-AML3 and HL-60 cells, and the treatment with quizartinib and midostaurin in MOLM-13 and MV4-11 cells, was less effective in ΔNp73-transduced AML cell lines, in comparison with the empty vector control (Figure 12A-D, second panel). Since it is well established the role of PIM kinases as modulators of AML drug resistance, we decided to investigate if ΔNp73 cells could up-regulate PIM2 upon cytotoxic therapy. As we can see, the ΔNp73 AML cell lines were able to up-regulate *PIM2* expression upon cytarabine treatment, suggesting that *PIM2* up-regulation could be one of many mechanisms for drug resistance in the context of ΔNp73 (Figure 12A-D, third panel). Additionally, *ΔNp73* expressing cells presented decreased levels of *LRP6*, a downstream target of *TAp73* (Figure 12A-D, Last panel).

Next, since the refractoriness to the main FLT3-inhibitors (ROSENBERG et al., 2020; ZHANG et al., 2019) in AML patients has been associated with loss-of-function mutations in *TP53* and *KRAS*, we evaluated if the ΔNp73 overexpression would mimic this phenotype due to downregulation of *TP53* expression or via an independent role of ΔNp73 per se. To do so, we transduced MOLM13 and MV4-11 cells with a pLKO-shP53-mCherry vector, and after sorting the $mCherry^+$ cells (with decreased *TP53* levels) we transduced these cells with the different ΔNp73 isoforms (GFP^+ cells) and sorted the double-positive population ($GFP^+mCherry^+$) to perform the experiments. Interestingly, the knockdown of *TP53* was able to abrogate the effects observed upon *ΔNp73* overexpression, regarding the drug-induced apoptosis with FLT3-inhibitors, as well as cytarabine and venetoclax (Figure 12E). In accordance with these observations, the *ΔNp73* overexpression in *TP53* mutant AML cell lines (TF1 and KG1) resulted in no differences regarding cell proliferation and drug-induced apoptosis (Figure 12F-G). Together, this data suggests that at least in AML cells, the effects of ΔNp73 isoforms seem to be related to the downregulation of the TP53 pathway.

Figure 12. Differential TP73 isoforms content in AML cell lines reveal molecular targets related to cell cycle and apoptosis control.

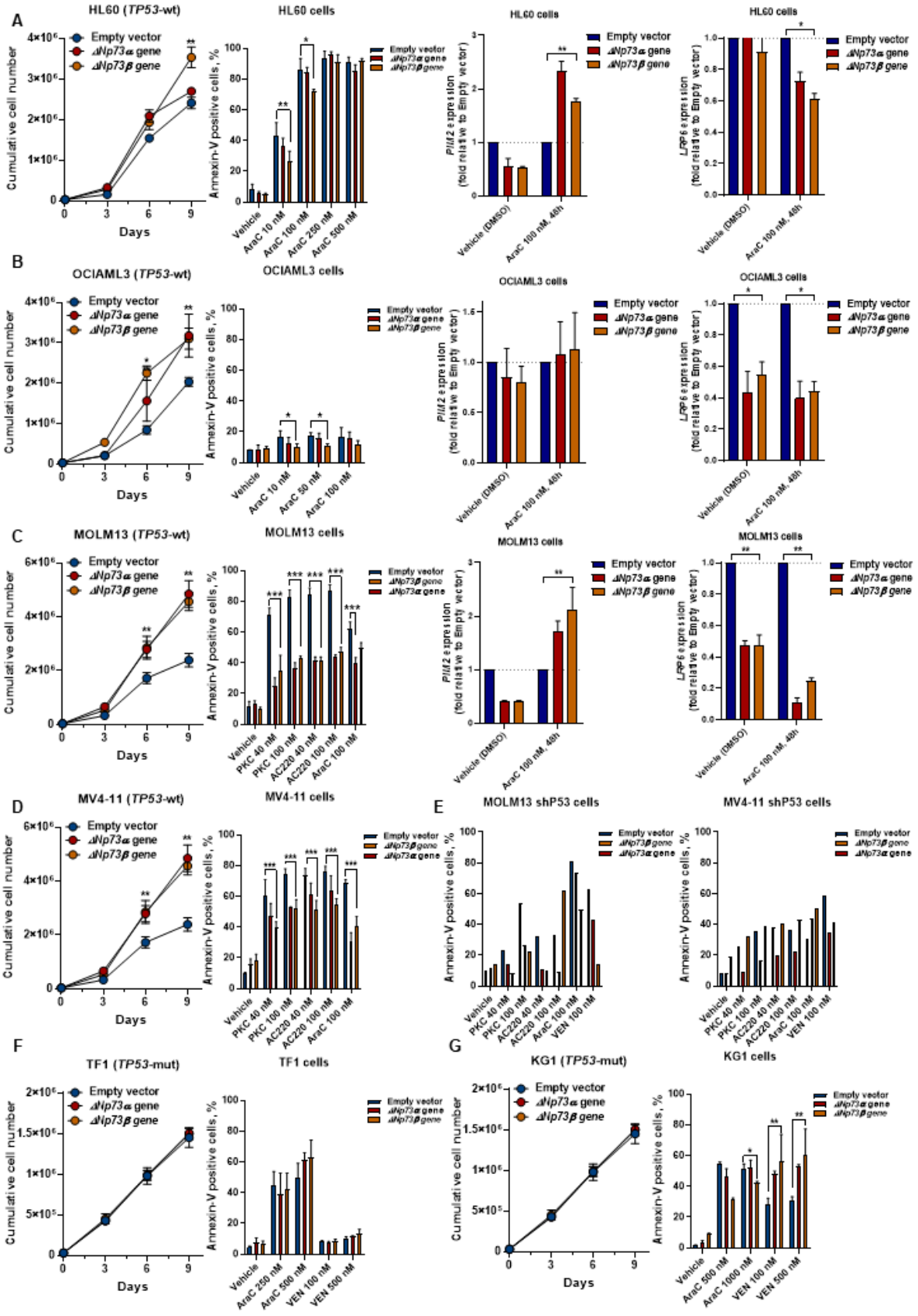

Growth curves (First panel), drug induced apoptosis after 72h of treatment (second panel) and quantitative gene expressions of *PIM2* (Third panel) and *LRP6* (fourth panel) were analyzed in ΔNp73 overexpressing HL60 (A), OCI-AML3 (B), MOLM13 (C) and MV4-11 (D) cells relative to the EV control. Apoptosis was evaluated using Annexin V APC and DAPI to distinguish the apoptotic cells, by FACS. Gene expression values were normalized to the expression level of housekeeping genes (*ACTB* and *RLP30*). Results are shown as mean ± standard error mean (SEM) of, at least, 4 independent experiments. Each independent experiment was performed in triplicate. Student's t-test was used for statistical analysis. (E) Drug-induced apoptosis in MOLM13 and MV4-11 cells transduced with pLKO-shTP53-mCherry and overexpressing the different ΔNp73 isoforms. Analysis was performed after 72h of treatment. Growth curves (First panel) and drug induced apoptosis after 72h of treatment (second panel) in TF1 (F) and KG1 (G) AML cell lines (TP53 mutant).

4.9 ΔNp73 overexpression in AML cell lines resulted in reduced ATRA-induced myeloid differentiation

Finally, we investigated whether ΔNp73 overexpression in AML cell lines would result in decreased sensitivity to ATRA-induced myeloid differentiation (since we demonstrated previously that overexpression of *ΔNp73* in NB4 cells resulted in decreased response to ATRA). As we can see, the ATRA treatment was less effective to induce myeloid differentiation in ΔNp73 cells in comparison to empty vector control (Figure 13A-C, first two panels). Among the down-regulated targets in patients with a high *ΔNp73*/*TAp73* ratio, the *PHF8* gene is an interesting one since upon ATRA treatment, the increased expression of *PHF8* results in the recruitment of additional histone modification enzymes and RNA pol II to drive differentiation (HEUSER et al., 2007; PEREIRA-MARTINS et al., 2021). In addition to that, a previous publication demonstrated that *ΔNp73* expressing AML cells exhibited increased levels of *NANOG* (VOELTZEL et al., 2018), suggesting a more immature state for those cells. In our dataset of AML cells, we observed that at basal levels, ΔNp73-transduced AML cell lines exhibit lower *PHF8* levels than the empty vector control, which remains decreased even upon ATRA treatment. Regarding *NANOG* expression, at baseline conditions, AML cell lines overexpressing ΔNp73 exhibited similar levels as the empty vector control. Interestingly, upon ATRA treatment for 72h, cells transduced with *ΔNp73* displayed increased expression of *NANOG*, in comparison with the empty vector control (Figure 13A-C, last two panels). Finally, as observed regarding the cell proliferation and resistance to drug-induced apoptosis, the *ΔNp73* overexpression resulted in no differences regarding drug-induced differentiation in *TP53* mutant AML cells (Figure 13D). These results support the idea that at least in AML cells, *ΔNp73* may act as a downregulating factor for the activation of the TP53 signaling pathway.

Figure 13. ΔNp73 overexpression in AML cell lines resulted in reduced ATRA-induced myeloid differentiation.

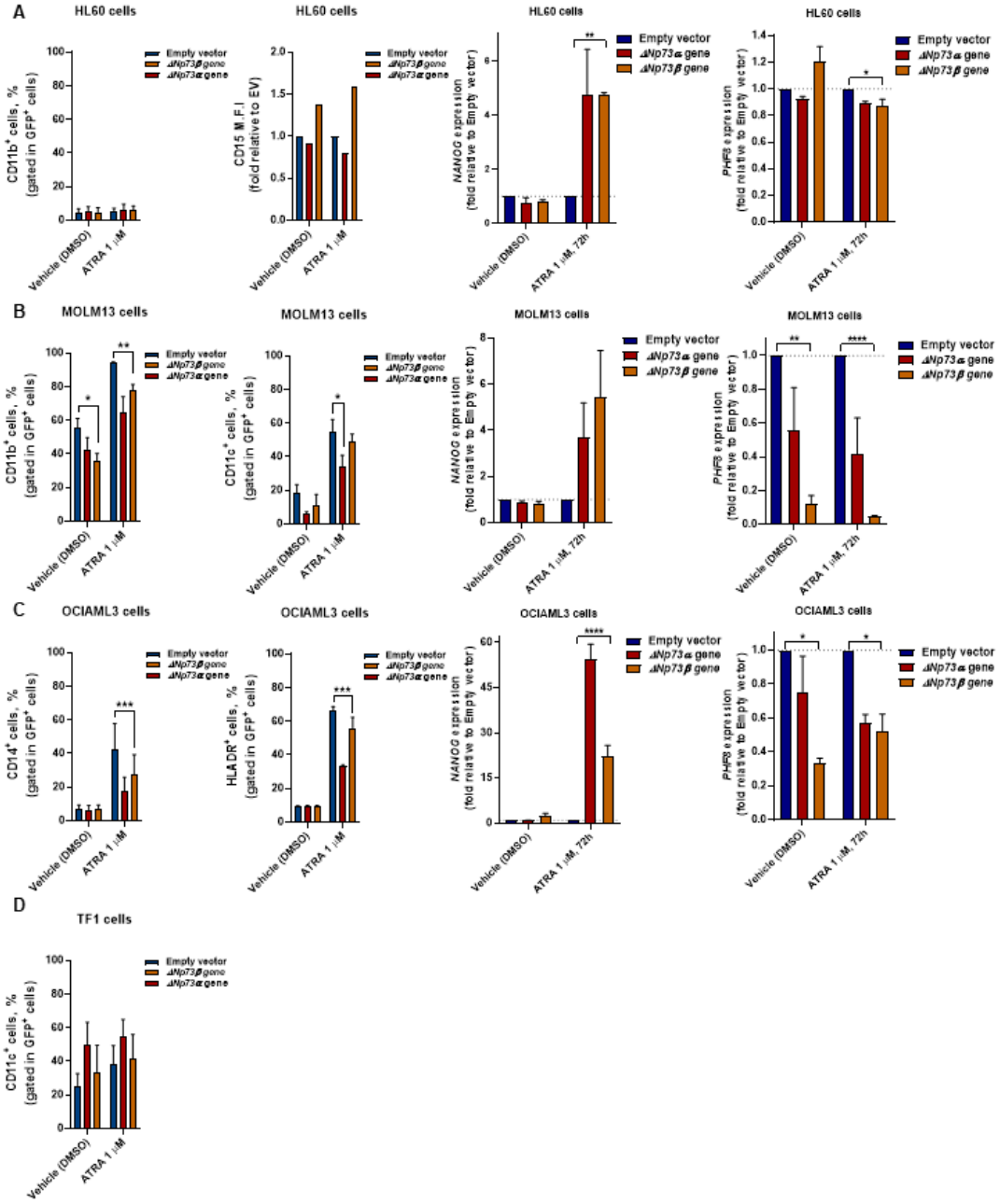

Percentage of $CD11b^+$, $CD11c^+$, $CD14^+$, $CD15^+$ and $HLA\text{-}DR^+$ in AML cell lines – HL60 (A), MOLM13 (B), OCI-AML3 (C) and TF1 (D) infected with empty vector or pMEG-ΔNp73 lentiviruses after 72 (right panel) hours of ATRA (1 μM) treatment used as the standard stimulus for differentiation (First two panels). Gene expression analysis of *NANOG* and *PHF8* in AML cell lines transduced with pMEG-ΔNp73 and empty vector controls upon ATRA treatment (1 μM). The gene expression was quantified by Real-time quantitative PCR (RQ-PCR) using *RLP30* and *ACTB* as endogenous control. Note: Data from continuous variable were all expressed as mean ± standard error of the mean. * Indicates $P < 0.05$. *** indicates $P < 0.001$. NS indicates not significant.

Discussion

5 DISCUSSION

According to our literature review, our study provided one of the first xenograft model that satisfactorily promoted engraftment of transduced human APL samples in xenotransplantation models (PEREIRA-MARTINS et al., 2021). Our data demonstrate a role of the *ΔNp73* gene in the APL cell proliferation *in vitro* and *in vivo*, with decreased response to the main differentiating agents used in clinical practice to treat APL and AML patients in general (DÖHNER et al., 2017). Although we previously associated high *ΔNp73* expression with increased resistance to drug-induced apoptosis, this work investigated these effects in transformed leukemic cells, and not cells containing only the PML-RARα translocation (LUCENA-ARAUJO et al., 2017b), opening new questions regarding the importance of the ΔNp73α in the context of the disease itself.

It is important to highlight that the present work presents some critical technical points that could impair some of the observations, such as: 1) the reduced number of animals used in the xenotransplantation experiment in each group (10 animals in total per group, being 2 animals per patient sample), 2) the non-preconditioning of the animals using sub-lethal irradiation to favor the engraftment of APL cells and 3) the murine model used in the experiment (NSGS), which present a constitutive secretion of cytokines at levels much higher than those found in the normal human BM (20 times higher in NSGS animals). Additionally, we noticed that the mice used for PDX experiments using APL samples usually displayed superior levels of engraftment in the bone marrow, in earlier time-points (around week 3), which also highlights the necessity of monitoring the engraftment levels using BM samples, as a more reliable source for evaluation. Of note, APL patients usually display lower levels of blast counts in the PB, which can be one of the reasons why we do not detect these cells in the PB of the transplanted mice, although the biological reasons for that observation are still at large to be explored.

Due to several logistic reasons, we unfortunately were unable to pre-condition the recipient mice before the transplant. Thus, we decided to test whether transplantation without preconditioning could be a way out, and our data showed that it is possible to perform xenotransplantation without previously conditioning the mice. Other studies showed similar results for other types of AML and MPN/SMD PDX models (PACZULLA et al., 2017; RAU, 2017; WUNDERLICH; MULLOY, 2016) in which the authors did not show differences between the levels of engraftment with or without preconditioning with sublethal irradiation. But additional experiments comparing side-by-side the conditions would be necessary to

further confirm these observations. We evaluated whether conditioning with the cytotoxic drug Busulfan (50 mg/kg; widely used in clinical settings – (CIUREA; ANDERSSON, 2009) in combination with cyclophosphamide (25 mg/kg) could be a strategy to overcome the fragility of our SGM3 animals to X-radiation. Our data demonstrated no significant improvement in engraftment levels comparing Busulfan versus non-preconditioning (data not shown). Finally, regarding the third point, we intend to use two different xenotransplantation systems (one containing scaffolds filled with human mesenchymal stromal cells and the other using genetically modified animals - MISTRG (RONGVAUX et al., 2014; WUNDERLICH; MULLOY, 2016) – which display similar levels of human cytokines to those found in normal human BM) in collaboration with the laboratory of Prof. Schuringa (UMCG – Groningen/NL).

Finally, we believe that it is imperative to evaluate the mutational and expression status of the *TP53* gene as well as for the *TP73* per se, for a better understanding of the real effect of ΔNp73 isoforms on transduced APL cells. To do so, we plan to carry out the global genome sequencing of the samples used in the xenotransplantation experiments at three different points: 1) at diagnosis, 2) after transduction (as control of non-alterations upon lentiviral insertion) with the constructs, and 3) at the endpoint of the experiment (with the sorted cells based on the expression of GFP, human CD45, and CD33).

Overall, regarding our evaluation in the APL context, our data suggest that the presence of ΔNp73α in APL cells favored an increased cell proliferation capacity, which directly affects resistance to treatment with cytotoxic drugs, associated to a lower responsiveness to drug- induced cell differentiation. These findings are important, as the induction of apoptosis and cellular differentiation of leukemic blast cells are the main pillars for the treatment in APL (ABLAIN et al., 2014). Thus, understanding how ΔNp73 isoforms can modulate cellular outcomes in response to these processes is of great importance in the hematology field, regarding the development of new therapeutic approaches.

Evaluating the functional role of TAp73 in APL cells, we showed its antagonistic role in comparison to the observed phenotypes upon ΔNp73 overexpression in APL models. These findings motivate us to study how the insertion of both isoforms (considering the ratio ΔNp73/TAp73) into APL and AML cells can functionally modulate the balance between apoptosis and differentiation, contributing to a more aggressive disease phenotype. In this regard, we evaluated the expression of the TP73 isoforms using a broad panel of AML cell lines, harboring different genetic alterations and molecular signatures, included in the CCLE dataset (PEREIRA-MARTINS et al., 2021; WEINHÄUSER et al., 2020). Our results

demonstrated that overall, in AML cells, the expression of the ΔNp73 is superior to the TAp73, suggesting a ratio towards a high ΔNp73/TAp73 setting, and the high ratio is correlated with downregulation of the TP53 downstream signaling pathway. Altogether, this data suggests that in AML, the role of ΔNp73 is more as an antagonist of TP53/TAp73, than as a gain-of-function effect observed in solid tumors (STEDER et al., 2013).

Evaluating the role of *TP73* isoforms in healthy HSPCs ($CD34^+$ cells isolated from cord blood), we were able to demonstrate that high *ΔNp73* expression resulted in increased cell proliferation and survival. Furthermore, *ΔNp73* overexpression resulted in increased levels of CD34 expression, which resulted also in increased clonogenic capacity. Together, these results suggested a role for the TP73 isoforms in the regulation of malignant transformation and leukemia. Further studies will be necessary to address the role of ΔNp73 isoforms in combination with different oncogenes that are not able to promote malignant transformation alone, such as the PML-RARA and the FLT3-ITD (MATSUSHITA et al., 2014; REGO et al., 2006; ZHANG et al., 2019), to identify possible additive effects regarding cell transformation capacity. Additionally, we observed that overexpression of ΔNp73 isoform beta, but not the alpha one, resulted in increased cell proliferation and decreased myeloid differentiation in primary AML blasts, cultured *ex vivo*. These results point to the high heterogeneity observed in AML samples, which often displayed a broad genetic background that in combination with TP73 isoforms, can result in different phenotypes. Additionally, further studies to investigate the role of TP73 isoforms in AML samples in vivo would be necessary to clarify some of the conclusions.

Here, we were also able to demonstrate that patients with AML as well as most of the AML cell lines presented increased levels of ΔNp73 isoforms. In AML patients, high ΔNp73/TAp73 ratio was correlated with increased leukocyte counts and had a trend to be associated with poor clinical outcomes. We and others (LUCENA-ARAUJO et al., 2015; VOELTZEL et al., 2018), demonstrated that AML patients, different than healthy $CD34^+$ cells, displayed high levels of ΔNp73, in comparison with TAp73 expression, suggesting a high ΔNp73/TAp73 ratio in AML. But the role of the ΔNp73/TAp73 ratio as a marker of clinical outcomes in AML, still not well established, and additional cohorts will need to be evaluated, to improve these observations. Mechanistically, a transcriptomic analysis comparing AML patients with high versus low ΔNp73/TAp73 ratio, associated a high ratio with an LSC-like transcriptional program, while a low ratio was correlated with a progenitor-like signature. It is well known that AMLs with a more stem-like signature (LSC/HSC-like leukemias) are associated with poor clinical outcomes (CHAO et al., 2010; NG et al., 2016;

VAN GALEN et al., 2019). Therefore, the association between high ΔNp73/TAp73 ratio and the clinical outcomes in AML patients could be possibly linked to differences in their cell-of-origin and metabolic state. We also noticed that patients with a high ΔNp73/TAp73 ratio were often harboring mutations in genes associated with the spliceosome machinery, which are often altered in AML patients, such as the *SF3B1*, *SRSF2*, and *U2AF1* (DÖHNER et al., 2017; PAPAEMMANUIL et al., 2016). The ΔNp73 isoforms are often generated by initiated transcription in a second promoter region, and not by differential splicing mechanisms, therefore, additional studies will be necessary to explain the functional mechanisms associated with this observation.

This observation provided us the opportunity to use the AML cell lines as models to evaluate the functional consequences of ΔNp73 overexpression. As observed in APL models, the increased expression of ΔNp73 in AML cells resulted in increased cell proliferation and survival. Interestingly, we were able to show that the phenotypes observed upon ΔNp73 expression, most likely rely on the downregulation of the TP53 pathway. Overexpression of ΔNp73 in AML cell lines harboring mutations in *TP53* or with reduced expression of *TP53* transcripts (induced by lentiviral mediated knockdown of the gene), resulted in non-significative changes in the cell proliferation and survival phenotypes, reinforcing our previous conclusions about ΔNp73 acting as an antagonist of the TP53 pathway.

As an alternative to the genetic models, we demonstrated that treatment with decitabine was able to induce the TAp73 expression, resulting in decreased ratio ΔNp73/TAp73 in AML cell lines with *TP53* wild type. These observations might represent a therapeutic opportunity for the combination between decitabine and the commonly used drugs in AML patients. Additionally, we also observed that AML cells with high *ΔNp73* expression presented increased levels of *DHODH*, which might represent a potential target to treat patients with high *ΔNp73* expression. Our results demonstrated that the use of AML cell lines as models of primary AML patients is suitable to help to understand the role of TP73 isoforms in AML. We also demonstrated that as observed in APL, the ΔNp73 overexpression resulted in decreased drug-induced differentiation, associated with increased expression of *NANOG* and decreased expression of *PHF8*, which is a marker of responsiveness to ATRA efficacy in APL models (PEREIRA-MARTINS et al., 2021). A previous report demonstrated that ΔNp73 is associated with increased *BMRP1* and *NANOG* expression in AML cells (VOELTZEL et al., 2018), although the direct correlation between *NANOG* expression and response to ATRA was not yet studied until now.

To complete these studies, we will perform a ChIP-seq associated with a protein pull-out to evaluate the molecular consequences of the high ΔNp73/TAp73 ratio in AML/APL. Evaluating the chromatin accessibility and the protein interactome in AML/APL cells overexpressing the ΔNp73 isoforms. Secondly, we would like to address the effects of ΔNp73 overexpression on normal HSPCs in vitro (in combination with other genetic alterations, such as the PML-RARα, MLL-AF9, FLT3-ITD mutations, and NPM1 mutations).

Conclusion

6 CONCLUSION

Taking into account our results we can draw the following conclusions:

- In AML and APL patients, regarding the expression of TP73 isoforms:

  - The expression of ΔNp73 isoforms was significantly higher than the TAp73 isoforms, which was not the case in heatlhy $CD34^+$ cells;
  - Patients with increased ΔNp73/TAp73 ratio displayed poor clinical outcomes and were associated with the terms *LSC-UP* and *HSC-UP*;
  - The ΔNp73/TAp73 ratio correlated negatively with the expression of TP53 and its target genes.

- In AML/APL cell lines and primary samples, as well as using the shTP53 models, the overexpression of TP73 isoforms: ΔNp73α/β and TAp73α promoted:

  - Increased cell proliferation and colony formation capacity (ΔNp73), being the isoform ΔNp73β superior in the phenotypes observed;
  - Reduction of drug-induced apoptosis and granulocytic differentiation capacity in response to treatment with the main drugs used in the clinical context of AML/APL (ΔNp73), by up-regulation of pro-survival genes like *NANOG*, *PIM2* and *DHODH*, with downregulation of *PHF8* gene, associated with response to ATRA;
  - Reduction of cell proliferation and colony formation capacity (TAp73α);
  - Increase in drug-induced apoptosis and granulocytic differentiation capacity in response to treatment with the main drugs used in the clinical context of APL (TAp73α);
  - Restored the sensitivity to ATO in an ATO-resistant APL model (TAp73α);
  - In the context of mutated *TP53* or its reduced expression (using shTP53 strategies), no pro-survival phenotype was observed in the context of ΔNp73 overexpression.

- In primary cells isolated from APL patients transduced with ΔNp73α and xenotransplanted into NSGS mice, it was possible to observe:

- Presence of ΔNp73α cells in the peripheral blood of NSGS animals 4 weeks after transplantation at higher levels than cells transduced with the empty vector (control);
- Leukocytosis and thrombocytopenia in animals transplanted with primary blasts transduced with ΔNp73α compared to animals transplanted with blasts transduced with the empty vector;
- Superior engraftment of APL blasts in the BM, spleen, liver and peripheral blood of animals transplanted with ΔNp73α cells than that found in animals transplanted with blasts transduced with the empty vector, with detectable levels of PML-RARα transcripts in the peripheral blood of the ΔNp73α animals.

Tables

7 TABLES

Table 1. Clinical characteristics of AML patients included

Characteristics		All patients (n=88)		
		No.	**%**	**Median (range)**
Gender				
	Female	43	54.4	
	Male	36	45.6	
	Unknown	9	-	
Age, years				60.7 (21, 86)
	18-40	10	14.5	
	41-60	22	31.9	
	≥60	37	53.6	
	Unknown	19	-	
Leukocyte counts, $\times 10^9$/L				61.4 (1.5, 335.6)
Platelet counts, $\times 10^9$/L				41.5 (2, 281)
Hemoglobin, g/dL				5.8 (3.2, 11.4)
Bone marrow blasts, %				76 (3, 99)
Lactate dehydrogenase, U/dL				655.5 (197, 4632)
FAB classification				
	M1	18	32.1	
	M2	5	8.9	
	M3	17	30.4	
	M4	7	12.5	
	M5	9	16.1	
	Unknown	32	-	
ELN2017 risk stratification				
	Favorable	15	24.2	
	Intermediate	32	51.6	
	Adverse	15	24.2	
	Unknown	26	-	
FLT3 mutational status				
	Non-mutant	35	57.4	
	ITD/TKD mutant	25	42.6	
	Missing	26	-	
HSCT status				
	Yes	39	66.1	
	No	20	33.9	
	Unknown	29	-	

Characteristics		All patients (n=88)		
		No.	**%**	**Median (range)**
Treatment scheme				
	Intensive chemotherapy (3+7)	48	76.2	
	Hypomethylating agents	12	19	
	Best supportive care	3	4.8	
	Unknown	25	-	
Treatment response				
	CHR	42	72.4	
	CRi	7	12.1	
	No response/refractory	9	15.5	
	Unknown	30	-	
Relapse status				
	Relapse	15	25	
	Non-relapse	45	75	
	Unknown	28	-	
Survival status				
	Dead	48	70.6	
	Alive	20	29.4	
	Unknown	20	-	

FAB, French-American-British classification; ELN, European Leukemia-Net; *FLT3*, Fms Related Receptor Tyrosine Kinase 3 gene; ITD, Internal tandem duplication; TKD, Tyrosine kinase domain; HSCT, Hematopoietic stem cell transplant; CHR, Complete hematological remission; CRi, Incomplete remission

Table 2. APL samples used in the PDX models

Table 1. Xenograft samples after first transplantation						
Patient no.	**Vectors**	***PML-RARα*⁺ expression (7^{th} week)**	**Bcr (7^{th} week)**	**hu*ΔNp73α* expression (7^{th} week)**	**Time of evaluation (week)**	**%hCD45⁺/GFP⁺**
#1	Empty vector (pMEG)	-	-	-	**5**/10/**15**	**0.23**/5.41/**1.27**
#2	Empty vector (pMEG)	Positive	Bcr1	Yes	**5**/10/**15**	**1.59**/6.02/**0.84**
#3	Empty vector (pMEG)	Positive	Bcr3	Yes	**5**/10/**15**	**0.46**/5.14/**0.64**
#4	Empty vector (pMEG)	-	-	-	**5**/10/**15**	**0.38**/8.88/**0.39**
#5	Empty vector (pMEG)	-	-	-	**5**/10/**15**	**0.51**/4.83/**1.05**
#1	pMEG-ΔNp73α	Positive	Bcr3	Yes	**5**/10/**15**	**4.56**/13.6/**1.16**
#2	pMEG-ΔNp73α	Positive	Bcr1	Yes (5x)	**5**/10/**15**	**1.92**/8.37/**3.02**
#3	pMEG-ΔNp73α	Positive	Bcr3	Yes (equal)	**5**/10/**15**	**3.27**/11.4/**1.07**
#4	pMEG-ΔNp73α	Positive	Bcr3	Yes	**5**/10/**15**	**0.97**/9.17/**1.06**
#5	pMEG-ΔNp73α	Positive	Bcr1	Yes	**5**/10/**15**	**0.95**/11.1/**5.56**

References

8 REFERENCES

ABARRATEGI, Ander; FOSTER, Katie; HAMILTON, Ashley; MIAN, Syed A.; PASSARO, Diana; GRIBBEN, John; MUFTI, Ghulam; BONNET, Dominique. Versatile humanized niche model enables study of normal and malignant human hematopoiesis. **Journal of Clinical Investigation**, *[S. l.]*, v. 127, n. 2, p. 543–548, 2017. DOI: 10.1172/JCI89364.

ABLAIN, Julien; RICE, Kim; SOILIHI, Hassane; DE REYNIES, Aurélien; MINUCCI, Saverio; DE THÉ, Hugues. Activation of a promyelocytic leukemia-tumor protein 53 axis underlies acute promyelocytic leukemia cure. **Nature Medicine**, *[S. l.]*, v. 20, n. 2, p. 167–174, 2014. DOI: 10.1038/nm.3441.

ADOLFSSON, Jörgen et al. Identification of Flt3+ lympho-myeloid stem cells lacking erythro-megakaryocytic potential: A revised road map for adult blood lineage commitment. **Cell**, *[S. l.]*, v. 121, n. 2, p. 295–306, 2005. DOI: 10.1016/j.cell.2005.02.013.

ADOLFSSON, Jörgen; BORGE, Ole Johan; BRYDER, David; THEILGAARD-MÖNCH, Kim; ÅSTRAND-GRUNDSTRÖM, Ingbritt; SITNICKA, Ewa; SASAKI, Yutaka; JACOBSEN, Sten E. W. Upregulation of Flt3 expression within the bone marrow Lin- Sca1+c-kit+ stem cell compartment is accompanied by loss of self-renewal capacity. **Immunity**, *[S. l.]*, v. 15, n. 4, p. 659–669, 2001. DOI: 10.1016/S1074-7613(01)00220-5.

AKASHI K; TRAVER D; MIYAMOTO T; IL, Weissman. A clonogenic common myeloid progenitor that gives rise to all myeloid lineages. **Nature**, *[S. l.]*, v. 404, n. 6774, p. 193–197, 2000.

ALFONSO, V. et al. Early and sensitive detection of PML-A216V mutation by droplet digital PCR in ATO-resistant acute promyelocytic leukemia. **Leukemia**, *[S. l.]*, v. 33, n. 6, p. 1527–1530, 2019. DOI: 10.1038/s41375-018-0298-3. Disponível em: http://dx.doi.org/10.1038/s41375-018-0298-3.

AMODEO, Valeria et al. A PML/Slit Axis Controls Physiological Cell Migration and Cancer Invasion in the CNS. **Cell Reports**, *[S. l.]*, v. 20, n. 2, p. 411–426, 2017. DOI: 10.1016/j.celrep.2017.06.047. Disponível em: http://dx.doi.org/10.1016/j.celrep.2017.06.047.

ANA CUMANO; FRANCOISE DIETERIAN-LIEVRE; ISABELLE GODIN. Lymphoid Potential, Probed before Circulation in Mouse, Is Restricted to Caudal Intraembryonic Splanchnopleura. **Cell**, *[S. l.]*, v. 86, p. 907–916, 1996. Disponível em: http://ac.els-cdn.com/S009286740080166X/1-s2.0-S009286740080166X-main.pdf?_tid=97a5d510-7d49-11e7-92bf-00000aacb362&acdnat=1502314249_f55a839e9bc65ebb1efad0d5c1f60608.

ANTONELLI, Antonella et al. **Establishing human leukemia xenograft mouse models by implanting human bone marrow-like scaffold-based niches**. [s.l: s.n.]. v. 128 DOI: 10.1182/blood-2016-05-719021.

BAGGER, Frederik Otzen; KINALIS, Savvas; RAPIN, Nicolas. BloodSpot: A database of healthy and malignant haematopoiesis updated with purified and single cell mRNA sequencing profiles. **Nucleic Acids Research**, *[S. l.]*, v. 47, n. D1, p. D881–D885, 2019. DOI: 10.1093/nar/gky1076.

BARABÉ, Frédéric; KENNEDY, James A.; HOPE, Kristin J.; DICK, John E. Modeling the initiation and progression of human acute leukemia in mice. **Science**, *[S. l.]*, v. 316, n. 5824, p. 600–604, 2007. DOI: 10.1126/science.1139851.

BENNETT, J. M.; CATOVSKY, D.; DANIEL, Marie- Theregse - T; FLANDRIN, G.; GALTON, D. A. G.; GRALNICK, H. R.; SULTAN, C. Proposals for the Classification of the Acute Leukaemias French- American- British (FAB) Co- operative Group. **British Journal of Haematology**, *[S. l.]*, v. 33, n. 4, p. 451–458, 1976. DOI: 10.1111/j.1365-2141.1976.tb03563.x.

BERNARDI, Rosa; SCAGLIONI, Pier Paolo; BERGMANN, Stephan; HORN, Henning F.; VOUSDEN, Karen H.; PANDOLFI, Pier Paolo. PML regulates p53 stability by sequestering Mdm2 to the nucleolus. **Nature Cell Biology**, *[S. l.]*, v. 6, n. 7, p. 665–672, 2004. DOI: 10.1038/ncb1147.

BEZERRA, M. F. et al. Co-occurrence of DNMT3A, NPM1, FLT3 mutations identifies a subset of acute myeloid leukemia with adverse prognosis. **Blood**, *[S. l.]*, v. 135, n. 11, 2020. DOI: 10.1182/blood.2019003339.

BIOLOGY, Leukocyte. Particular TP73-DAPK2-ATG5 autophagy and cell death pathways in response to APL therapy Magali Humbert. *[S. l.]*, v. 924, 2016.

BOLTON, Kelly L. et al. Cancer therapy shapes the fitness landscape of clonal hematopoiesis. **Nature Genetics**, *[S. l.]*, v. 52, n. 11, p. 1219–1226, 2020. DOI: 10.1038/s41588-020-00710-0. Disponível em: http://dx.doi.org/10.1038/s41588-020-00710-0.

BOYAPATI, Anita; KANBE, Eiki; ZHANG, Dong Er. P53 Alterations in Myeloid Leukemia. **Acta Haematologica**, *[S. l.]*, v. 111, n. 1–2, p. 100–106, 2004. DOI: 10.1159/000074489.

BOYER, Scott W.; SCHROEDER, Aaron V.; SMITH-BERDAN, Stephanie; FORSBERG, E. Camilla. All Hematopoietic Cells Develop from Hematopoietic Stem Cells through Flk2/Flt3-Positive Progenitor Cells. **Cell Stem Cell**, *[S. l.]*, v. 9, n. 1, p. 64–73, 2011. DOI: 10.1016/j.stem.2011.04.021. Disponível em: http://dx.doi.org/10.1016/j.stem.2011.04.021.

CABEZAS-WALLSCHEID, Nina et al. Identification of regulatory networks in HSCs and their immediate progeny via integrated proteome, transcriptome, and DNA methylome analysis. **Cell Stem Cell**, *[S. l.]*, v. 15, n. 4, p. 507–522, 2014. DOI: 10.1016/j.stem.2014.07.005.

CALLENS, C. et al. Prognostic implication of FLT3 and Ras gene mutations in patients with acute promyelocytic leukemia (APL): A retrospective study from the European APL Group. **Leukemia**, *[S. l.]*, v. 19, n. 7, p. 1153–1160, 2005. DOI: 10.1038/sj.leu.2403790.

CAMPBELL, Peter J. et al. Pan-cancer analysis of whole genomes. **Nature**, *[S. l.]*, v. 578, n. 7793, p. 82–93, 2020. DOI: 10.1038/s41586-020-1969-6.

CARRETTA, Marco et al. Genetically engineered mesenchymal stromal cells produce IL-3 and TPO to further improve human scaffold-based xenograft models. **Experimental Hematology**, *[S. l.]*, v. 51, p. 36–46, 2017. DOI: 10.1016/j.exphem.2017.04.008. Disponível em: http://dx.doi.org/10.1016/j.exphem.2017.04.008.

CELLS, Stem et al. Repression of BMI1 in normal and leukemic human CD34. **Blood**, *[S. l.]*, v. 114, n. 8, p. 1498–1506, 2016. DOI: 10.1182/blood-2009-03-209734.The.

CHANG, Chung; HSIEH, Meng Ke; CHANG, Wen Yi; CHIANG, An Jen; CHEN, Jiabin. Determining the optimal number and location of cutoff points with application to data of cervical cancer. **PLoS ONE**, *[S. l.]*, v. 12, n. 4, p. 1–13, 2017. DOI: 10.1371/journal.pone.0176231.

CHAO, Mark P. et al. Calreticulin is the dominant pro-phagocytic signal on multiple human cancers and is counterbalanced by CD47. **Science Translational Medicine**, *[S. l.]*, v. 2, n. 63, 2010. DOI: 10.1126/scitranslmed.3001375.

CHIM, Chor S.; WONG, Seung Y.; KWONG, Yok L. Aberrant gene promoter methylation in acute promyelocytic leukaemia: Profile and prognostic significance. **British Journal of Haematology**, *[S. l.]*, v. 122, n. 4, p. 571–578, 2003. DOI: 10.1046/j.1365-2141.2003.04462.x.

CHOI, Kyunghee; KENNEDY, Marion; KAZAROV, Alexander; PAPADIMITRIOU, John C.; KELLER, Gordon. A common precursor for hematopoietic and endothelial cells. **Development**, *[S. l.]*, v. 125, n. 4, p. 725–732, 1998. DOI: 10.1242/dev.125.4.725.

CHRISTENSEN, Julie L.; WEISSMAN, Irving L. Flk-2 is a marker in hematopoietic stem cell differentiation: A simple method to isolate long-term stem cells. **Proceedings of the National Academy of Sciences of the United States of America**, *[S. l.]*, v. 98, n. 25, p. 14541–14546, 2001. DOI: 10.1073/pnas.261562798.

CHUNG, Yun Shin; ZHANG, Wen Jie; ARENTSON, Elizabeth; KINGSLEY, Paul D.; PALIS, James; CHOI, Kyunghee. Lineage analysis of the hemangioblast as defined by FLK1 and SCL expression. **Development**, *[S. l.]*, v. 129, n. 23, p. 5511–5520, 2002. DOI: 10.1242/dev.00149.

CIUREA, Stefan O.; ANDERSSON, Borje S. Busulfan in Hematopoietic Stem Cell Transplantation. **Biology of Blood and Marrow Transplantation**, *[S. l.]*, v. 15, n. 5, p. 523–536, 2009. DOI: 10.1016/j.bbmt.2008.12.489. Disponível em: https://linkinghub.elsevier.com/retrieve/pii/S1083879108011002.

CONCIN, Nicole et al. Transdominant ΔTAp73 Isoforms Are Frequently Up-regulated in Ovarian Cancer. Evidence for Their Role as Epigenetic p53 Inhibitors in Vivo. **Cancer Research**, *[S. l.]*, v. 64, n. 7, p. 2449–2460, 2004. DOI: 10.1158/0008-5472.CAN-03-1060.

CORRÊA DE ARAUJO KOURY, Luisa; GANSER, Arnold; BERLINER, Nancy; REGO, Eduardo M. Treating acute promyelocytic leukaemia in Latin America: lessons from the International Consortium on Acute Leukaemia experience. **British Journal of Haematology**, *[S. l.]*, v. 177, n. 6, p. 979–983, 2017. DOI: 10.1111/bjh.14589.

DE BOER, Bauke et al. Prospective Isolation and Characterization of Genetically and Functionally Distinct AML Subclones. **Cancer Cell**, *[S. l.]*, v. 34, n. 4, p. 674- 689.e8, 2018. DOI: 10.1016/j.ccell.2018.08.014.

DI, Cuixia et al. Mechanisms, function and clinical applications of DNp73. **Cell Cycle**, *[S. l.]*, v. 12, n. 12, p. 1861–1867, 2013. DOI: 10.4161/cc.24967.

DÖHNER, Hartmut et al. Diagnosis and management of acute myeloid leukemia in adults: Recommendations from an international expert panel, on behalf of the European LeukemiaNet. **Blood**, *[S. l.]*, v. 115, n. 3, p. 453–474, 2010. DOI: 10.1182/blood-2009-07-235358.

DÖHNER, Hartmut et al. Diagnosis and management of AML in adults: 2017 ELN recommendations from an international expert panel. **Blood**, *[S. l.]*, v. 129, n. 4, p. 424–447, 2017. DOI: 10.1182/blood-2016-08-733196.

DROPULIĆ, Boro. Lentiviral Vectors: Their Molecular Design, Safety, and Use in Laboratory and Preclinical Research. **Human Gene Therapy**, *[S. l.]*, v. 22, n. 6, p. 649–657, 2011. DOI: 10.1089/hum.2011.058. Disponível em: http://www.liebertonline.com/doi/abs/10.1089/hum.2011.058.

ELLEGAST, Jana M. et al. inv(16) and NPM1mut AMLs engraft human cytokine knock-in mice. **Blood**, *[S. l.]*, v. 128, n. 17, p. 2130–2134, 2016. DOI: 10.1182/blood-2015-12-689356.

EMA, Hideo; NAKAUCHI, Hiromitsu. Expansion of hematopoietic stem cells in the developing liver of a mouse embryo. **Blood**, *[S. l.]*, v. 95, n. 7, p. 2284–2288, 2000. DOI: 10.1182/blood.v95.7.2284. Disponível em: http://dx.doi.org/10.1182/blood.V95.7.2284.

ESTEY, Elihu. Acute Myeloid Leukemia — Many Diseases, Many Treatments. **New England Journal of Medicine**, *[S. l.]*, v. 375, n. 21, p. 2094–2095, 2016. DOI: 10.1056/NEJMe1611424. Disponível em: http://www.nejm.org/doi/10.1056/NEJMe1611424.

FALOON, Patrick; ARENTSON, Elizabeth; KAZAROV, Alexander; DENG, Chu Xia; PORCHER, Catherine; ORKIN, Stuart; CHOI, Kyunghee. Faloon P, 2000.pdf. *[S. l.]*, v. 1941, p. 1931–1941, 2000.

FORSBERG, E. Camilla; SERWOLD, Thomas; KOGAN, Scott; WEISSMAN, Irving L.; PASSEGUÉ, Emmanuelle. New Evidence Supporting Megakaryocyte-Erythrocyte Potential of Flk2/Flt3+ Multipotent Hematopoietic Progenitors. **Cell**, *[S. l.]*, v. 126, n. 2, p. 415–426, 2006. DOI: 10.1016/j.cell.2006.06.037.

GAILLARD, Coline; SURIANARAYANAN, Sangeetha; BENTLEY, Trevor; WARR, Matthew R.; FITCH, Briana; GENG, Huimin; PASSEGUÉ, Emmanuelle; DE THÉ, Hugues; KOGAN, Scott C. Identification of IRF8 as a potent tumor suppressor in murine acute promyelocytic leukemia. **Blood Advances**, *[S. l.]*, v. 2, n. 19, p. 2462–2466, 2018. DOI: 10.1182/bloodadvances.2018018929.

GARCIA-PORRERO, Juan A.; GODIN, Isabelle E.; DIETERLEN-LIÈVRE, Françoise. Potential intraembryonic hemogenic sites at pre-liver stages in the mouse. **Anatomy and Embryology**, *[S. l.]*, v. 192, n. 5, p. 425–435, 1995. DOI: 10.1007/BF00240375.

GASPARETTO, Maura et al. Targeted therapy for a subset of acute myeloid leukemias that lack expression of aldehyde dehydrogenase 1A1. **Haematologica**, *[S. l.]*, v. 102, n. 6, p. 1054–1065, 2017. DOI: 10.3324/haematol.2016.159053.

GHANDI, Mahmoud et al. Next-generation characterization of the Cancer Cell Line Encyclopedia. **Nature**, *[S. l.]*, v. 569, n. 7757, p. 503–508, 2019. DOI: 10.1038/s41586-019-1186-3. Disponível em: http://dx.doi.org/10.1038/s41586-019-1186-3.

GOMEZ-PUERTO, Maria Catalina; FOLKERTS, Hendrik; WIERENGA, Albertus T. J.; SCHEPERS, Koen; SCHURINGA, Jan Jacob; COFFER, Paul J.; VELLENGA, Edo. Autophagy Proteins ATG5 and ATG7 Are Essential for the Maintenance of Human CD34+Hematopoietic Stem-Progenitor Cells. **Stem Cells**, *[S. l.]*, v. 34, n. 6, p. 1651–1663, 2016. DOI: 10.1002/stem.2347.

GOULD, Stephen E.; JUNTTILA, Melissa R.; DE SAUVAGE, Frederic J. Translational value of mouse models in oncology drug development. **Nature Medicine**, *[S. l.]*, v. 21, n. 5, p. 431–439, 2015. DOI: 10.1038/nm.3853.

GRENIER-PLEAU, Isabelle et al. Blood extracellular vesicles from healthy individuals regulate hematopoietic stem cells as humans age. **Aging Cell**, *[S. l.]*, v. 19, n. 11, p. 1–6, 2020. DOI: 10.1111/acel.13245.

GRIMWADE, David; HILLS, Robert K.; MOORMAN, Anthony V.; WALKER, Helen; CHATTERS, Stephen; GOLDSTONE, Anthony H.; WHEATLEY, Keith; HARRISON, Christine J.; BURNETT, Alan K. Refinement of cytogenetic classification in acute myeloid leukemia: Determination of prognostic significance of rare recurring chromosomal abnormalities among 5876 younger adult patients treated in the United Kingdom Medical Research Council trials. **Blood**, *[S. l.]*, v. 116, n. 3, p. 354–365, 2010. DOI: 10.1182/blood-2009-11-254441.

GROB, T. J. et al. Human ΔNp73 regulates a dominant negative feedback loop for TAp73 and p53. **Cell Death and Differentiation**, *[S. l.]*, v. 8, n. 12, p. 1213–1223, 2001. DOI: 10.1038/sj.cdd.4400962.

GU, Xiaorong et al. Leukemogenic nucleophosmin mutation disrupts the transcription factor hub that regulates granulomonocytic fates. **Journal of Clinical Investigation**, *[S. l.]*, v. 128, n. 10, p. 4260–4279, 2018. DOI: 10.1172/JCI97117.

HEUSER, Michael et al. MN1 overexpression induces acute myeloid leukemia in mice and predicts ATRA resistance in patients with AML. **Blood**, *[S. l.]*, v. 110, n. 5, p. 1639–1647, 2007. DOI: 10.1182/blood-2007-03-080523.

HIRAI, Hideyo; OGAWA, Minetaro; SUZUKI, Norio; YAMAMOTO, Masayuki; BREIER, Georg; MAZDA, Osam; IMANISHI, Jiro; NISHIKAWA, Shin Ichi. Hemogenic and nonhemogenic endothelium can be distinguished by the activity of fetal liver kinase (Flk)-1 promoter/enhancer during mouse embryogenesis. **Blood**, *[S. l.]*, v. 101, n. 3, p. 886–893, 2003. DOI: 10.1182/blood-2002-02-0655.

IKUTA, Koichi; WEISSMAN, Irving L. Evidence that hematopoietic stem cells express. **Proc.Natl.Acad.Sci., USA**, *[S. l.]*, v. 89, n. 4, p. 1502–1506, 1992.

INSINGA, Alessandra et al. Impairment of p53 acetylation, stability and function by an oncogenic transcription factor. **EMBO Journal**, *[S. l.]*, v. 23, n. 5, p. 1144–1154, 2004. DOI: 10.1038/sj.emboj.7600109.

ISHIMOTO, Osamu; KAWAHARA, Chikashi; ENJO, Kentaro; OBINATA, Masuo; NUKIWA, Toshihiro; IKAWA, Shuntaro. Possible oncogenic potential of ΔNp73: A newly identified isoform of human p73. **Cancer Research**, *[S. l.]*, v. 62, n. 3, p. 636–641, 2002.

JOST, Christine A.; MARIN, Maria C.; KAELIN, William G. P73 Is a Human P53-Related Protein That Can Induce Apoptosis. **Nature**, *[S. l.]*, v. 389, n. 6647, p. 191–194, 1997. DOI: 10.1038/38298.

KAGHAD, Mourad et al. Monoallelically expressed gene related to p53 at 1p36, a region frequently deleted in neuroblastoma and other human cancers. **Cell**, *[S. l.]*, v. 90, n. 4, p. 809–819, 1997. DOI: 10.1016/S0092-8674(00)80540-1.

KAMLER, M.; PIZANIS, N. Aktueller Stand der Lungentransplantation. **Zeitschrift für Herz-,Thorax- und Gefäßchirurgie**, *[S. l.]*, v. 27, n. 4, p. 235–242, 2013. DOI: 10.1007/s00398-012-0935-5. Disponível em: http://link.springer.com/10.1007/s00398-012-0935-5.

KARTASHEVA, Natalia N.; CONTENTE, Ana; LENZ-STÖPPLER, Claudia; ROTH, Judith; DOBBELSTEIN, Matthias. p53 induces the expression of its antagonist p73ΔN, establishing an antoregulatory feedback loop. **Oncogene**, *[S. l.]*, v. 21, n. 31, p. 4715–4727, 2002. DOI: 10.1038/sj.onc.1205584.

KAWASAKI, Akira; MATSUMURA, Itaru; KATAOKA, Yoshihisa; TAKIGAWA, Eri; NAKAJIMA, Koichi; KANAKURA, Yuzuru. Opposing effects of PML and PML/RARα on STAT3 activity. **Blood**, *[S. l.]*, v. 101, n. 9, p. 3668–3673, 2003. DOI: 10.1182/blood-2002-08-2474.

KLCO, Jeffery M. et al. Functional heterogeneity of genetically defined subclones in acute myeloid leukemia. **Cancer Cell**, *[S. l.]*, v. 25, n. 3, p. 379–392, 2014. DOI: 10.1016/j.ccr.2014.01.031. Disponível em: http://dx.doi.org/10.1016/j.ccr.2014.01.031.

KOKKALIARIS, Konstantinos D. et al. Identification of factors promoting ex vivo maintenance of mouse hematopoietic stem cells by long-term single-cell quantification. **Blood**, *[S. l.]*, v. 128, n. 9, p. 1181–1192, 2016. DOI: 10.1182/blood-2016-03-705590.

KORNBLAU, Steven M. et al. Distinct protein signatures of acute myeloid leukemia bone marrow-derived stromal cells are prognostic for patient survival. **Haematologica**, *[S. l.]*, v. 103, n. 5, p. 810–821, 2018. DOI: 10.3324/haematol.2017.172429.

LEVRERO, M.; DE LAURENZI, V.; COSTANZO, A.; GONG, J.; MELINO, G.; WANG, J. Y. J. Structure, function and regulation of p63 and p73. **Cell Death and Differentiation**, *[S. l.]*, v. 6, n. 12, p. 1146–1153, 1999. DOI: 10.1038/sj.cdd.4400624.

LEVRERO, M.; DE LAURENZI, V.; COSTANZO, A.; SABATINI, S.; GONG, J.; WANG, J. Y. J.; MELINO, G. The p53/p63/p73 family of transcription factors: Overlapping and distinct functions. **Journal of Cell Science**, *[S. l.]*, v. 113, n. 10, p. 1661–1670, 2000. DOI: 10.1242/jcs.113.10.1661.

LEY, Timothy J. et al. Genomic and epigenomic landscapes of adult de novo acute myeloid leukemia. **New England Journal of Medicine**, *[S. l.]*, v. 368, n. 22, p. 2059–2074, 2013. DOI: 10.1056/NEJMoa1301689.

LI, Sheng; MASON, Christopher; MELNICK, Ari. Genetic and epigenetic heterogeneity in acute myeloid leukemia. **Current Opinion in Genetics and Development**, *[S. l.]*, v. 36, p. 100–106, 2016. DOI: 10.1016/j.gde.2016.03.011. Disponível em: http://dx.doi.org/10.1016/j.gde.2016.03.011.

LINNEKIN, Diana. Early signaling pathways activated by c-Kit in hematopoietic cells. **International Journal of Biochemistry and Cell Biology**, *[S. l.]*, v. 31, n. 10, p. 1053–1074, 1999. DOI: 10.1016/S1357-2725(99)00078-3.

LORENZ, E.; CONGDON, C.; UPHOFF, D. Modification of acute irradiation injury in mice and guinea-pigs by bone marrow injections. **Radiology**, *[S. l.]*, v. 58, n. 6, p. 863–877, 1952. DOI: 10.1148/58.6.863.

LUCENA-ARAUJO, Antonio R. et al. The expression of ΔnTP73, TATP73 and TP53 genes in acute myeloid leukaemia is associated with recurrent cytogenetic abnormalities and in vitro susceptibility to cytarabine cytotoxicity. **British Journal of Haematology**, *[S. l.]*, v. 142, n. 1, p. 74–78, 2008. DOI: 10.1111/j.1365-2141.2008.07160.x.

LUCENA-ARAUJO, Antonio R. et al. High Δnp73/TAp73 ratio is associated with poor prognosis in acute promyelocytic leukemia. **Blood**, *[S. l.]*, v. 126, n. 20, p. 2302–2306, 2015. DOI: 10.1182/blood-2015-01-623330.

LUCENA-ARAUJO, Antonio R. et al. DeltaNp73 overexpression promotes resistance to apoptosis but does not cooperate with PML/RARA in the induction of an APL-leukemic phenotype. **Oncotarget**, *[S. l.]*, v. 8, n. 5, p. 8475–8483, 2017. a. DOI: 10.18632/oncotarget.14295.

LUCENA-ARAUJO, Antonio R. et al. ΔNp73 overexpression promotes resistance to apoptosis but does not cooperate with PML/RARA in the induction of an APL-leukemic phenotype. **Oncotarget**, *[S. l.]*, v. 8, n. 5, p. 8475–8483, 2017. b. DOI: 10.18632/oncotarget.14295.

LUCENA-ARAUJO, Antonio R. et al. Clinical impact of *BAALC* expression in high-risk acute promyelocytic leukemia. **Blood Advances**, *[S. l.]*, v. 1, n. 21, p. 1807–1814, 2017. c. DOI: 10.1182/bloodadvances.2017005926. Disponível em: http://www.bloodadvances.org/lookup/doi/10.1182/bloodadvances.2017005926.

MAINARDI, S. et al. ΔN-p73 is a transcriptional target of the PML/RARα oncogene in myeloid differentiation [1]. **Cell Death and Differentiation**, *[S. l.]*, v. 14, n. 11, p. 1968–1971, 2007. DOI: 10.1038/sj.cdd.4402210.

MATSUOKA, Sahoko et al. Generation of definitive hematopoietic stem cells from murine early yolk sac and paraaortic splanchnopleures by aorta-gonad-mesonephros region-derived stromal cells. **Blood**, *[S. l.]*, v. 98, n. 1, p. 6–12, 2001. DOI: 10.1182/blood.V98.1.6.

MATSUSHITA, Hiromichi et al. Establishment of a humanized apl model via the transplantation of PML-rara-transduced human common myeloid progenitors into immunodeficient mice. **PLoS ONE**, *[S. l.]*, v. 9, n. 11, 2014. DOI: 10.1371/journal.pone.0111082.

MCKEON, Frank; MELINO, Gerry. Fog of war: The emerging p53 family. **Cell Cycle**, *[S. l.]*, v. 6, n. 3, p. 229–232, 2007. DOI: 10.4161/cc.6.3.3876.

MEDVINSKY, Alexander; DZIERZAK, Elaine. Definitive hematopoiesis is autonomously initiated by the AGM region. **Cell**, *[S. l.]*, v. 86, n. 6, p. 897–906, 1996. DOI: 10.1016/S0092-8674(00)80165-8.

MEIER, Claudia; HARDTSTOCK, Philip; JOOST, Sophie; ALLA, Vijay; PÜTZER, Brigitte M. P73 and IGF1R regulate emergence of aggressive cancer stem-like features via miR-885-5p control. **Cancer Research**, *[S. l.]*, v. 76, n. 2, p. 197–205, 2016. DOI: 10.1158/0008-5472.CAN-15-1228.

MENDELSON, Avital; FRENETTE, Paul S. Hematopoietic stem cell niche maintenance during homeostasis and regeneration. **Nature Medicine**, *[S. l.]*, v. 20, n. 8, p. 833–846, 2014. DOI: 10.1038/nm.3647.

MÉNDEZ-FERRER, Simón; BONNET, Dominique; STEENSMA, David P.; HASSERJIAN, Robert P.; GHOBRIAL, Irene M.; GRIBBEN, John G.; ANDREEFF, Michael; KRAUSE, Daniela S. Bone marrow niches in haematological malignancies. **Nature Reviews Cancer**, *[S. l.]*, v. 20, n. 5, p. 285–298, 2020. DOI: 10.1038/s41568-020-0245-2. Disponível em: http://dx.doi.org/10.1038/s41568-020-0245-2.

MORITA, Kiyomi et al. Author Correction: Clonal evolution of acute myeloid leukemia revealed by high-throughput single-cell genomics (Nature Communications, (2020), 11, 1, (5327), 10.1038/s41467-020-19119-8). **Nature Communications**, *[S. l.]*, v. 12, n. 1, p. 41467, 2021. DOI: 10.1038/s41467-021-23280-z. Disponível em: http://dx.doi.org/10.1038/s41467-021-23280-z.

MORRISON, Sean J.; SCADDEN, David T. The bone marrow niche for haematopoietic stem cells. **Nature**, *[S. l.]*, v. 505, n. 7483, p. 327–334, 2014. DOI: 10.1038/nature12984.

MORRISON, Sean J.; WANDYCZ, Antoni M.; HEMMATI, Houman D.; WRIGHT, Douglas E.; WEISSMAN, Irving L. Development-1997-Morrison-1929-39. *[S. l.]*, v. 1939, p. 1–11, 1997. Disponível em: papers2://publication/uuid/44A71CA9-CF17-462D-851D-B2A305E52759.

MORRISON, Sean J.; WEISSMAN, Irving L. The long-term repopulating subset of hematopoietic stem cells is deterministic and isolatable by phenotype. **Immunity**, *[S. l.]*, v. 1, n. 8, p. 661–673, 1994. DOI: 10.1016/1074-7613(94)90037-X.

NAKORN, Thanyaphong Na; TRAVER, David; WEISSMAN, Irving L.; AKASHI, Koichi. Myeloerythroid-restricted progenitors are sufficient to confer radioprotection and provide the majority of day 8 CFU-S. **Journal of Clinical Investigation**, *[S. l.]*, v. 109, n. 12, p. 1579–1585, 2002. DOI: 10.1172/JCI200215272.

NG, Stanley W. K. et al. A 17-gene stemness score for rapid determination of risk in acute leukaemia. **Nature**, *[S. l.]*, v. 540, n. 7633, p. 433–437, 2016. DOI: 10.1038/nature20598. Disponível em: http://dx.doi.org/10.1038/nature20598.

PACZULLA, Anna M. et al. Long-term observation reveals high-frequency engraftment of human acute myeloid leukemia in immunodeficient mice. **Haematologica**, *[S. l.]*, v. 102, n. 5, p. 854–864, 2017. DOI: 10.3324/haematol.2016.153528.

PAPAEMMANUIL, Elli et al. Genomic Classification and Prognosis in Acute Myeloid Leukemia. **New England Journal of Medicine**, *[S. l.]*, v. 374, n. 23, p. 2209–2221, 2016. DOI: 10.1056/nejmoa1516192.

PASSLICK, B.; FLIEGER, D.; ZIEGLER-HEITBROCK, HW. Identification and characterization of a novel monocyte subpopulation in human peripheral blood. **Blood**, *[S. l.]*, v. 74, n. 7, p. 2527–2534, 1989. DOI: 10.1182/blood.v74.7.2527.2527. Disponível em: http://dx.doi.org/10.1182/blood.V74.7.2527.2527.

PATEL, S. et al. Successful xenografts of AML3 samples in immunodeficient NOD/shi-SCID IL2Rγ-/- mice. **Leukemia**, *[S. l.]*, v. 26, n. 11, p. 2432–2435, 2012. DOI: 10.1038/leu.2012.154.

PEREIRA-MARTINS, Diego A. et al. MLL5 improves ATRA driven differentiation and promotes xenotransplant engraftment in acute promyelocytic leukemia model. **Cell Death and Disease**, *[S. l.]*, v. 12, n. 4, 2021. DOI: 10.1038/s41419-021-03604-z. Disponível em: http://dx.doi.org/10.1038/s41419-021-03604-z.

PETRENKO, Oleksi; ZAIKA, Alexander; MOLL, Ute M. ΔNp73 Facilitates Cell Immortalization and Cooperates with Oncogenic Ras in Cellular Transformation In Vivo. **Molecular and Cellular Biology**, *[S. l.]*, v. 23, n. 16, p. 5540–5555, 2003. DOI: 10.1128/mcb.23.16.5540-5555.2003.

PIETRAS, Eric M.; REYNAUD, Damien; KANG, Yoon A.; CARLIN, Daniel; CALERO-NIETO, Fernando J.; LEAVITT, Andrew D.; STUART, Joshua A.; GÖTTGENS, Berthold; PASSEGUÉ, Emmanuelle. Functionally Distinct Subsets of Lineage-Biased Multipotent Progenitors Control Blood Production in Normal and Regenerative Conditions. **Cell Stem Cell**, *[S. l.]*, v. 17, n. 1, p. 35–46, 2015. DOI: 10.1016/j.stem.2015.05.003.

PÜTZER, Brigitte M.; TUVE, S.; TANNAPFEL, A.; STIEWE, T. Increased ΔN-p73 expression in tumors by upregulation of the E2F1-regulated, TA-promoter-derived ΔN′-p73 transcript [2]. **Cell Death and Differentiation**, *[S. l.]*, v. 10, n. 5, p. 612–614, 2003. DOI: 10.1038/sj.cdd.4401205.

RAU, Rachel E. CMML/JMML PDXs: As easy as 1, 2, NSG-SGM3. **Blood**, *[S. l.]*, v. 130, n. 4, p. 385–386, 2017. DOI: 10.1182/blood-2017-06-789123.

REGO, E. M.; RUGGERO, D.; TRIBIOLI, C.; CATTORETTI, G.; KOGAN, S.; REDNER, R. L.; PANDOLFI, P. P. Leukemia with distinct phenotypes in transgenic mice expressing PML/RARα, PLZF/RARα or NPM/RARα. **Oncogene**, *[S. l.]*, v. 25, n. 13, p. 1974–1979, 2006. DOI: 10.1038/sj.onc.1209216.

REGO, Eduardo M. et al. Improving acute promyelocytic leukemia (APL) outcome in developing countries through networking, results of the International Consortium on APL. **Blood**, *[S. l.]*, v. 121, n. 11, p. 1935–1943, 2013. DOI: 10.1182/blood-2012-08-449918.

REGO, Eduardo M.; WANG, Zhu Gang; PERUZZI, Daniela; HE, Le Zhen; CORDON-CARDO, Carlos; PANDOLFI, Pier Paolo. Role of promyelocytic leukemia (PML) protein in tumor suppression. **Journal of Experimental Medicine**, *[S. l.]*, v. 193, n. 4, p. 521–529, 2001. DOI: 10.1084/jem.193.4.521.

REINISCH, Andreas; MAJETI, Ravindra. Sticking It to the Niche: CD98 Mediates Critical Adhesive Signals in AML. **Cancer Cell**, *[S. l.]*, v. 30, n. 5, p. 662–664, 2016. DOI: 10.1016/j.ccell.2016.10.014.

REINISCH, Andreas; THOMAS, Daniel; CORCES, M. Ryan; ZHANG, Xiaohua; GRATZINGER, Dita; HONG, Wan Jen; SCHALLMOSER, Katharina; STRUNK, Dirk; MAJETI, Ravindra. A humanized bone marrow ossicle xenotransplantation model enables improved engraftment of healthy and leukemic human hematopoietic cells. **Nature Medicine**, *[S. l.]*, v. 22, n. 7, p. 812–821, 2016. DOI: 10.1038/nm.4103.

RONGVAUX, Anthony et al. Development and function of human innate immune cells in a humanized mouse model. **Nature Biotechnology**, *[S. l.]*, v. 32, n. 4, p. 364–372, 2014. DOI: 10.1038/nbt.2858.

ROSENBERG, Mara W.; WATANABE-SMITH, Kevin; TYNER, Jeffrey W.; TOGNON, Cristina E.; DRUKER, Brian J.; BORATE, Uma. Genomic markers of midostaurin drug sensitivity in FLT3 mutated and FLT3 wild-type acute myeloid leukemia patients. **Oncotarget**, *[S. l.]*, v. 11, n. 29, p. 2807–2818, 2020. DOI: 10.18632/oncotarget.27656.

RUFINI, Alessandro et al. P73 in cancer. **Genes and Cancer**, *[S. l.]*, v. 2, n. 4, p. 491–502, 2011. DOI: 10.1177/1947601911408890.

SAHU, Geeta Ram; MISHRA, Rajakishore; NAGPAL, Jatin Kumar; DAS, Bibhu Ranjan. Alteration of p73 in acute myelogenous leukemia. **American Journal of Hematology**, *[S. l.]*, v. 79, n. 1, p. 1–7, 2005. DOI: 10.1002/ajh.20284.

SANZ, Miguel A. et al. A modified AIDA protocol with anthracycline-based consolidation results in high antileukemic efficacy and reduced toxicity in newly diagnosed PML/RARα-positive acute promyelocytic leukemia. **Blood**, *[S. l.]*, v. 94, n. 9, p. 3015–3021, 1999. DOI: 10.1182/blood.V94.9.3015.

SANZ, Miguel A. et al. Management of acute promyelocytic leukemia: Updated recommendations from an expert panel of the European LeukemiaNet. **Blood**, *[S. l.]*, v. 133, n. 15, p. 1630–1643, 2019. DOI: 10.1182/blood-2019-01-894980.

SAWYERS, By Charles L.; GISHIZKY, Mikhail L.; QUAN, Shirley; GOLDE, David W.; WITTE, Owen N. Propagation of Human Blastic Myeloid Leukemias in the SCID Mouse. **Molecular Biology**, *[S. l.]*, v. 79, n. 8, p. 2089–2098, 1992.

SCHMELZ, Karin; WAGNER, Mandy; DÖRKEN, Bernd; TAMM, Ingo. 5-Aza-2′-deoxycytidine induces p21WAF expression by demethylation of p73 leading to p53-independent apoptosis in myeloid leukemia. **International Journal of Cancer**, *[S. l.]*, v. 114, n. 5, p. 683–695, 2005. DOI: 10.1002/ijc.20797.

SHIN, Jong Yeon; KIM, Hyun Seok; PARK, Jinseu; PARK, Jae Bong; LEE, Jae Yong. Mechanism for inactivation of the KIP family cyclin-dependent kinase inhibitor genes in gastric cancer cells. **Cancer Research**, *[S. l.]*, v. 60, n. 2, p. 262–265, 2000.

SHLUSH, Liran I. et al. Tracing the origins of relapse in acute myeloid leukaemia to stem cells. **Nature**, *[S. l.]*, v. 547, n. 7661, p. 104–108, 2017. DOI: 10.1038/nature22993. Disponível em: http://dx.doi.org/10.1038/nature22993.

SHULTZ, Leonard D.; ISHIKAWA, Fumihiko; GREINER, Dale L. Humanized mice in translational biomedical research. **Nature Reviews Immunology**, *[S. l.]*, v. 7, n. 2, p. 118–130, 2007. DOI: 10.1038/nri2017.

SILVA, Wellington F. d. et al. Real-life Outcomes on Acute Promyelocytic Leukemia in Brazil – Early Deaths Are Still a Problem. **Clinical Lymphoma, Myeloma and Leukemia**, *[S. l.]*, v. 19, n. 2, p. e116–e122, 2019. DOI: 10.1016/j.clml.2018.11.004. Disponível em: https://doi.org/10.1016/j.clml.2018.11.004.

SMITH, L. G.; WEISSMAN, I. L.; HEIMFELD, S. Clonal analysis of hematopoietic stem-cell differentiation in vivo. **Proceedings of the National Academy of Sciences of the United States of America**, *[S. l.]*, v. 88, n. 7, p. 2788–2792, 1991. DOI: 10.1073/pnas.88.7.2788.

SONTAKKE, P. et al. Modeling BCR-ABL and MLL-AF9 leukemia in a human bone marrow-like scaffold-based xenograft model. **Leukemia**, *[S. l.]*, v. 30, n. 10, p. 2064–2073, 2016. DOI: 10.1038/leu.2016.108. Disponível em: http://dx.doi.org/10.1038/leu.2016.108.

SPANGRUDE, Gerald J. Hematopoietic stem-cell differentiation. **Current Opinion in Immunology**, *[S. l.]*, v. 3, n. 2, p. 171–178, 1991. DOI: 10.1016/0952-7915(91)90046-4.

STEDER, Marc et al. DNp73 Exerts Function in Metastasis Initiation by Disconnecting the Inhibitory Role of EPLIN on IGF1R-AKT/STAT3 Signaling. **Cancer Cell**, *[S. l.]*, v. 24, n. 4, p. 512–527, 2013. DOI: 10.1016/j.ccr.2013.08.023.

STIEWE, T.; PÜTZER, B. M. P73 in Apoptosis. **Apoptosis**, *[S. l.]*, v. 6, n. 6, p. 447–452, 2001. DOI: 10.1023/A:1012433522902.

STIEWE, T.; PÜTZER, B. M. Role of p73 in malignancy: Tumor suppressor or oncogene? **Cell Death and Differentiation**, *[S. l.]*, v. 9, n. 3, p. 237–245, 2002. DOI: 10.1038/sj.cdd.4400995.

STIEWE, Thorsten. The p53 family in differentiation and tumorigenesis. **Nature Reviews Cancer**, *[S. l.]*, v. 7, n. 3, p. 165–167, 2007. DOI: 10.1038/nrc2072.

STIEWE, Thorsten; THESELING, Carmen C.; PÜTZER, Brigitte M. Transactivation-deficient ΔTA-p73 inhibits p53 by direct competition for DNA binding. Implications for tumorigenesis. **Journal of Biological Chemistry**, *[S. l.]*, v. 277, n. 16, p. 14177–14185, 2002. DOI: 10.1074/jbc.M200480200.

STIEWE, Thorsten; TUVE, Sebastian; PETER, Martin; TANNAPFEL, Andrea; ELMAAGACLI, Ahmet H.; PÜTZER, Brigitte M. Quantitative TP73 Transcript Analysis in Hepatocellular Carcinomas. **Clinical Cancer Research**, *[S. l.]*, v. 10, n. 2, p. 626–633, 2004. DOI: 10.1158/1078-0432.CCR-0153-03.

SUBRAMANIAN, Aravind et al. Gene set enrichment analysis: A knowledge-based approach for interpreting genome-wide expression profiles. **Proceedings of the National Academy of Sciences of the United States of America**, *[S. l.]*, v. 102, n. 43, p. 15545–15550, 2005. DOI: 10.1073/pnas.0506580102.

TAM, Patrick P. L.; BEHRINGER, Richard R. Mouse gastrulation: The formation of a mammalian body plan. **Mechanisms of Development**, *[S. l.]*, v. 68, n. 1–2, p. 3–25, 1997. DOI: 10.1016/S0925-4773(97)00123-8.

THEOCHARIDES, Alexandre P. A.; RONGVAUX, Anthony; FRITSCH, Kristin; FLAVELL, Richard A.; MANZ, Markus G. Humanized hemato-lymphoid system mice. **Haematologica**, *[S. l.]*, v. 101, n. 1, p. 5–19, 2016. DOI: 10.3324/haematol.2014.115212.

TILL, J. E.; MCCULLOCH, E. A. A Direct Measurement of the Radiation Sensitivity of Normal Mouse Bone Marrow Cells Author (s): J . E . Till and E . A . McCulloch Published by : Radiation Research Society Stable URL : http://www.jstor.org/stable/3570892 A Direct Measurement of the Rad. **Radiation Research Society**, *[S. l.]*, v. 14, n. 2, p. 213–222, 1961.

TOMASINI, Richard et al. TAp73 knockout shows genomic instability with infertility and tumor suppressor functions. **Genes and Development**, *[S. l.]*, v. 22, n. 19, p. 2677–2691, 2008. DOI: 10.1101/gad.1695308.

TYNER, Jeffrey W. et al. Functional genomic landscape of acute myeloid leukaemia. **Nature**, *[S. l.]*, v. 562, n. 7728, p. 526–531, 2018. DOI: 10.1038/s41586-018-0623-z.

VALENT, Peter et al. Cancer stem cell definitions and terminology: The devil is in the details. **Nature Reviews Cancer**, *[S. l.]*, v. 12, n. 11, p. 767–775, 2012. DOI: 10.1038/nrc3368. Disponível em: http://dx.doi.org/10.1038/nrc3368.

VAN GALEN, Peter et al. Single-Cell RNA-Seq Reveals AML Hierarchies Relevant to Disease Progression and Immunity. **Cell**, *[S. l.]*, v. 176, n. 6, p. 1265- 1281.e24, 2019. DOI: 10.1016/j.cell.2019.01.031. Disponível em: https://doi.org/10.1016/j.cell.2019.01.031.

VAN GOSLIGA, Djoke; SCHEPERS, Hein; RIZO, Aleksandra; VAN DER KOLK, Dorina; VELLENGA, Edo; SCHURINGA, Jan Jacob. Establishing long-term cultures with self-renewing acute myeloid leukemia stem/progenitor cells. **Experimental Hematology**, *[S. l.]*, v. 35, n. 10, p. 1538–1549, 2007. DOI: 10.1016/j.exphem.2007.07.001.

VARGAFTIG, J.; TAUSSIG, D. C.; GRIESSINGER, E.; ANJOS-AFONSO, F.; LISTER, T. A.; CAVENAGH, J.; OAKERVEE, H.; GRIBBEN, J.; BONNET, D. Frequency of leukemic initiating cells does not depend on the xenotransplantation model used. **Leukemia**, *[S. l.]*, v. 26, n. 4, p. 858–860, 2012. DOI: 10.1038/leu.2011.250. Disponível em: http://www.nature.com/doifinder/10.1038/leu.2011.250.

VERHAAK, Roel G. W.; WOUTERS, Bas J.; ERPELINCK, Claudia A. J.; ABBAS, Saman; BEVERLOO, H. Berna; LUGTHART, Sanne; LÖWENBERG, Bob; DELWEL, Ruud; VALK, Peter J. M. Prediction of molecular subtypes in acute myeloid leukemia based on gene expression profiling. **Haematologica**, *[S. l.]*, v. 94, n. 1, p. 131–134, 2009. DOI: 10.3324/haematol.13299.

VOELTZEL, Thibault et al. A new signaling cascade linking BMP4, BMPR1A, ΔNp73 and NANOG impacts on stem-like human cell properties and patient outcome. **Cell Death and Disease**, *[S. l.]*, v. 9, n. 10, 2018. DOI: 10.1038/s41419-018-1042-7. Disponível em: http://dx.doi.org/10.1038/s41419-018-1042-7.

WANG, K. et al. Patient-derived xenotransplants can recapitulate the genetic driver landscape of acute leukemias. **Leukemia**, *[S. l.]*, v. 31, n. 1, p. 151–158, 2017. DOI: 10.1038/leu.2016.166.

WARNER, J. K.; WANG, J. C. Y.; TAKENAKA, K.; DOULATOV, S.; MCKENZIE, J. L.; HARRINGTON, L.; DICK, J. E. Direct evidence for cooperating genetic events in the leukemic transformation of normal human hematopoietic cells. **Leukemia**, *[S. l.]*, v. 19, n. 10, p. 1794–1805, 2005. DOI: 10.1038/sj.leu.2403917.

WEINHÄUSER, I. et al. Reduced SLIT2 is associated with increased cell proliferation and arsenic trioxide resistance in acute promyelocytic Leukemia. **Cancers**, *[S. l.]*, v. 12, n. 11, 2020. DOI: 10.3390/cancers12113134.

WUNDERLICH, Mark; MULLOY, James C. MISTRG extends PDX modeling to favorable AMLs. **Blood**, *[S. l.]*, v. 128, n. 17, p. 2111–2112, 2016. DOI: 10.1182/blood-2016-09-738757.

YAMASHITA, Masayuki; DELLORUSSO, Paul V.; OLSON, Oakley C.; PASSEGUÉ, Emmanuelle. Dysregulated haematopoietic stem cell behaviour in myeloid leukaemogenesis. **Nature Reviews Cancer**, *[S. l.]*, v. 20, n. 7, p. 365–382, 2020. DOI: 10.1038/s41568-020-0260-3. Disponível em: http://dx.doi.org/10.1038/s41568-020-0260-3.

YANG, Annie et al. P73-Deficientmicehaveneurological, Pheromonal and Inflammatory Defectsbutlackspontaneoustumours. **Development**, *[S. l.]*, v. 117, n. 1997, p. 1321–1331, 1993.

YANG, Liping; BRYDER, David; ADOLFSSON, Jörgen; NYGREN, Jens; MÅNSSON, Robert; SIGVARDSSON, Mikael; JACOBSEN, Sten Eirik W. Identification of Lin-Sca1+kit+CD34 +Flt3- short-term hematopoietic stem cells capable of rapidly reconstituting and rescuing myeloablated transplant recipients. **Blood**, *[S. l.]*, v. 105, n. 7, p. 2717–2723, 2005. DOI: 10.1182/blood-2004-06-2159.

ZAIKA, Alex I.; SLADE, Neda; ERSTER, Susan H.; SANSOME, Christine; JOSEPH, Troy W.; PEARL, Michael; CHALAS, Eva; MOLL, Ute M. δNp73, a dominant-negative inhibitor of wild-type p53 and TAp73, is up-regulated in human tumors. **Journal of Experimental Medicine**, *[S. l.]*, v. 196, n. 6, p. 765–780, 2002. DOI: 10.1084/jem.20020179.

ZEHIR, Ahmet et al. Mutational landscape of metastatic cancer revealed from prospective clinical sequencing of 10,000 patients. **Nature Medicine**, *[S. l.]*, v. 23, n. 6, p. 703–713, 2017. DOI: 10.1038/nm.4333.

ZHANG, Haijiao et al. Clinical resistance to crenolanib in acute myeloid leukemia due to diverse molecular mechanisms. **Nature Communications**, *[S. l.]*, v. 10, n. 1, p. 244, 2019. DOI: 10.1038/s41467-018-08263-x. Disponível em: http://www.nature.com/articles/s41467-018-08263-x.

ZHANG, Yanyan et al. Engraftment of chronic myelomonocytic leukemia cells in immunocompromised mice supports disease dependency on cytokines. **Blood Advances**, *[S. l.]*, v. 1, n. 14, p. 972–979, 2017. DOI: 10.1182/bloodadvances.2017004903. Disponível em: http://www.ncbi.nlm.nih.gov/pubmed/29296739%0Ahttp://www.pubmedcentral.nih.gov/articlerender.fcgi?artid=PMC5737594%0Ahttp://www.bloodadvances.org/lookup/doi/10.1182/bloodadvances.2017004903.

Supplemental Material

9 SUPPLEMENTAL MATERIAL

UNIVERSIDADE DE SÃO PAULO
FACULDADE DE MEDICINA DE RIBEIRÃO PRETO
COMISSÃO DE ÉTICA NO USO DE ANIMAIS

CEUA FMRP-USP
Comissão de Ética no Uso de Animais

FMRP 65 anos USP

CERTIFICADO

Certificamos que o Protocolo intitulado *"Avaliação da via TP53/TP73 na enxertia de células de leucemia promielocítica aguda em modelo de xenotransplante"*, registrado com o número **067/2018**, sob a responsabilidade do **Prof. Dr. Eduardo Magalhães Rego,** envolvendo a produção, manutenção ou utilização de animais pertencentes ao *filo Chordata, subfilo Vertebrata* (exceto humanos) para fins de pesquisa científica, encontra-se de acordo com os preceitos da Lei nº 11.794 de 8 de outubro de 2008, do Decreto nº 6.899 de 15 de julho de 2009 e com as normas editadas pelo Conselho Nacional de Controle de Experimentação Animal (CONCEA), e foi **APROVADO** pela Comissão de Ética no Uso de Animais da Faculdade de Medicina de Ribeirão Preto da Universidade de São Paulo em reunião de 30 de maio de 2018.

Este Protocolo prevê a utilização de 80 camundongos NSG fêmeas pesando 22g oriundos do Serviço de Laboratório de Estudos Experimentais em Animais de Ribeirão Preto da Universidade de São Paulo. Vigência da autorização: 30/05/2018 a 06/06/2022.

We certify that the Protocol ***nº* 067/2018,** entitled ***"Evaluation of the TP53/TP73 pathway in the engraftment of acute promyelocytic leukemia cells using xenotransplantation models"***, is in accordance with the Ethical Principles in Animal Research adopted by the National Council for the Control of Animal Experimentation (CONCEA) and was approved by the Local Animal Ethical Committee from Ribeirão Preto Medical School of the University of São Paulo in *05/30/2018*. This protocol involves the production, maintenance or use of animals from *phylum Chordata, subphylum Vertebrata* (except humans) for research purposes, and includes the use of 80 female NSG mice weighing 22g from Laboratory of Experimental Studies in Animals of Ribeirão Preto Medical School, University of São Paulo. This certificate is valid until 06/06/2022.

Ribeirão Preto, 30 de maio de 2018

Prof. Dr. Fernando Silva Ramalho
Coordenador da CEUA–FMRP – USP

Faculdade de Medicina de Ribeirão Preto - USP - Av. Bandeirantes, 3900 - Ribeirão Preto - SP - Brasil -14049-900 - Tel.: (16) 3315-3301 / 3315.3275 - e-mail: ceua@fmrp.usp.br

COMISSÃO NACIONAL DE ÉTICA EM PESQUISA

PARECER CONSUBSTANCIADO DA CONEP

DADOS DO PROJETO DE PESQUISA

Título da Pesquisa: AVALIAÇÃO DA DAUNORRUBICINA COMO AGENTE ANTRACÍCLICO NA INDUÇÃO DE REMISSÃO E CONSOLIDAÇÃO DE PACIENTES COM LEUCEMIA PROMIELOCÍTICA AGUDA

Pesquisador: Eduardo Magalhães Rego

Área Temática: A critério do CEP

Versão: 3

CAAE: 81987818.5.1001.5440

Instituição Proponente: Hospital das Clínicas da Faculdade de Medicina de Ribeirão Preto da USP -

Patrocinador Principal: FUNDACAO DE AMPARO A PESQUISA DO ESTADO DE SAO PAULO

DADOS DO PARECER

Número do Parecer: 3.003.975

Apresentação do Projeto:

As informações elencadas nos campos "Apresentação do Projeto", "Objetivo da Pesquisa" e "Avaliação dos Riscos e Benefícios" foram retiradas do arquivo Informações Básicas da Pesquisa (PB_INFORMAÇÕES_BÁSICAS_DO_PROJETO_1049986.pdf, de 05/06/2018) e do Projeto Detalhado.

INTRODUÇÃO

A Leucemia Promielocítica Aguda (LPA) é um subtipo de Leucemia Mielóide Aguda (LMA) que se caracteriza pela parada da maturação do precursor mielóide no estágio de promielócito. Corresponde a cerca de 10% dos casos de LMA com incidência de 10.000 casos nos Estados Unidos em 2001. Entretanto, em alguns países, como Brasil e México a proporção de casos de LPA entre as LMAs é maior, situando-se entre 20 e 30%. Além das características morfológicas e citoquímicas peculiares, clinicamente apresenta-se com um quadro de coagulopatia que é o responsável pela maior morbidade dos pacientes. Do ponto de vista molecular, aproximadamente 95% dos casos de LPA apresentam uma translocação balanceada entre os cromossomos 15 e 17 (loci q22 e q21, respectivamente), gerando o gene PML-RAR. As conseqüências na regulação do ciclo celular e na terapêutica desta doença decorrentes desta alteração genética são de tal forma peculiares que, em 2001, a Organização Mundial de Saúde em sua reclassificação das hemopatias categorizou esta entidade como LMA com t(15;17). As recomendações atuais para o tratamento da

Endereço: SRNTV 701, Via W 5 Norte - Edifício PO 700, 3º andar
Bairro: Asa Norte **CEP:** 70.719-049
UF: DF **Município:** BRASILIA
Telefone: (61)3315-5877 **E-mail:** conep@saude.gov.br